

**acp-2018-603: Surface–atmosphere exchange of water-soluble gases and aerosols above agricultural grassland pre- and post-fertilisation**  
by Ramsay, R. et al.

**Response to Anonymous Referee #1**

We thank the reviewer for their time in reviewing our paper and providing comments. Before addressing the numbered points made by this reviewer individually, we would like to respond to the reviewer's overall question "does this manuscript offer a real advancement of the current state of knowledge?" We believe our paper provides novelty and advancement for the following reasons:

Firstly, there is currently a lack of data for simultaneous time-resolved fluxes of trace inorganic gases and associated aerosol counterparts, particularly for the reactive nitrogen species  $\text{NH}_3/\text{NH}_4^+$  and  $\text{HNO}_3/\text{NO}_3^-$ . Our paper presents flux data for these species over agricultural grassland at hourly resolution for one month at high precision and with appropriate consideration of the uncertainties in the flux values. This dataset also includes fluxes for trace gas and aerosol species during a period of flux divergence post-application of urea fertiliser. By careful consideration of the issues present in analysing fluxes during periods of flux divergence, we present a robust dataset which considers total nitrate and total ammonium fluxes during this period and discusses the changes in flux behaviour post-fertiliser application. Furthermore, it provides strong field evidence of a ground source of both HONO and  $\text{HNO}_3$  after fertilisation.

Secondly, this paper presents bulk deposition velocities for particulate  $\text{Cl}^-$ ,  $\text{NO}_3^-$  and  $\text{SO}_4^{2-}$ , which are themselves important values for deposition modelling. From observation of these deposition velocities, it was hypothesized there was a link between deposition velocity and the proportion of fine to coarse aerosol. Using the ratio of  $\text{PM}_{2.5}/\text{PM}_{10}$ , as measured by a nearby instrument, we were able to demonstrate this association. While this proportion acts as a proxy measurement for particle size measurements, we believe this is novel evidence for demonstrating a link between enhancement of aerosol deposition velocity and proportion of particles contained in the coarse fraction.

Thirdly, we believe we present the first intercomparison data for nitrous acid measurements made by the Gradient of Aerosols and Gases Online Registration (GRAEGOR) and by the Long Path Absorption Photometer (LOPAP), which not only compares concentrations, but also gradients. We also present an intercomparison of ammonia measurements made by the GRAEGOR and by a Quantum Cascade Laser (QCL).

We now respond to the individual points raised in the review, with the reviewer's comments presented in blue, italicized font.

*1) "As illustrated by many of the figures using gradients to determine fluxes is extremely difficult (see the concentration plots in Fig 3 & 4). Indeed direct flux measurements are also very difficult! Thus although the fluxes shown in Figure 7 and Figure 9 are presented without error bars I suspect the error bars are in fact VERY large. This is not a new problem and is certainly not unique to these authors or this study. BUT Figure 10 actually tells an important part of the story as does in Figure 14...that the concentrations are themselves rather uncertain."*

We agree that it would be helpful to include error bars on the time series for fluxes and will add these to Figures 7 and 9 in the revised manuscript. We have included in this response a revised version of Figure 7 – the time series of trace gas fluxes - which includes error bars as an example. We will also add a summary of median flux error values to Tables 4 and 5.

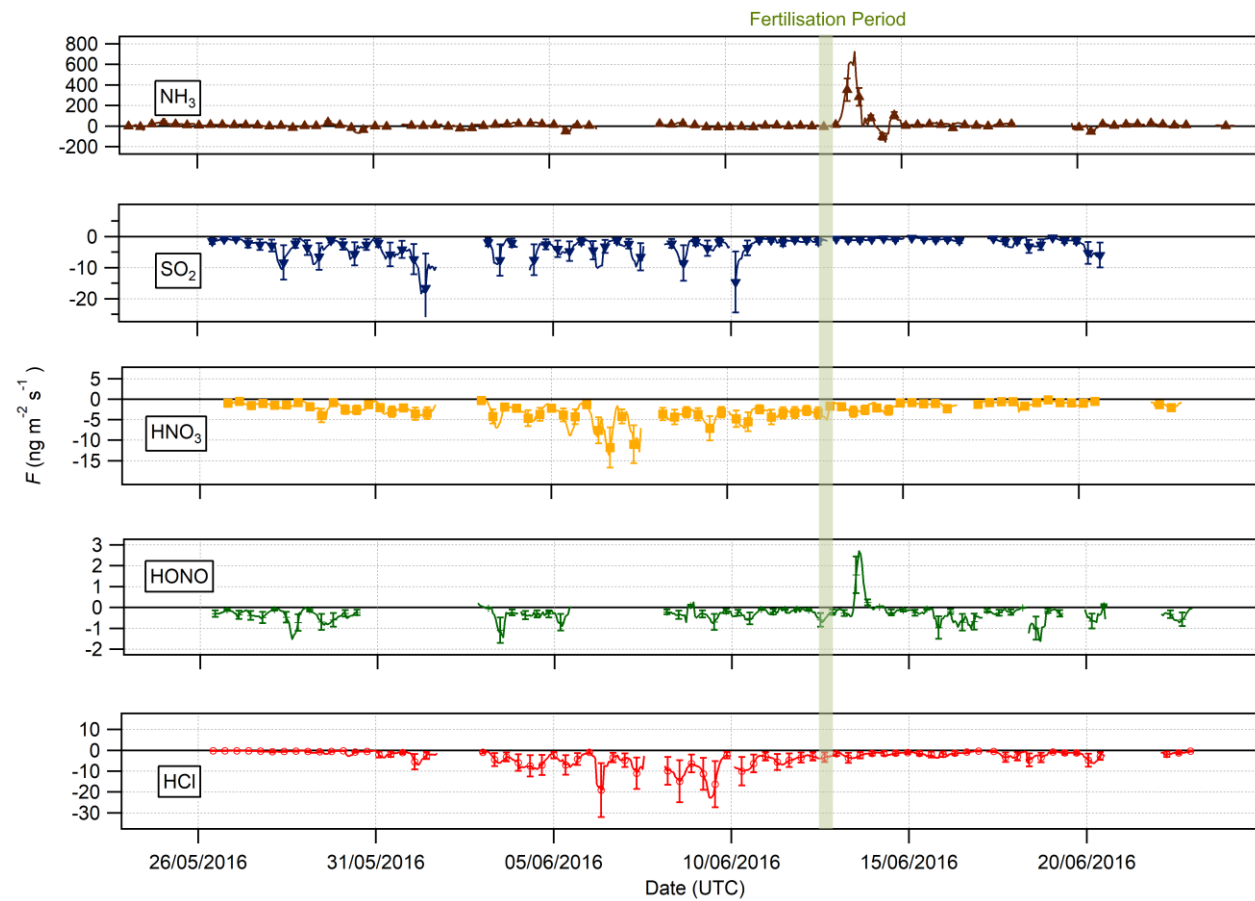


Figure 7: Time series of hourly trace gas fluxes measured during the Easter Bush campaign. Results smoothed using a 5-point moving point average. The fertilisation period was 08:00 – 09:00 on 13th June, and is highlighted in green. Flux uncertainties for each trace gas are included as error bars.

Figure 10 (which compares measurements of NH<sub>3</sub> taken by the GRAEGOR to that by a QCL system) and Figure 14 (similarly comparing measurements of HONO taken by the GRAEGOR to that by a LOPAP) are intercomparison studies between instruments. These comparisons do not reflect the uncertainty of GRAEGOR concentration measurements, only that there exists a difference between measurement techniques that should be accounted for when considering measurements of concentration. Crucially, the difference in measurements between two different systems does not directly impact on the error in the concentration gradient of the GRAEGOR, which is the critical part in calculating flux values. The two GRAEGOR detector boxes share the same analytical system and therefore uncertainties in the concentrations at the two heights are not independent, and the error on the gradient is significantly smaller than the combined error between the two concentrations.

It is our view that the flux uncertainties in this study are not “very large” in respect to previously published studies using the GRAEGOR. The median flux error for NH<sub>3</sub>, for example, was 32%, which is similar to values obtained for measurements made over grassland using the GRAEGOR by Wolff et al. (2010) and Thomas et al. (2009). By inclusion of median flux error values in Tables 2 and 3 of the revised manuscript, we anticipate we can satisfy readers that our flux errors are in the range expected for use of this instrument.

*2) “Fundamentally is GRAEGOR ‘fit for purpose’? Some basic statistics could be brought into play to consider what fraction of flux periods (of each of the considered species) exceeded the uncertainty bounds FOR each individual measurement.”*

The reviewer raises an important point that was considered during flux calculations, but which was not included in the manuscript. As outlined by Thomas et al. (2009), it is possible to calculate the minimum flux that the GRAEGOR can measure for each species, effectively providing a limit of detection for flux measurements. Fluxes presented have been filtered using these values, but discussion of their development, beyond mentioning that fluxes were filtered according to these values was not included, nor were they included in Tables 4 and 5. We will include a brief discussion of calculating this value in the Methods section of the revised manuscript, which, together with inclusion of minimum detectable flux values for each species in Tables 2 and 3, should resolve this issue.

It is important to emphasize that the capability of the GRAEGOR to measure fluxes is dependent upon its ability to measure concentration differences with sufficient precision. As documented in the manuscript, a side-by-side comparison of the GRAEGOR sample boxes was used to develop a linear regression profile, from which – after correction – the residuals were used to determine the precision of the concentration measurements. As we state in our manuscript: “From the results obtained, it was found that for the gases NH<sub>3</sub>, HCl, HONO, HNO<sub>3</sub> and SO<sub>2</sub> that deviation from the 1:1 fit resulted in a precision of measurements <4% (3σ). For the aerosol species Cl<sup>-</sup>, NO<sub>3</sub><sup>-</sup> and SO<sub>4</sub><sup>2-</sup>, precision was calculated as <8% (3σ), while for NH<sub>4</sub><sup>+</sup> was calculated as <9% (3σ).” These precision values are in line with those previously calculated by those using the GRAEGOR to measure fluxes (Thomas et al., 2009; Wolff et al., 2010; Twigg et al., 2011), and we maintain that these are sufficient precision values to resolve the vertical concentration gradients necessary for flux calculations.

The GRAEGOR shares its principle of operation and many components with other instrumentation that has routinely been used for gradient flux measurements, such as the AMANDA/GRAHAM for NH<sub>3</sub> (same denuder but based on selective membrane / conductivity; Erisman and Wyers, 1993; Flechard and Fowler, 1998; Milford et al., 2001, 2009; Wichink Kruij et al., 2007; Neiryneck et al., 2008) and the MARGA-based gradient system of Rumsey et al. (2016). Considering the similar architecture of the GRAEGOR to these instruments which have been successfully used to measure gradient fluxes, the statement that the GRAEGOR would not be fit for purpose is therefore surprising.

Finally, the good agreement between expected and measured deposition velocities for HNO<sub>3</sub> and HCl may be taken as independent evidence (though not proof) of the high quality of the measured fluxes.

*"The authors describe some efforts at determining uncertainty in concentrations and fluxes but they do not appear to be applied"*

As described in responses above, we will resolve issues of clarity surrounding the uncertainty measurements by revising quoted figures in the text so that they include their error values. We will also include error bars in figures where appropriate, and revise Tables 2 and 3 to include further details on error measurements.

*"...the description is quiet[sic] vague and associated with statements I find it hard to comprehend; 'Uncertainties for the trace gases and water-soluble aerosols measured calculated by error propagation ranged from 8% - 18% (3 $\sigma$ ) throughout the campaign, varying primarily due to fluctuations in the measured flow rate and analysed concentration of the internal Br standard.' Does this really mean ALL species for ALL hours had an uncertainty of 8-18% of the measured concentration?"*

We agree with the reviewer that the wording of this section lacks clarity. The determination of concentration measurement error results in the error for concentration measurement. Side-by-side measurements measure the error in concentration difference. Error in flux calculations are determined from this error in concentration difference and the error in flux transfer velocity. The error of 8 – 18% in concentration measurements is reasonable in comparison to past campaigns with the GRAEGOR (Thomas et al., 2009; Wolff et al., 2010). We will clarify this issue in the revised manuscript.

*' $\sigma_u$ \* was estimated at 12% median, which, in combination with  $\sigma_{\Delta c}$ , was used to calculate  $\sigma_F$ ' – I can't see uncertainties are presented... 'While most exceedances fall within the uncertainty range of the measurement' How many do not? And why?*

*3) Addressing point 2) and doing so in a manner that actually uses uncertainties for EACH measurement not for the sample as a whole would be useful in contextualizing the flux estimates and allowing the authors to determine if the 'good enough' threshold is achieved."*

As discussed above, we shall resolve this issue through the inclusion of the necessary values in the text.

*4) "I think Figure 12 is partly a response to particle size but since no data on particle size were provided is it also a story of large measurement uncertainty?"*

In our discussion of the investigation into the dependence of measured deposition velocity ( $V_d$ ) on particle size, we repeatedly emphasize that our value for particle size is a proxy (the ratio  $PM_{2.5}/PM_{10}$  as measured by an instrument nearby). As stated in the text – "Although measurements of particle size were not made during this campaign, measurements of aerosol species (including Cl<sup>-</sup> and SO<sub>4</sub><sup>2-</sup>) in the  $PM_{2.5}$  and  $PM_{10}$  size fractions were taken by a two-channel Monitor for Aerosols and Gases in Ambient Air (MARGA, Applikon B.V, The Netherlands) instrument located at Auchencorth Moss, 12 km south west of Easter Bush...As proxy for a particle size measurement, the proportion of  $PM_{2.5}$  to  $PM_{10}$  was used, with a lower proportion of  $PM_{2.5}$  indicating a greater proportion of coarse aerosol, and a corresponding larger deposition velocity based on process-orientated modelling". Particle size measurements were not available. As summarised at the start of this response document, the proxy measurement was used to investigate a hypothesis that was developed from observations of aerosol  $V_d$  values. Our use of such a proxy measurement is not related to measurement uncertainty. Figure 12 shows strong and statistically significant relationships. The scatter indicated may reflect measurement uncertainty, but could equally reflect limitations in a concentration ratio from a nearby site to describe the full size-distribution at our measurement site, the additional effect of atmospheric stability on  $V_d/u$  (e.g. Wesely et al., 1985) or a number of additional processes (e.g. surface wetness). We anticipate that the reviewer's concern will be resolved by further clarifying the proxy nature of the aerosol size measurement in our manuscript.

**Commented [RR1]:** A revised statement from the original response, which directly clarifies the calculation of concentration measurement error and flux error.

5) *"The manuscript title implies a focus on fluxes ("Surface-atmosphere exchange of water-soluble gases and aerosols above agricultural grassland pre- and post-fertilisation") why are so many of the figures and so much of the text about concentrations and/or the ion balance in the aerosols?"*

5 We believe it is necessary to include figures and text discussing concentrations as a precursor to discussion of fluxes. It is also important to present these findings for the discussions relating to (i) the deposition velocities (which makes references to elevated periods of  $\text{Cl}^-$  concentrations that are visually apparent in Figure 3), (ii) the HONO fluxes (the presence of HONO concentrations above the detection limit suggests a day time source for HONO; this is then linked to discussion of HONO fluxes), and (iii) the instrument intercomparison studies (which compare concentrations).

10 The inclusion of a brief discussion of ionic balance, with an accompanying figure, was necessary to discuss the development of the hypothesis of aerosol bulk deposition velocities being enhanced by particles in the coarse fraction. As mentioned in the text – "[the ionic balance study]...suggests a deficit of  $\text{NH}_4^+$ , suggesting that some of the  $\text{NO}_3^-$  and/or  $\text{SO}_4^{2-}$  was balanced by ions other than  $\text{NH}_4^+$ . A likely candidate is  $\text{Na}^+$ : some of the  $\text{SO}_4^{2-}$  is likely to have represented sea-salt  $\text{SO}_4^{2-}$  and some  $\text{NaNO}_3$  is formed by reaction of  $\text{NaCl}$  with  $\text{HNO}_3$ ." This is then followed by discussion of atmospheric chemical processes that would give rise to the formation of these coarse particles, providing the framework for the eventual discussion of aerosol  $V_d$  and particle size proxy. Without the inclusion of this section, we believe that it would harm the coherence of a novel discussion point in the paper.

20 In conclusion, we believe that the discussion of concentration data is a necessary part of further discussion surrounding surface-atmosphere exchange. We could alternatively have called the manuscript "Concentrations and surface/atmosphere exchange fluxes of water-soluble ...", but we feel that beyond making the title even more cumbersome than it is already, this would not add any more information.

25 6) *"With only a single fertilization event I wonder how generalizable this is? If a data set could be developed that comprises many fertilization events it may be possible to extract a signal, but at the moment the S2N ratio is very low."*

30 Our paper provides rare field evidence of a ground source of both HONO and  $\text{HNO}_3$  following fertilisation, corroborating previous evidence of Sutton et al. (1998) and Twigg et al. (2011). These results are quite remarkable because it is certainly not clear why the application of fertiliser, characterised by a high pH, should result in  $\text{HNO}_3$  release. We do not suggest in the paper that our results should be generalized to fit all grassland fertilization events. However, the observations may well trigger follow-on laboratory process studies of these fertiliser emissions of HONO and  $\text{HNO}_3$ .

35 Here, we aimed only to observe the fluxes of trace gases and aerosols, particularly reactive nitrogen species, pre- and post- fertilisation of a grassland site with urea fertiliser, and to discuss any observed changes. We believe that through our use of the chemical conservative tracers total-nitrate and total-ammonium, we have accounted for the period of flux divergence while drawing relevant conclusions about the behaviour of reactive nitrogen species post-fertilisation. These results add to the literature on fluxes of reactive nitrogen above fertilised grassland, much of which has also described study of only one fertilisation event.

45 7) *"I think IF a numerical model (that accounts for flux divergence) could be brought into the research it would be very useful in trying to extract more information and provide greater insights. As it stands I did not find it compelling and thus the conclusions seem to really over-state what is shown in the manuscript."*

50 The senior author of this publication is indeed a global leader in the 1D modelling of the  $\text{NH}_3$ - $\text{HNO}_3$ - $\text{NH}_4\text{NO}_3$  interaction (e.g. Nemitz et al., 1998; Nemitz et al., 2000; Nemitz et al., 2009; Ryder et al., 2016). A general thread running through these model studies has been that the models are able to explore the observations qualitatively,

but that it is difficult to constrain the model sufficiently to provide fully quantitative results. For example, a fully quantitative model run would require treatment and measurement information of the aerosol composition as a function of size, including any potential external mixing. Such model application is, however, well beyond the scope of this paper or the comprehensiveness of the dataset.

We do not believe that we have overstated our conclusions, as all conclusions cited in the abstract and conclusion sections are argued through the results and discussion section appropriately. We maintain that the data is robust, but we shall emphasize in the revised manuscript why we believe that to be the case, providing more information on flux errors and minimum detectable fluxes, as well as clarifying the issue of concentration measurement errors. We will also reword one conclusion in the abstract, which currently reads “providing direct evidence of a size-dependence of aerosol deposition velocity for aerosol chemical compounds” to remove the phrase “direct evidence”, which we hope in combination with emphasizing the proxy nature of aerosol size measurements should clarify our hypothesis regarding aerosol  $V_d$  and aerosol size. In conclusion, we believe that the work presented in the paper remains suitable for publication by ACP, with the above-discussed amendments to highlight the robustness of our dataset.

*“It’s a minor point given the above but although the manuscript is quite lengthy, I did not find all the details of the measurements.”*

We think the reviewer may be referring here to some lack of information on the source of the NO<sub>2</sub> concentrations and on the MARGA instrument measurements, to which Reviewer #2 also referred. The NO<sub>2</sub> concentrations were determined by chemiluminescence analyser operated to standard UK national network protocols. Details will be added to the revised paper. A full description of the MARGA set-up and operation at the Auchencorth site is available in Twigg et al. (2015). The processed and ratified MARGA data are publicly available online at [https://uk-air.defra.gov.uk/data/data\\_selector](https://uk-air.defra.gov.uk/data/data_selector) from which concentrations of any of the species measured by the MARGA can be selected. We will add the references and online resources to the paper.

#### References:

Erisman, J. W. and Wyers, G. P.: Continuous measurements of surface exchange of SO<sub>2</sub> and NH<sub>3</sub>; Implications for their possible interaction in the deposition process, *Atmos. Environ. Part A. Gen. Top.*, 27(13), 1937–1949, doi:10.1016/0960-1686(93)90266-2, 1993.

Flechard, C. R. and Fowler, D.: Atmospheric ammonia at a moorland site. II: Long-term surface-atmosphere micrometeorological flux measurements, *Q. J. R. Meteorol. Soc.*, 124(547), 759–791, doi:10.1002/qj.49712454706, 1998.

Milford, C., Theobald, M. R., Nemitz, E. and Sutton, M. A.: Dynamics of ammonia exchange in response to cutting and fertilising in an intensively-managed grassland, *Water, Air Soil Pollut.*, 1, 167–176 [online] Available from: <http://link.springer.com/article/10.1023/A:1013142802662>, 2001.

Milford, C., Theobald, M. R., Nemitz, E., Hargreaves, K. J., Horvath, L., Raso, J., Dämmgen, U., Neftel, A., Jones, S. K., Hensen, A., Loubet, B., Cellier, P. and Sutton, M. A.: Ammonia fluxes in relation to cutting and fertilization of an intensively managed grassland derived from an inter-comparison of gradient measurements, *Biogeosciences*, 6(5), 819–834, doi:10.5194/bg-6-819-2009, 2009.

Neiryneck, J., Janssens, I. A., Roskams, P., Quataert, P., Verschelde, P. and Ceulemans, R.: Nitrogen biogeochemistry of a mature Scots pine forest subjected to high nitrogen loads, *Biogeochemistry*, 91(2–3), 201–222, doi:10.1007/s10533-008-9280-x, 2008.

- Nemitz, E., Sutton, M. A., Choulaton, T. W., Wyers, P. G. and Otjes, R. P.: Investigations into vertical gradients of the gas-aerosol phase equilibrium  $\text{NH}_3(\text{g}) - \text{NH}_4(\text{s, aq})$  above vegetative surfaces, *J. Aerosol Sci.*, 29(SUPPL.2), S885–S886, doi:10.1016/S0021-8502(98)90625-5, 1998.
- 5 Nemitz, E., Sutton, M. A., Schjoerring, J. K., Husted, S. and Paul Wyers, G.: Resistance modelling of ammonia exchange over oilseed rape, *Agric. For. Meteorol.*, 105(4), 405–425, doi:10.1016/S0168-1923(00)00206-9, 2000.
- 10 Nemitz, E., Loubet, B., Lehmann, B. E., Cellier, P., Neftel, A., Jones, S. K., Hensen, A., Ihly, B., Tarakanov, S. V and Sutton, M. A.: Turbulence characteristics in grassland canopies and implications for tracer transport, *Biogeosciences*, 6(8), 1519–1537, doi:10.5194/bg-6-1519-2009, 2009.
- 15 Ryder, J., Polcher, J., Peylin, P., Ottlé, C., Chen, Y., Van Gorsel, E., Haverd, V., McGrath, M. J., Naudts, K., Otto, J., Valade, A. and Luyssaert, S.: A multi-layer land surface energy budget model for implicit coupling with global atmospheric simulations, *Geosci. Model Dev.*, 9(1), 223–245, doi:10.5194/gmd-9-223-2016, 2016.
- 20 Sutton, M. A., Milford, C., Dragosits, U., Place, C. J., Singles, R. J., Smith, R. I., Pitcairn, C. E. R., Fowler, D., Hill, J., ApSimon, H. M., Ross, C., Hill, R., Jarvis, S. C., Pain, B. F., Phillips, V. C., Harrison, R., Moss, D., Webb, J., Espenhahn, S. E., Lee, D. S., Hornung, M., Ullyett, J., Bull, K. R., Emmett, B. A., Lowe, J. and Wyers, G. P.: Dispersion, deposition and impacts of atmospheric ammonia: Quantifying local budgets and spatial variability, *Environ. Pollut.*, 102(SUPPL. 1), 349–361, doi:10.1016/S0269-7491(98)80054-7, 1998.
- 25 Thomas, R. M., Trebs, I., Otjes, R., Jongejan, P. A. C. C., Ten Brink, H., Phillips, G., Kortner, M., Meixner, F. X. and Nemitz, E.: An automated analyzer to measure surface-atmosphere exchange fluxes of water soluble inorganic aerosol compounds and reactive trace gases, *Environ. Sci. Technol.*, 43(5), 1412–1418, doi:10.1021/es8019403, 2009.
- 30 Twigg, M. M., House, E., Thomas, R., Whitehead, J., Phillips, G. J., Famulari, D., Fowler, D., Gallagher, M. W., Cape, J. N., Sutton, M. A. and Nemitz, E.: Surface/atmosphere exchange and chemical interactions of reactive nitrogen compounds above a manured grassland, *Agric. For. Meteorol.*, 151(12), 1488–1503, doi:10.1016/j.agrformet.2011.06.005, 2011.
- 35 Twigg, M. M., Di Marco, C. F., Leeson, S., Van Dijk, N., Jones, M. R., Leith, I. D., Morrison, E., Coyle, M., Proost, R., Peeters, A. N. M., Lemon, E., Frelink, T., Braban, C. F., Nemitz, E. and Cape, J. N.: Water soluble aerosols and gases at a UK background site – Part 1: Controls of  $\text{PM}_{2.5}$  and  $\text{PM}_{10}$  aerosol composition, *Atmos. Chem. Phys.*, 15(14), 8131–8145, doi:10.5194/acp-15-8131-2015, 2015.
- 40 Wesely, M. L., Cook, D. R., Hart, R. L. and Speer, R. E.: Measurements and parameterization of particulate sulfur dry deposition over grass, *J. Geophys. Res. Atmos.*, 90(D1), 2131–2143, doi:10.1029/JD090iD01p02131, 1985.
- 45 Wichink Kruit, R. J., van Pul, W. A. J., Otjes, R. P., Hofschreuder, P., Jacobs, A. F. G. and Holtslag, A. A. M.: Ammonia fluxes and derived canopy compensation points over non-fertilized agricultural grassland in The Netherlands using the new gradient ammonia-high accuracy-monitor (GRAHAM), *Atmos. Environ.*, 41(6), 1275–1287, doi:10.1016/j.atmosenv.2006.09.039, 2007.
- 50 Wolff, V., Trebs, I., Foken, T. and Meixner, F. X.: Exchange of reactive nitrogen compounds: Concentrations and fluxes of total ammonium and total nitrate above a spruce canopy, *Biogeosciences*, 7(5), 1729–1744, doi:10.5194/bg-7-1729-2010, 2010.

**acp-2018-603: Surface–atmosphere exchange of water-soluble gases and aerosols above agricultural grassland pre- and post-fertilisation  
by Ramsay, R. et al.**

5

**Response to Anonymous Referee #2**

We thank the reviewer for their time spent reading our paper and providing comments.

10 Clearly we have failed to convince this reviewer of the merits of our dataset and of our interpretations of this dataset. Below we provide responses to the reviewer's criticisms on a point-by-point basis (the reviewer's comments are provided in italics and blue font), but first we wish to reiterate the aims of our study and the relevancy of its conclusions.

15 The aim of this work was to determine, at hourly resolution for a month, the concentrations and fluxes of water-soluble trace gases and their associated particle-phase ionic counterparts as measured by the Gradient of Aerosols and Gases Online Registration (GRAEGOR) at two heights over agricultural grassland. The vertical fluxes of these species were calculated using the modified aerodynamic gradient method and co-located micrometeorological measurements. Simultaneous time-resolved fluxes of these atmospheric components have not been widely determined because of the sophistication of the instrumentation required to do so. We carefully considered issues of limits of detection and flux divergence.

20 A further aim of this study was to discuss any change in flux of reactive nitrogen species after an inorganic fertilizer application to the grassland part way through the measurement period. Such a change was observed.

25

It was not an aim of this study to measure fluxes of particles, total or size-resolved. The use of the word 'aerosol' without qualification in the title of this paper may have unintentionally raised expectation that full particle flux characterisation is included – we expand on this remark, and suggest a refinement to the title, further below.

30 Our paper presents bulk deposition velocities of the water-soluble aerosol-phase ions  $\text{Cl}^-$ ,  $\text{NO}_3^-$  and  $\text{SO}_4^{2-}$  which is important knowledge for deposition models. In examining the deposition velocities we derived we hypothesised a relationship with the proportion of fine and coarse particulate matter. We were able to demonstrate this association by plotting hourly deposition velocity as a function of the temporal  $\text{PM}_{2.5}/\text{PM}_{10}$  ratio measured nearby. We emphasise throughout our paper that use of this ratio is a proxy only for particle size. This reviewer might have liked to see additional measurements that would have allowed a more quantitative analysis. However, to our knowledge, this is the first study that through composition-resolved bulk flux measurements confirms the enhancement in the bulk deposition velocity of aerosol constituents partly contained in the coarse fraction. Direct particle number flux measurements in the coarse fraction are notoriously difficult due to the limited counting statistics. The only ambient measurements available are from fog droplet deposition (see reviews, e.g. by Pryor et al., 2008), based on the (non-validated) assumption that aerosols and fog droplets interact with vegetation in similar manner.

35 A final aim of our work was to present a novel intercomparison between measurements of nitrous acid as gathered by two wet-chemistry instruments.

45 We maintain that fundamentally the depth of our dataset, its presentation and the conclusions it supports are appropriate for publication in ACP.

*After thorough reading the manuscript I come to the conclusion that it does not meet the standards of atmospheric chemistry and physics and has to be rejected. My rating is based on several points: Title and abstract promise*

*measurements, findings, and discussions which are not given. Title and abstract are very broadly formulated, while the paper itself lacks of focus.*

5 We do not agree that the abstract is broadly formulated or promises measurements and discussions that are not subsequently presented. The method by which the trace gases and associated aerosol counterparts were measured is specifically mentioned in the abstract, as is the method by which flux was calculated. All findings referred to in the abstract are directly referred to in the results section, and the discussion points in the abstract are likewise presented in the discussion sections of the paper. We acknowledge, however, that the following wording in the abstract "direct evidence of a size-dependence of aerosol deposition velocity" is overstated, since aerosol size distributions were not directly measured at the site; but the conclusion itself is supported by use of a proxy measurement of aerosol size, which we stress is a proxy measurement throughout the text, including later in this same sentence in the abstract. We will reword this sentence in the revised paper to remove the phrasing "direct evidence." We will also add to the abstract the location of the study. Other than that we do not see anything in the abstract which is not supported by data discussed in the paper.

15 We do acknowledge that the title of the paper is potentially too broad in that it does not specifically qualify that the aspect of aerosol fluxes measured are the water-soluble ionic counterparts of the measured trace gases not full particle distribution fluxes. However, we believe that the exact scope of the aerosol-phase measurements made in our work is readily clear from the abstract and the main text. To avoid ambiguity we will extend the title of our paper to "Surface-atmosphere exchange of inorganic water-soluble gases and associated ions in bulk aerosol above agricultural grassland pre- and post-fertilisation."

20 *Substantial supportive measurements are lacking (e.g. aerosol size distribution or even size resolved chemical analysis of the aerosol).*

25 We believe that the origin of this comment may relate to the issue raised above concerning the abstract, which mentions aerosol size, but which is clarified within the abstract and throughout the text as being a proxy measurement of fine to coarse particle ratio. As indicated above, we will amend the phrasing on this in the abstract and in the title. Measurement of aerosol size distributions and full size-dependent chemical composition was not a component of our study, and we only base our conclusions on data that were available to us. We state in Section 4.2.2 that we did not make size-resolved aerosol measurements: "Although measurements of particle size were not made during this campaign, measurements of aerosol species (including Cl<sup>-</sup> and SO<sub>4</sub><sup>2-</sup>) in the PM<sub>2.5</sub> and PM<sub>10</sub> size fractions were taken by a two-channel Monitor for Aerosols and Gases in Ambient Air (MARGA, Applikon B.V, The Netherlands) instrument located at Auchencorth Moss, 12 km south west of Easter Bush...As proxy for a particle size measurement, the proportion of PM<sub>2.5</sub> and PM<sub>10</sub> was used, with a lower proportion of PM<sub>2.5</sub> indicating a greater proportion of coarse aerosol, and a corresponding larger deposition velocity based on process-orientated modelling".

30 We also state in our Conclusions section that "Future measurements of aerosol deposition velocities should aim to investigate the effect of particle size upon deposition velocity, using a more robust measurement of particle size than used here".

35 We believe that re-emphasis of the proxy nature of aerosol measurements in the abstract will clarify this matter.

*The text is not structured clearly and way too long.*

The reviewer has not amplified on aspects of the paper that they feel are not structured clearly. We have followed the standard structure of presenting primary results and discussions in separate sections. The Discussion includes secondary analysis of the results data, and/or other data brought in, where this supports the points we wish to draw out at a particular place in the Discussion.

*Some sections contradict each other.*

We cannot provide a response to this since the reviewer has not specified where they believe there is contradiction. We do not see a contradiction in what we present.

*When studying reactive trace gas exchange fluxes, possible flux divergence needs to be addressed. The typical sources for flux divergences are introduced in the introduction but not analyzed and discussed in the paper.*

*There are several indications for flux divergence in the results. Nonetheless the authors calculate a 'flux' from the measured gradients and even derive a canopy resistance.*

We agree that the period of measurement includes periods of flux divergence due to changes in the gas-aerosol partitioning. However, this has been explicitly addressed throughout the manuscript. At the end of Section 2.3.3 we state that we initially process the data ignoring chemistry and discuss the validity of this assumption later. Divergence of  $V_d(\text{HNO}_3)$  (as calculated neglecting chemistry) from  $V_{\text{max}}$  has often been taken as an indicator of the importance of flux divergence as have very large deposition velocities of  $\text{NH}_4^+$ . Thus, in Section 4.2.3 it is shown that the influence of chemistry is within the measurement uncertainty, except for the period after fertilisation. To overcome this problem, this period is treated separately by calculating the conservative tracers of total-ammonium and total-nitrate, as per our text: "It should be noted that during this period the aerodynamic gradient method does not derive accurate fluxes because the condition of flux conservation is not met... By contrast, fluxes of total ammonium and total nitrate would be conserved, as the effect of gas-particle interactions are not considered, and their assessment provides additional information on the processes occurring during periods when fluxes are not conserved with height." Our conclusions based on the behaviour of ammonia, ammonium nitrate and nitric acid fluxes are grounded in this analysis.

We have also taken care to exclude the period of flux divergence from the statistical analysis of canopy resistance and deposition velocity for the entirety of the campaign. This latter point was perhaps not clear in the paper and we will add text to stress this exclusion.

It is also worth noting in this context, that previous analyses indicate that size-segregated particle number fluxes (e.g. Nemitz and Sutton, 2004) and even total particle number fluxes (Nemitz et al., 2009) can be highly perturbed by gas-aerosol partitioning, an artefact that is usually completely ignored. This implies that eddy-covariance particle number fluxes do not have a methodological advantage over the bulk composition gradient flux measurements presented here.

*Flux limits of detection are explained in the material and method section, but no results are given. Small and bidirectional fluxes most probably were within the detection limit.*

The flux limits of detection for all trace gas and aerosol species measured will be added to Tables 4 and 5, respectively, of the manuscript. The bidirectional fluxes of HONO and  $\text{NH}_3$  that were observed throughout the campaign – including the period before fertilisation – remained above the flux detection limit calculated. This point will also be added to the text.

*At a well-studied site like Easter Bush there should be more information on aerosol chemistry than just the GRAEGOR measurements. The comparison with MARGA results (measured at a distance of 12 km) itself plus the very rough aerosol size analysis is not sufficient.*

5 As outlined in Section 2.1., Easter Bush periodically hosts campaigns but it is not a site which hosts a suite of long-term measurements of aerosol chemistry. Aerosol size measurements, if they had been available, would have been used. Standard continuous measurements of size distribution would not have greatly aided this campaign: scanning mobility particle sizers (SMPS) and Aerosol Mass Spectrometers (AMS) measure in the sub-micron fraction and the AMS only non-refractory aerosol, whilst analysis focuses on the influence of the coarse fraction and refractory material on deposition velocity. Whilst impactor measurements of aerosol size segregated ion composition would have been helpful, they were not available and indeed are not a routine measurement even at Supersites.

*Furthermore the supportive measurements of the MARGA are not described in the corresponding section. Nor are the NO<sub>2</sub> measurements.*

15 We thank the reviewer for pointing out these omissions. A full description of the MARGA set-up and operation at the Auchencorth site is available in (Twigg et al, 2015). The processed and ratified MARGA data are publicly available online at [https://uk-air.defra.gov.uk/data/data\\_selector](https://uk-air.defra.gov.uk/data/data_selector) from which concentrations of any of the species measured by the MARGA can be selected. We will add the references and online resources to the paper.

20 We also acknowledge that whilst measurements of NO<sub>2</sub> are mentioned in Section 4.4.1 the details of this measurement are not included. The NO<sub>2</sub> concentrations were determined by chemiluminescence analyser operated to standard UK national network protocols. Details will be added to the revised paper.

25 *In the comparison of GRAEGOR measurements with LOPAP and QCL measurements discussion is mixed with contents that should better be placed in the material and method and/or the results section. Data for both comparison lack in number, range and supportive measurements, which would help to understand agreement and disagreement.*

30 During the preparation of this paper the authors discussed the best placements within the paper of the material on the LOPAP and QCL comparisons. We consider that the comparison between GRAEGOR and LOPAP, and GRAEGOR and QCL, is best placed in the Discussion Section as this was not the motivation of the study and we felt that it would become disjointed if material was split between several sections. If reviewers collectively feel strongly on this point we are happy to rearrange the sections.

35 With respect to the comment on amount of intercomparison data, for the comparison between the QCL and the GRAEGOR there is a limited (n = 72) number of measurements. This is considered in the discussion of the comparison (Section 4.4.2), where we mention that lack of measurements restricted comparison to only concentrations of ammonia. On the other hand, the comparison between the LOPAP and the GRAEGOR spans 6 days (n = 148).

40 We are mindful of the novelty of the comparisons – the first that we are aware of to be presented for publication – and we believe the data and our observations on it are worth inclusion in the paper.

*The presented measurements and results do not lead to the presented conclusions.*

45 *Conclusions remain speculative, unfounded and airy.*

*Conclusion*

*The discussion paper does not keep up to the promising title and abstract. The data basis does not appear to bring sufficient material to a paper on its own. Maybe the data can be presented as supportive data in another paper, such as the cited Di Marco et al. one on HONO fluxes.*

50

These final comments from the reviewer essentially re-iterate the same concerns the reviewer has expressed in their earlier comments, and to which we have responded. In summary, we present one full month of hourly-resolved multi-species flux measurements, and throughout the results and discussion section, present carefully considered findings and conclusions which we have made based on our understanding of atmosphere science, the scientific literature, and analysis of the data gathered. We will make modifications to the title and the abstract to avoid any interpretation that this study included size-resolved aerosol flux measurements, plus the other modifications indicated above.

#### References:

- 10 Pryor, S. C.; Gallagher, M. W.; Sievering, H.; Larsen, S. E.; Barthelme, R. J.; Birsan, F.; Nemitz, E.; Rinne, J.; Kulmala, M.; Groenholm, T.; Taipale, R.; Vesala, T., A review of measurement and modelling results of particle atmosphere-surface exchange. *Tellus B* **2008**, *60*, 42-75.
- 15 Nemitz, E.; Sutton, M. A., Gas-particle interactions above a Dutch heathland: III. Modelling the influence of the NH<sub>3</sub>-HNO<sub>3</sub>-NH<sub>4</sub>NO<sub>3</sub> equilibrium on size-segregated particle fluxes. *Atmospheric Chemistry and Physics* **2004**, *4*, 1025-1045.
- 20 Nemitz, E.; Dorsey, J. R.; Flynn, M.; Gallagher, M. W.; Hensen, A.; Erisman, J. W.; Owen, S.; Daemmgen, U.; Sutton, M. A., Aerosol fluxes and particle growth above grassland following the application of NH<sub>4</sub>NO<sub>3</sub> fertilizers. *Biogeosciences* **2009**, *6*, 1627-1645.
- 25 Twigg, M. M.; Di Marco, C. F.; Leeson, S.; Van Dijk, N.; Jones, M. R.; Leith, I. D.; Morrison, E.; Coyle, M.; Proost, R.; Peeters, A. N. M.; Lemon, E.; Frelink, T.; Braban, C. F.; Nemitz, E.; Cape, J. N., Water soluble aerosols and gases at a UK background site – Part 1: Controls of PM<sub>2.5</sub> and PM<sub>10</sub> aerosol composition, *Atmospheric Chemistry and Physics* **2015**, *15*, 8131–8145; doi:10.5194/acp-15-8131-2015; 2015.

# Surface–atmosphere exchange of **inorganic** water–soluble gases and associated ions in bulk aerosols above agricultural grassland pre– and post– fertilisation

Robbie Ramsay<sup>1,2</sup>, Chiara F. Di Marco<sup>1</sup>, Mathew R. Heal<sup>2</sup>, Marsailidh M. Twigg<sup>1</sup>, Nicholas Cowan<sup>1</sup>,  
Matthew R. Jones<sup>1</sup>, Sarah R. Leeson<sup>1</sup>, William J. Bloss<sup>3</sup>, Louisa J. Kramer<sup>3</sup>, Leigh Crilley<sup>3</sup>, Matthias  
Sörge<sup>4</sup>, Meinrat Andreae<sup>4,5</sup>, Eiko Nemitz<sup>1</sup>

<sup>1</sup> Centre for Ecology & Hydrology (CEH), Edinburgh, EH26 0QB, United Kingdom

<sup>2</sup> School of Chemistry, University of Edinburgh, West Mains Road, EH9 3JJ, United Kingdom

<sup>3</sup> School of Geography, Earth and Environmental Sciences, University of Birmingham, Birmingham, B15 2TT, United Kingdom

<sup>4</sup> Max Plank Institute for Chemistry, Biogeochemistry Department, Mainz, P.O. Box 3060, Germany

<sup>5</sup> Scripps Institution of Oceanography, University of California San Diego, La Jolla, CA 92093, USA

Correspondence to: Eiko Nemitz (en@ceh.ac.uk)

**Abstract.** The increasing use of intensive agricultural practices can lead to damaging consequences for the atmosphere through enhanced emissions of air pollutants. However, there are few direct measurements of the surface-atmosphere exchange of trace gases and water–soluble aerosols over agricultural grassland, particularly of reactive nitrogen compounds. In this study, we present measurements of the concentrations, fluxes and deposition velocities of the trace gases HCl, HONO, HNO<sub>3</sub>, SO<sub>2</sub> and NH<sub>3</sub>, and their associated water-soluble aerosol counterparts Cl<sup>-</sup>, NO<sub>2</sub><sup>-</sup>, NO<sub>3</sub><sup>-</sup>, SO<sub>4</sub><sup>2-</sup>, NH<sub>4</sub><sup>+</sup> as determined hourly for one month in May–June 2016 over agricultural grassland **near Edinburgh, UK**, pre- and post- fertilisation. Measurements were made using the Gradient of Aerosols and Gases Online Registration (GRAEGOR) wet–chemical two–point gradient instrument. Emissions of NH<sub>3</sub> peaked at 1460 ng m<sup>-2</sup> s<sup>-1</sup> three hours after fertilisation, with an emission of HONO peaking at 4.92 ng m<sup>-2</sup> s<sup>-1</sup> occurring five hours after fertilisation. Apparent emissions of NO<sub>3</sub><sup>-</sup> aerosol were observed after fertilisation which, coupled with a divergence of HNO<sub>3</sub> deposition velocity ( $V_d$ ) from its theoretical maximum value, suggested the reaction of emitted NH<sub>3</sub> with atmospheric HNO<sub>3</sub> to form ammonium nitrate aerosol. The use of the conservative exchange fluxes of tot-NH<sub>4</sub><sup>+</sup> and tot-NO<sub>3</sub><sup>-</sup> indicated net emission of tot-NO<sub>3</sub><sup>-</sup>, implying a ground source of HNO<sub>3</sub> after fertilisation. Daytime concentrations of HONO remained above the detection limit (30 ng m<sup>-3</sup>) throughout the campaign, suggesting a daytime source for HONO at the site. Whilst the mean  $V_d$  of NH<sub>4</sub><sup>+</sup> was with 0.93 mm/s in the range expected for the accumulation mode, the larger average  $V_d$  for Cl<sup>-</sup> (3.65 mm/s), NO<sub>3</sub><sup>-</sup> (1.97 mm/s), SO<sub>4</sub><sup>2-</sup> (1.89 mm/s) reflected the contribution of a super-micron fraction and decreased with increasing PM<sub>2.5</sub>/PM<sub>10</sub> ratio (a proxy measurement for aerosol size), **providing direct evidence of providing evidence – although limited by the use of a proxy for aerosol size - of a size-dependence of aerosol deposition velocity for aerosol chemical compounds, which has been suggested from process orientated models of aerosol deposition.**

**Commented [RR2]:** Response to Reviewer #2 - We do acknowledge that the title of the paper is potentially too broad in that it does not specifically qualify that the aspect of aerosol fluxes measured are the water-soluble ionic counterparts of the measured trace gases not full particle distribution fluxes. However, we believe that the exact scope of the aerosol-phase measurements made in our work is readily clear from the abstract and the main text. To avoid ambiguity we will extend the title of our paper to "Surface-atmosphere exchange of inorganic water-soluble gases and associated ions in bulk aerosol above agricultural grassland pre- and post-fertilisation."

**Commented [RR3]:** Response to Reviewer #2 - We will also add to the abstract the location of the study

**Commented [RR4]:** Response to Reviewer #1 - We will also reword one conclusion in the abstract, which currently reads "providing direct evidence of a size-dependence of aerosol deposition velocity for aerosol chemical compounds" to remove the phrase "direct evidence", which we hope in combination with emphasizing the proxy nature of aerosol size measurements should clarify our hypothesis regarding aerosol  $V_d$  and aerosol size.

Response to Reviewer #2 - We acknowledge, however, that the following wording in the abstract "direct evidence of a size-dependence of aerosol deposition velocity" is overstated, since aerosol size distributions were not directly measured at the site; but the conclusion itself is supported by use of a proxy measurement of aerosol size, which we stress is a proxy measurement throughout the text, including later in this same sentence in the abstract. We will reword this sentence in the revised paper to remove the phrasing "direct evidence."

## 1 Introduction

As the demand for food production grows in line with an increasing global population, so too does the development of intensive agricultural practices. These can have deleterious impacts on the environment and human health (Godfray et al., 2010; Foley et al., 2011), particularly through the emission of trace gases and the formation of airborne particles generated by their reactive chemistry. The application of nitrogen-based fertilisers and the keeping of livestock are two systems that are important to the formation of atmospheric reactive nitrogen ( $N_r$ ) compounds, such as the gases ammonia ( $NH_3$ ), and nitrous acid ( $HONO$ ), the latter of which, together with nitric acid ( $HNO_3$ ), also derives from the oxidation of nitrogen oxides ( $NO_x$ ) emitted by combustion sources. The associated condensed-phase components of ammonium ( $NH_4^+$ ) and nitrate ( $NO_3^-$ ) exist in equilibrium (as ammonium nitrate ( $NH_4NO_3$ )) with  $NH_3$  and  $HNO_3$  (Robertson et al., 2013). The emission of these  $N_r$  species and their subsequent deposition by washout (wet deposition) or uptake on the surface (dry deposition) have high spatial and temporal variability, and can have critical impacts on terrestrial and aquatic ecosystems, especially those which are nitrogen limited (Galloway et al., 2003; Fowler et al., 2013). The deposition of  $NH_3$  has been specifically linked to eutrophication and to changes in ecosystem composition from nitrogen sensitive to nitrogen tolerant plant species (Bobbink et al., 2010), as well as to reduction in biodiversity of coastal waters (Camargo and Alonso, 2006). The seepage of  $N_r$  compounds into soil can also affect the nitrification/denitrification cycle, giving rise to increased emissions of the greenhouse gas nitrous oxide ( $N_2O$ ) as well as of nitric oxide ( $NO$ ), which in turn effects the formation of  $HNO_3$  and  $HONO$  (Medinets et al., 2014).

As the primary basic gas in the atmosphere,  $NH_3$  also reacts with other trace acidic gases, such as hydrogen chloride ( $HCl$ ) and sulfuric acid ( $H_2SO_4$ ). The products of these reactions give rise to the aerosols, ammonium chloride ( $NH_4Cl$ ) and ammonium sulfate ( $(NH_4)_2SO_4$ ), which along with  $NH_4NO_3$  act as scattering aerosols that alter the Earth's total albedo and contribute significantly to regional and global climate (Fiore et al., 2015). Ammonium sulfate is particularly long lived, and its transport and subsequent deposition to surfaces such as agricultural soils can affect plant health (van der Eerden et al., 1992) and lower soil pH (Elliott et al., 2008). The dry deposition of the acidic gases themselves can also induce soil acidification, which on agricultural soils can limit the growth of crops through perturbing the uptake of nutrients. The ammonium salts make a significant contribution to inhalable particulate matter (PM) associated with human health impacts, with  $NH_4NO_3$  often dominating PM pollution events in northern Europe (Vieno et al., 2014).

It is therefore important that measurements be made of the surface-atmosphere exchange of trace gases and associated aerosol compounds to quantify the emissions from – and deposition to – land used for agriculture. This also provides important process understanding to represent better the dry deposition processes in chemistry and transport models used to predict air quality and climate change. Understanding the impact of agricultural activities on the environment informs the development of abatement strategies and legislation designed to control emissions, for example through instructing agricultural managers on how best to apply their fertiliser inputs.

Measurements of trace gases and associated aerosols are, however, restricted by the availability of appropriate instrumentation, complications in their measurement due to their reactivity and water solubility, as well as the potential interference of gas-particle interactions.

5

Of particular importance is the interaction between  $\text{NH}_3$  and  $\text{HNO}_3$ . These gases, and their aerosol equivalents  $\text{NH}_4^+$  and  $\text{NO}_3^-$ , are the primary contributors to atmospheric N, dry deposition (Andersen and Hovmand, 1999). The majority of  $\text{NH}_3$  emissions originate from agricultural sources, either from direct point sources from the application of N-containing fertilisers, or from long-term sources from livestock (Behera et al., 2013). The use of urea as a fertiliser is associated with particularly large losses of  $\text{NH}_3$  after application, due to the action of the urease enzyme present in soil, which leads to  $\text{NH}_3$  volatilization (Suter et al., 2013). Ferm et al. (1998) estimate that fertiliser losses as  $\text{NH}_3$  average 14% of the N applied. Nitrogen losses from animal waste present on grassland used for sheep grazing has also been observed (Cowan et al., 2015). While  $\text{NH}_3$  is predominantly deposited close to source, resulting  $\text{NH}_4^+$  aerosol can be transported over large distances.

10

15  $\text{HNO}_3$  is primarily formed from the oxidation of nitrogen oxides ( $\text{NO}_x$ ), which are principally anthropogenic in origin but also have a soil biogenic origin (Pilegaard, 2013).  $\text{HNO}_3$  is extremely water soluble and is rapidly removed from the atmosphere through deposition or by gas-particle interactions, leading to a high deposition velocity. The gas-phase equilibrium reaction of  $\text{HNO}_3$  with  $\text{NH}_3$ , which is dependent upon temperature and relative humidity (Mozurkewich, 1993), gives rise to ammonium nitrate (R1).



Higher temperatures and humidity favour the decomposition of  $\text{NH}_4\text{NO}_3$ , and its transportation – and subsequent evaporation – can result in the deposition of reactive nitrogen to the surface. The interaction of  $\text{NH}_3$  with  $\text{HNO}_3$  can also lead to over estimation of the  $\text{HNO}_3$  deposition rate, as the additional sink for  $\text{HNO}_3$  deposition provided for by the reaction violates the theoretical deposition rate modelled on a zero surface resistance model for  $\text{HNO}_3$ . The dissociation of  $\text{NH}_4\text{NO}_3$  over vegetation can induce an opposite effect, with apparent emissions of  $\text{HNO}_3$  occurring with associated high deposition rates for  $\text{NO}_3^-$  and  $\text{NH}_4^+$  (Nemitz and Sutton, 2004). The sums of the total ammonium ( $\text{tot-NH}_4^+ = \text{NH}_3 + \text{NH}_4^+$ ) and of total nitrate ( $\text{tot-NO}_3^- = \text{HNO}_3 + \text{NO}_3^-$ ), however, are conservative quantities (Kramm and Dlugi, 1994), and the use of them in the measurement of exchange fluxes can help to account for the  $\text{NH}_3$ - $\text{HNO}_3$ - $\text{NH}_4\text{NO}_3$  triad on overall deposition rates.

25

30 The reaction is complicated by the presence of  $\text{SO}_2$  and  $\text{HCl}$  that also compete with  $\text{HNO}_3$  for the  $\text{NH}_3$ .  $\text{HCl}$ , like  $\text{HNO}_3$ , is highly water soluble, is deposited quickly to the surface, and consequently has a high deposition velocity. It can be formed by the reaction of other acidic gases, such as  $\text{HNO}_3$  and  $\text{SO}_2$ , with sodium chloride found in sea spray (Pio and Harrison, 1983). The reaction of  $\text{NH}_3$  and  $\text{HCl}$  gives rise to ammonium chloride, which has a similar volatility as  $\text{NH}_4\text{NO}_3$  (Allen et al., 1989).

SO<sub>2</sub>, which is the precursor for H<sub>2</sub>SO<sub>4</sub> in the atmosphere, is primarily anthropogenic in origin, being emitted via the burning of fossil fuels that contain sulfur.

5 HONO is similar to HNO<sub>3</sub> in that it can derive from oxidation of NO<sub>x</sub> precursors. Although it can be formed homogeneously in the atmosphere by the reaction of the hydroxyl radical OH with NO (R2) (Pagsberg et al., 1997), the rate of this reaction is too slow to account for measured concentrations of HONO. Similarly, the heterogeneous reaction involving the reaction of NO<sub>2</sub> with H<sub>2</sub>O on terrestrial surfaces, while potentially a contributory source to atmospheric HONO, has also been found to be too slow to account for measured concentrations (Kleffman, 2007). HONO is photolyzed during daytime, being a primary source of OH-radicals depending on the source and sink mechanisms that govern its abundance (Sörgel et al., 2015). However, a growing number of field measurements of non-zero HONO concentrations during the day points to the presence of daytime sources (Acker et al., 2006), including the emissions of HONO from soils (Su et al., 2011; Oswald et al., 2013; Scharko et al., 2015).



15 Techniques to measure concentrations and fluxes of these trace gas and associated aerosol components require multispecies quantification, low detection limits and fast temporal resolution. Eddy covariance, the most direct micrometeorological technique for the measurement of trace gas fluxes, requires fast-response sensors that are not available for some species (such as HNO<sub>3</sub>) or are limited by the time-response and potential for chemical interferences of the inlet (Neuman et al., 1999). While eddy covariance has been used to measure NH<sub>3</sub> concentrations using laser absorption spectroscopy, such as through the use of quantum cascade lasers (QCL) (Famulari et al., 2004; Zöll et al., 2016), intercomparisons with more established techniques are still lacking.

25 The aerodynamic gradient method derives fluxes of a tracer from its vertical concentration gradient, which can be obtained from concentration measurements at two or more heights, avoiding the requirement for fast response measurement. Developments in automated wet chemistry instrumentation have in turn led to the development of the Gradient of Aerosols and Gases Online Registrator (GRAEGOR), a two-point gradient system that measures the concentrations of HCl, HONO, HNO<sub>3</sub>, SO<sub>2</sub> and NH<sub>3</sub>, and their associated aerosol counterparts Cl<sup>-</sup>, NO<sub>2</sub><sup>-</sup>, NO<sub>3</sub><sup>-</sup>, SO<sub>4</sub><sup>2-</sup> and NH<sub>4</sub><sup>+</sup> (Thomas et al., 2009). One of the advantages of the modified aerodynamic gradient method is the ability to determine the deposition velocities (*V<sub>d</sub>*) of chemical tracers, provided the flux and concentration at a reference height have been calculated. With the use of the GRAEGOR, which takes measurements of tracers at two heights over one hour, high-resolution time scale measurements of deposition velocities can be acquired.

30 Other wet chemistry instruments have also been developed to measure individual species at one height, such as the Long Path Absorption Photometer (LOPAP), which measures concentrations of HONO with fewer artefacts than the GRAEGOR (Heland

et al., 2001). A comparison study between LOPAP HONO measurements and the Gas and Aerosol Collector (GAC) - an instrument which uses similar measurement techniques to the GRAEGOR – was conducted by Dong et al. (2012), but there has not yet been a published comparison between the LOPAP and GRAEGOR in measurements of HONO. Similarly, measurements of trace gases and aerosols above agricultural grassland using the GRAEGOR are limited, and previous studies above these land systems have been restricted to measurements of a limited number of species within a limited particle size range.

The aim of this study was to use the GRAEGOR to measure concentrations and fluxes of the trace gases HCl, HONO, HNO<sub>3</sub>, SO<sub>2</sub> and NH<sub>3</sub> and their water-soluble aerosol counterparts Cl<sup>-</sup>, NO<sub>2</sub><sup>-</sup>, NO<sub>3</sub><sup>-</sup>, SO<sub>4</sub><sup>2-</sup> and NH<sub>4</sub><sup>+</sup> over agricultural grassland in Scotland during a period in early summer (May–June 2016) that included a fertilisation event using urea pellets. The possible formation of NH<sub>4</sub>NO<sub>3</sub> post fertilisation, a link between aerosol deposition velocity and size (specifically, a proxy for size based on the PM<sub>2.5</sub>/PM<sub>10</sub> ratio from measurements nearby), and the potential ground source formation of HONO are discussed. A further aim of this study was to undertake intercomparisons between the measurements of HONO by the GRAEGOR and two LOPAP instruments, and between measurements of NH<sub>3</sub> recorded by a parallel quantum cascade laser eddy covariance system.

## 2 Methodology

### 2.1 Easter Bush Site Description

The campaign was conducted during the late spring/summer 2016 (21<sup>st</sup> May – 24<sup>th</sup> June) at the Easter Bush measurement site (3°12'W, 55°52'N, 190 m above sea level), located 10 km south of Edinburgh, UK. Measurements were made at a 3 m tower situated on the boundary of two intensively managed grassland fields (hereafter referred to as North and South Field) of 16 ha total area, composed principally of *Lolium perenne* (perennial Rye grass) (Fig. 1). Due to the presence of the Pentland Hills close by to the west, local wind direction is channelled such that SW winds – the predominant wind direction at the site – yield flux footprints over the South field, while NE winds produces flux footprints over the North field.

Both fields are used for year-round (although not continuous) sheep grazing, in rotation with adjacent fields, but the South Field also typically has an annual cutting for silage. Mineral fertilisation is carried out twice a year on both fields. During this study, fertilisation of the two fields occurred between 08:00 – 09:00 on the 13<sup>th</sup> June, using urea mineral fertiliser at a rate of 69.9 kg N ha<sup>-1</sup>. In preparation for this application, sheep that had been present in the fields since April were removed from the South Field on the 2<sup>nd</sup> June and removed from the North Field on the 9<sup>th</sup> June. Sheep were reintroduced to the North Field on the 21<sup>st</sup> June.

Over the years the Easter Bush field site has hosted several long-term measurements of CO<sub>2</sub>, CH<sub>4</sub> and NO<sub>2</sub>, and has participated in a number of international projects, such as GRAMINAE (GRassland AMmonia INTERactions Across Europe) (Sutton et al.,

**Commented [RR5]:** Response to Reviewer #1 - ...in combination with emphasizing the proxy nature of aerosol size measurements should clarify our hypothesis regarding aerosol Vd and aerosol size.

Response to Reviewer #2 - We believe that re-emphasis of the proxy nature of aerosol ... will clarify this matter.

2009), Greengrass (Soussana et al., 2007) and NitroEurope (Sutton et al., 2007). It has also supported several individual campaigns of trace gas measurements (Di Marco et al., 2004; Famulari et al., 2004; Jones et al., 2017). In particular, fluxes of  $\text{NH}_3$  were measured over an 18-month period (Milford et al., 2000) and the GRAEGOR was operated during a period of manure application (Twiggy et al., 2011).

## 5 2.2 Instrumentation

### 2.2.1 Gradient of Aerosols and Gases Online Registrator

The GRAEGOR (Energy Research Centre of the Netherlands) is a wet chemistry instrument that measures the concentrations of reactive trace gases ( $\text{HCl}$ ,  $\text{HONO}$ ,  $\text{HNO}_3$ ,  $\text{SO}_2$  and  $\text{NH}_3$ ) and water-soluble aerosols ( $\text{Cl}^-$ ,  $\text{NO}_2^-$ ,  $\text{NO}_3^-$ ,  $\text{SO}_4^{2-}$ ,  $\text{NH}_4^+$ ) continuously, semi-autonomously, and with online analysis at hourly resolution (Thomas et al., 2009; Wolff et al., 2010). The instrument consists of two sampling boxes placed at two heights (during this campaign,  $z_1 = 0.6$  m,  $z_2 = 2.4$  m), from which concentration gradients and hence fluxes can be derived.

Each sample box contains a horizontal wet rotating annular denuder (WRD) (Keuken, 1988) and a steam jet aerosol collector (SJAC) (Khylstov et al., 1995; Slanina et al., 2001) connected in series. Air is drawn through each sample box simultaneously by an air pump at a rate of  $16.7 \text{ L min}^{-1}$ , passing first through the WRD, which is continuously coated with a feeding solution of double-deionized water (DDI) of  $18.2 \text{ M}\Omega$  resistance. Trace gases within the laminar air flow are absorbed into the sorption solution which is then fed from the sample box to a detection unit located at ground level. The trace-gas-free air then passes through the SJAC, where particles within the air flow are mixed with steam generated from the DDI water feeding solution, precipitating a supersaturation event causing the water-soluble particles to grow into droplets. The enlarged droplets are separated out of the air stream by a cyclone and fed as a liquid sample to the detection unit. Liquid samples from the SJAC and WRD of each sample box are analysed for  $\text{NH}_3/\text{NH}_4^+$  using flow injection analysis (FIA) (Wyers, 1993; Norman et al., 2009). An ion chromatography (IC) unit equipped with a Dionex AS12 column, quantifies the concentration of  $\text{HONO}/\text{NO}_2^-$ ,  $\text{HNO}_3/\text{NO}_3^-$  and  $\text{SO}_2/\text{SO}_4^{2-}$  based on the measured conductivity of the respective anions within the liquid sample compared to a reference standard of  $50 \text{ ppb Br}^-$  added to the sample solution. Analysis by FIA and IC is carried out over 15 minutes, and using a flow control scheme, a half-hourly averaged concentration of trace gases and water-soluble aerosols is generated for each height every hour.

A high-density polyethylene tube (0.3 m length, and 1/3" outer diameter) with a HDPE filter is placed at the inlet of the WRD in order to minimise the loss of  $\text{HNO}_3$  and  $\text{NH}_3$  and to ensure a particle diameter cutoff of 0.2  $\mu\text{m}$ . A biocide of 0.6 mL of hydrogen peroxide (30%) is added to every 1 L of the DDI water feeding solution to prevent biological contamination in the WRD of each sample box. Air flow is controlled using a critical orifice downstream of the SJAC.

Autonomous calibration of the FIA system was carried out 24 h after the beginning of the campaign, and every 72 h thereafter, giving a total of 5 internal calibrations of this system. Calibration was conducted using three liquid  $\text{NH}_4^+$  standards of 0, 50 and 500 ppb concentration. The IC unit is continuously checked for analytical performance by the addition of a liquid  $\text{Br}^-$  internal standard (50 ppb concentration) to each column injection. Calibration of the IC unit was conducted twice during the campaign (23<sup>rd</sup> May and the 28<sup>th</sup> June, prior to and after the campaign respectively) using a mixed ionic liquid standard consisting of 25 ppb  $\text{SO}_4^{2-}$ , 20 ppb  $\text{NO}_3^-$  and 20 ppb  $\text{Cl}^-$ .

Measurements of the air flow into the sample boxes were conducted using an independent device (TSI Mass Flowmeter 4140) once every fortnight during the campaign. Additional checks of the field performance of the instrument included daily checks of the WRD tubes and sample box air inlets for signs of visible contamination.

The GRAEGOR sampling boxes have very short inlets with no size-selection. Consequently, the aerosol concentration reflects water-soluble total suspended particulate (TSP). It detects any compound that dissociates to form the measured ions and therefore has a number of artefacts. These include interferences in HONO measurements through  $\text{NO}_2$ , particularly during periods of high  $\text{SO}_2$  concentrations (Spindler et al., 2003); the inclusion of dinitrogen pentoxide ( $\text{N}_2\text{O}_5$ ) concentrations in measurements of  $\text{HNO}_3$  during the night-time measurement periods, though the magnitude of this unclear in rural environments (Phillips et al., 2013); and the potential for organic chloride compounds to be included in measurements of overall  $\text{Cl}^-$  aerosol (Nemitz et al., 2000a).

[The GRAEGOR has been demonstrated to be capable of measuring fluxes in a number of studies both in identical form to the one used here \(Wolff et al., 2010, 2011; Twigg et al., 2011\) or in related variants \(Nemitz et al, 2004; Rumsey and Walker, 2016\). Ammonia-specific instruments based on the same technology \(AMANDA, GRAHAM, ECN Petten, NL; Wyers et al., 1993\) represent the most commonly used instrument for the automated measurement of ammonia fluxes.](#)

### 2.2.2 Supplementary Measurements

Vertical profiles of temperature were measured at the tower using fine-thread, custom-made thermocouples set at the same heights as the GRAEGOR sample boxes. Located 0.4 m from the tower, an eddy covariance system (Gill Anemometer R01012 with LI-COR-7000) at a height of 2.6 m measured three-dimensional wind speed, sensible heat flux ( $H$ ), frictional velocity ( $u_*$ ) and wind direction. Ongoing, long-term measurements of relative humidity (RH) (Vaisla 50/Y humitter), global radiation (Skye Instruments SKS 110 pyranometer), and total rainfall (Campbell Scientific ARG110 tipping bucket rain gauge) were also available at the site for the campaign period. Measurements of HONO taken by a LOPAP (QUMA Elektronik & Analytik, Wuppertal, Germany) and  $\text{NH}_3$  measurements taken by a Quantum Cascade laser (QCL) (Aerodyne Research Inc., Billerica, USA) during the campaign period were used for comparison studies with GRAEGOR measurements. [Measurements of  \$\text{NO}\_2\$](#)

concentration, used in Section 4.4.1 to quantify an artefact in GRAGOR HONO measurements, were recorded by a chemiluminescence NO<sub>2</sub> detector (200E, Teledyne API, San Diego, California, USA) located 300 m south-east of the Easter Bush site.

## 2.3 Micrometeorological Theory

### 2.3.1 Aerodynamic Gradient Method

- 5 The aerodynamic gradient method (AGM), based upon flux-gradient similarity theory, calculates the flux of a tracer ( $\chi$ , such as a gas or aerosol species) based on its vertical concentration gradient coupled with turbulence parameters (Fokken, 2008). In this paper a hybrid version of the AGM is used, in which the flux is calculated as (Flechard, 1998):

$$F_{\chi} = -u_* \kappa \frac{\partial \chi}{\ln\left(\frac{z_2-d}{z_1-d}\right) - \Psi_H\left(\frac{z_2-d}{L}\right) + \Psi_H\left(\frac{z_1-d}{L}\right)} \quad (1)$$

- 10 where the friction velocity ( $u_*$ ) is derived from eddy-covariance measurements with a sonic anemometer;  $\kappa$  is the von Karman constant ( $\kappa = 0.41$ );  $z_2$  and  $z_1$  are the heights of the sample boxes;  $d$  is the displacement height; and  $\zeta$  is a dimensionless stability parameter expressing the ratio  $(z-d)/L$ , where  $L$  is the Obukhov length, a measure for atmospheric stability. The parameter  $\Psi_H$ , an integrated form of the heat stability correction term, accounts for deviations from the log-linear profile under non-neutral stratification. By convention, negative and positive flux values denote deposition and emission, respectively.

### 2.3.2 Choice of displacement height, $d$ , value

- 15 A temperature gradient profile for the campaign was derived from measurements of air temperature at the two heights at which concentrations were measured (0.6 m and 2.4 m). Sensible heat flux ( $H$ ) was calculated from the temperature gradient as per Wang and Bras (1998):

$$H = -\rho_{\text{air}} c_p K_H (z-d) \frac{dT}{dz}, \quad (2)$$

- 20 where  $c_p$  is the heat capacity of air,  $\rho_{\text{air}}$  is the density of air, and  $K_H$  is the eddy diffusivity constant for heat.  $K_H$  can be calculated as

$$K_H (z-d) = \frac{(z-d)u_*}{\Phi_H\left(\frac{z-d}{L}\right)}, \quad (3)$$

- 25 where  $z$  is the absolute height above ground,  $d$  is the displacement height,  $u_*$  is the friction velocity, and  $\Phi_H$  is the stability correction for sensible heat. Sensible heat flux and, by extension, the flux of the trace gas and aerosol species, are dependent upon the value of  $d$ . In order to ensure that the correct displacement height was chosen, the sensible heat flux based upon the temperature gradient developed from thermocouple measurements was calculated using a variety of different values for displacement height. The resulting values for the sensible heat flux were then compared through linear regression to the value for the sensible heat flux recorded by the eddy covariance system also present. A displacement height value of 0.14 m gave the

**Commented [RR6]:** Response to Reviewer #1 - The NO<sub>2</sub> concentrations were determined by chemiluminescence analyser operated to standard UK national network protocols. Details will be added to the revised paper

Response to Reviewer #2 - We also acknowledge that whilst measurements of NO<sub>2</sub> are mentioned in Section 4.4.1 the details of this measurement are not included. The NO<sub>2</sub> concentrations were determined by chemiluminescence analyser operated to standard UK national network protocols. Details will be added to the revised paper.

closest agreement between the sensible heat fluxes derived by the aerodynamic gradient approach and eddy-covariance, with a linear regression slope of 0.997 and  $R^2 = 0.945$ .

### 2.3.3 Determination of Dry Deposition Velocities

The dry deposition velocity ( $V_d$ ) of a tracer is the negative ratio of its flux to its concentration ( $\chi$ ) at height  $z - d$

$$5 \quad V_d(z - d) = - \frac{F_\chi}{\chi(z-d)}, \quad (4)$$

The  $V_d$  for gas species may also be expressed as the reciprocal of the total resistance for deposition, which is composed of  $R_a$  (the aerodynamic resistance),  $R_b$  (the quasi-laminar boundary layer resistance) and  $R_c$  (the canopy resistance) as per the resistance analogy for dry deposition (Fowler and Unsworth, 1979; Wesley, 1989).  $R_a$  and  $R_b$  were calculated from (5) and (6) using meteorological measurements taken at the site using (Myles et al., 2014; Garland, 1977)

$$10 \quad R_a(z-d) = \frac{u(z-d)}{u_*^2}, R_a(z-d) = \frac{u(z-d)}{u_*^2} - \frac{\Psi_H(\zeta) - \Psi_M(\zeta)}{\kappa u_*}, \quad (5)$$

$$R_b = \frac{0.4 \sqrt{S_c^2}}{u_*}, R_b = (B u_*)^{-1}, \quad (6)$$

where  $B = B^{-1}$ ,  $B$  being the Stanton number, is the mean streamwise parametrized by the turbulent Reynold's number,  $R_{e*}$  (the ratio of the frictional force to the kinematic velocity of air) wind speed and  $S_c$  is the Schmidt number,  $S_c$  (the ratio of kinematic velocity of air to the molecular diffusivity coefficient of the gas species):

$$15 \quad B^{-1} = 1.45 R_{e*}^{0.24} S_c^{0.8}, \quad (7)$$

If  $R_a$  and  $R_b$  are calculated from measurements,  $R_c$  can be inferred via:

$$R_c = \frac{1}{V_d(z-d)} - R_a(z-d) - R_b, \quad (78)$$

For gases, a theoretical maximum deposition velocity can be calculated when it is assumed that the gas is completely absorbed by the canopy (i.e. for  $R_c = 0$ ):

$$20 \quad V_{max} = \frac{1}{(R_a + R_b)}, \quad (89)$$

The canopy resistance approach can only describe deposition and fails when the exchange of a gas is bi-directional, such as often the case with  $\text{NH}_3$ . In this case, the canopy compensation point model can be adopted, which considers the surface interaction of  $\text{NH}_3$  in terms of parallel resistance pathways, composed of individual resistances such as stomatal resistance and cuticular resistance (Nemitz et al., 2000b; Flechard et al., 1999).

**Commented [RR7]:** The previous version of the document which outlined the calculation of  $R_a$  and  $R_b$  did not include a function for stability correction. This section has now been revised to resolve this issue.

The gradient technique is only applicable for inert species whose flux is constant with height. Most studies of surface-exchange fluxes of reactive compounds do not have the information to assess whether chemical reactions might interfere with the flux measurement, but in this study the behaviour of HNO<sub>3</sub> and HCl allows us to draw conclusions on flux divergence (Section 4.2.1). Following precedence in the literature (e.g. Nemitz et al., 2004) we initially evaluate fluxes assuming that chemistry can be ignored, and then discuss the validity of this discussion based on the results. Whether this was always the case during this study, is discussed later.

#### 2.3.4 Limits of detection and estimation of uncertainties in concentration measurements and flux calculations

The concentration limit of detection (LOD) of the instrument for each of the species measured was quantified from a field blank test. The field blank test was carried out prior to the campaign on the 20<sup>th</sup> March over 24 hours by switching off the sample box air pump and sealing the air inlets, but leaving the rest of the system unaltered, as per Thomas (2009). Limits of detection were then calculated as three standard deviations from the average background signal. Results from this test are presented in Table 1, expressed as LOD values for each trace gas and corresponding water-soluble aerosol species.

The minimum detectable flux for each aerosol and gas species measured by the GRAEGOR is dependent upon atmospheric stability and the ambient concentration of the given trace gas or aerosol species. Based on the method described by Thomas et al. (2009), median minimum detectable fluxes ( $F_{LOD}$ ) were calculated for each trace gas and aerosol species measured and are detailed in Tables 2 and 3 respectively.

When calculating the flux of a species using the aerodynamic gradient method, it is apparent that errors in individual concentration measurements propagate into an error in the concentration differences, and subsequently, affect the accuracy of the calculated vertical concentration gradient. Some errors systematically affect both heights and therefore affect the gradient to a lesser extent than systemic errors in sampling efficiency at a single height, such as difference in capture efficiency of the WRD tubes or slight differences in air flow caused by differences in the critical orifices, may impact on the accuracy of concentration measurements and resultantly affect the precision in the error of concentration difference.

The overall random error in the measurements of the trace gas and water-soluble aerosol concentrations ( $\sigma_m$ ) can be determined using a Gaussian error propagation approach, in which the concentration error is expressed as a product of several individual measurement errors with the mixing ratio,  $m$  (Trebs et al., 2004) (eq. 9) –

$$\sigma_m = m \sqrt{\left(\frac{\sigma_{m_{liq}}}{m_{liq}}\right)^2 + \left(\frac{\sigma_{Br(std)}}{Br(std)}\right)^2 + \left(\frac{\sigma_{Q_{Br}}}{Q_{Br}}\right)^2 + \left(\frac{\sigma_{m_{Br}}}{m_{Br}}\right)^2 + \left(\frac{\sigma_{Q_{air}}}{Q_{air}}\right)^2} \quad (910)$$

**Commented [RR8]:** Response to Reviewer #2 - We have also taken care to exclude the period of flux divergence from the statistical analysis of canopy resistance and deposition velocity for the entirety of the campaign. This latter point was perhaps not clear in the paper and we will add text to stress this exclusion.

**Commented [RR9]:** Response to Reviewer #1 - The reviewer raises an important point that was considered during flux calculations, but which was not included in the manuscript. As outlined by Thomas et al. (2009), it is possible to calculate the minimum flux that the GRAEGOR can measure for each species, effectively providing a limit of detection for flux measurements. Fluxes presented have been filtered using these values, but discussion of their development, beyond mentioning that fluxes were filtered according to these values was not included, nor were they included in Tables 4 and 5. We will include a brief discussion of calculating this value in the Methods section of the revised manuscript, which, together with inclusion of minimum detectable flux values for each species in Tables 4 and 5, should resolve this issue.

Here,  $m_{liq}$  is the mixing ratio of the compounds found in the analysed liquid sample in ppb,  $Br_{(std)}$  the stated mixing ratio of the internal Br<sup>-</sup> standard,  $Q_{Br}$  the flow rate of the internal Br<sup>-</sup> standard,  $m_{Br}$  the analysed Br<sup>-</sup> mixing ratio and  $Q_{air}$  the air mass flow through the system. All values have an associated standard deviation,  $\sigma_x$ . This formulation holds strictly for the species measured by ion chromatography; for NH<sub>3</sub> and NH<sub>4</sub><sup>+</sup>, the equation is altered by omitting the factor relating to Br<sup>-</sup> addition and substituting the factor for  $Q_{Br}$  and its associated standard deviation with the term  $Q_s$ , the flow of the analysed liquid sample of NH<sub>3</sub> or NH<sub>4</sub><sup>+</sup>.

Uncertainties for the trace gases and water-soluble aerosols measured calculated by error propagation ranged from 8% - 18% (3 $\sigma$ ) throughout the campaign, varying primarily due to fluctuations in the measured flow rate and analysed concentration of the internal Br<sup>-</sup> standard.

Alternatively, the full random error in the concentration difference ( $\sigma_{\Delta c}$ ) can be characterised experimentally, by placing both sample boxes can at one height, or – provided that the absolute difference between sample heights is small – by using one common air inlet at a specified height, with the instrument operated normally. From this side-by-side measurement, linear regression analysis accompanied by orthogonal best of fit between the concentrations measured by each sample box can be conducted, with deviation from a 1:1 fit between sample heights defined as a systemic error. Using the calculated orthogonal fit equation, corrections in the concentrations can then be applied, accounting for the systemic bias (Wolff et al., 2010b). After correction using the orthogonal fit, the remaining scatter – termed the residuals – was used to determine the error in the concentration difference. During this campaign, one side-by-side measurement was conducted on the 8<sup>th</sup> June for 16 hours by connecting a common air inlet set at  $z = 1.2$  m between each sample box. From the results obtained, it was found that for the gases NH<sub>3</sub>, HCl, HONO, HNO<sub>3</sub> and SO<sub>2</sub> that deviation from the 1:1 fit resulted in a precision of measurements <4% (3 $\sigma$ ). For the aerosol species Cl<sup>-</sup>, NO<sub>3</sub><sup>-</sup> and SO<sub>4</sub><sup>2-</sup>, precision was calculated as <8% (3 $\sigma$ ), while for NH<sub>4</sub><sup>+</sup> was calculated as <9% (3 $\sigma$ ).

Errors in flux calculations can similarly be determined through the Gaussian error propagation method applied to Eq. (1). Wolff et al. (2010b), using an analogous form of this equation, showed that total error in the flux is composed of the error in the concentration difference ( $\sigma_{\Delta c}$ ) and the error in the flux-gradient relationship (expressed as a transport velocity by Wolff et al., 2010b), which is dominated by the error in  $u^*$  ( $\sigma_{u^*}$ ).

$$\sigma_F = F \sqrt{\left(\frac{\sigma_{u^*}}{u^*}\right)^2 + \left(\frac{\sigma_{\Delta c}}{\Delta c}\right)^2} \quad (11)$$

This simplification neglects the detailed secondary errors associated with the stability correction which to quantify fully is beyond the scope of this paper.

**Commented [RR10]:** Response to Reviewer #1 - We agree with the reviewer that the wording of this section lacks clarity... We will clarify this issue in the revised manuscript  
 -Calculation of uncertainty in the concentration – Gaussian Propagation method as detailed in equation 10.  
 -Calculation of uncertainty in the flux – Gaussian Propagation method as detailed in equation 11, where the uncertainty in the concentration gradient (different from the measurement of concentration uncertainty) is determined by side-by-side measurements.

$\sigma_{u^*}$  is dependent upon the sonic anemometer used and whether conditions are neutral or non-neutral (Foken, 2008; Nemitz et al., 2009a). For neutral conditions, and based on the sonic anemometer used,  $\sigma_{u^*}$  was estimated at  $\leq 10\%$ . For non-neutral conditions,  $\sigma_{u^*}$  was estimated at 12% median, which, in combination with  $\sigma_{\Delta c}$ , was used to calculate  $\sigma_F$ .

Throughout this paper, stated errors for concentration measurements are derived from the measurement uncertainty as calculated by Eq. (10), while stated errors for flux calculations are derived from the flux uncertainty as calculated by Eq. (11). Calculated errors for the uncertainty in concentration measurements, the error in the concentration difference, and the error in the calculated fluxes for all species measured are similar to values determined by previous studies which have used the GRAEGOR successfully to measure flux gradients (Thomas et al., 2009; Wolff et al., 2010; Twigg et al., 2011).

**Commented [RR11]:** Response to Reviewer #1 - Crucially, the difference in measurements between two different systems does not directly impact on the error in the concentration gradient of the GRAEGOR, which is the critical part in calculating flux values. The two GRAEGOR detector boxes share the same analytical system and therefore uncertainties in the concentrations at the two heights are not independent, and the error on the gradient is significantly smaller than the combined error between the two concentrations.

### 2.3.5 Data Post Processing

Concentrations that were less than five times the limit of detection as calculated before the campaign began (20<sup>th</sup> March) were discarded. Calculated fluxes were filtered according to a standard protocol. Fluxes were not calculated for periods of low wind speed ( $u < 1 \text{ m s}^{-1}$ ), low friction velocity ( $u < 0.15 \text{ m s}^{-1}$ ), and very stable conditions as indicated by the Obukhov length absolute value ( $|L| < 5 \text{ m}$ ). Fluxes were also discarded for periods when the wind was obstructed by the measurement cabin and other towers ( $270^\circ > \text{wd} < 320^\circ$ , and  $120^\circ > \text{wd} < 160^\circ$ ). Calculated fluxes which were below the minimum detectable flux value for their respective trace gas or aerosol species were discarded.

**Commented [RR12]:** Response to Reviewer #1 - It is our view that the flux uncertainties in this study are not "very large" in respect to previously published studies using the GRAEGOR. The median flux error for NH<sub>3</sub>, for example, was 32%, which is similar to values obtained for measurements made over grassland using the GRAEGOR by Wolff et al. (2010) and Thomas et al. (2009). By inclusion of median flux error values in Tables 4 and 5, we anticipate we can satisfy readers that our flux errors are in the range expected for use of this instrument.

## 3 Results

### 3.1 Meteorology

Figure 2 shows time series of the rainfall, radiation, relative humidity, air temperature and wind speed and direction measured during the campaign. The meteorology splits into two episodes. From 24<sup>th</sup> May to 5<sup>th</sup> June 2016, the dominant prevailing wind direction was north easterly, accompanied by dry and sunny conditions with air temperature displaying a characteristic diel cycle that increased each day. Following a period of cloudier conditions from 6<sup>th</sup> to 10<sup>th</sup> June, the prevailing wind direction shifted to south westerly for the remainder of the measurement period. Conditions became wetter and the diel air temperature amplitude was reduced. Relative humidity remained high throughout the campaign, with only occasional periods  $< 70\%$ , such as 3<sup>rd</sup> – 4<sup>th</sup> June and the 21<sup>st</sup> – 23<sup>rd</sup> June. Wind speed was variable throughout, ranging between 0.05 and 5.87  $\text{m s}^{-1}$ , with a median value of 2.16  $\text{m s}^{-1}$ . During the fertilisation period, the prevailing wind direction was from the SW, and therefore over the South Field, with no precipitation but high ( $> 90\%$ ) relative humidity.

**Commented [RR13]:** Response to Reviewer #1 - We agree with the reviewer that the wording of this section lacks clarity. The inclusion of the determination of instrument error was part of a development to determine flux error. However, as detailed in Section 2.3.4 "Alternatively, the full random error can be characterised experimentally...", the full random error was found through side by side measurements of the GRAEGOR sample boxes. This vagueness is compounded by an error in stating that concentration errors were developed from the calculation of instrument error, rather than from the side-by-side measurements. We will clarify this issue in the revised manuscript

### 3.2 Concentrations of trace gases and water-soluble aerosols

Summary statistics for the concentrations of the trace gas and water-soluble aerosol species measured at both heights 2.4 m during the campaign are presented in Table 2 and Table 3. Median values for the concentrations of water-soluble aerosol

**Commented [RR14]:** Response to Reviewer #1 and #2 - Due to concerns of length and the focus on concentration data, we have amalgamated three tables of concentration data into one. Limits of detection for each species are now contained in a single column, and the statistical data for only one height (2.4 m) is shown. Limits of detection for HNO<sub>3</sub> and SO<sub>2</sub> have also been corrected.

species were similar to those measured in PM<sub>10</sub> at the nearby rural background monitoring site of Auchencorth Moss (Twigg et al., 2015). The time series of the measured aerosol and trace gas concentrations are displayed in Figures 3 and 4, respectively. Data gaps in the time series are due to in-field calibrations, poor chromatograms, or instability in liquid or air flow.

5 Mean concentrations of NO<sub>3</sub><sup>-</sup> were 1.53 µg m<sup>-3</sup> (2.4 m), whereas its gaseous counterpart, HNO<sub>3</sub>, had mean concentrations of 0.19 µg m<sup>-3</sup> (2.4 m). The mean particulate NO<sub>3</sub><sup>-</sup> concentrations were therefore almost 6 times greater than the gaseous HNO<sub>3</sub> counterpart. The same dominance of particulate SO<sub>4</sub><sup>2-</sup> concentrations over gaseous SO<sub>2</sub> concentrations was also observed.

10 Median concentrations of particulate Cl<sup>-</sup> were 0.37 µg m<sup>-3</sup> and 0.36 µg m<sup>-3</sup> at 0.6 m and 2.4 m, respectively. The mean concentrations of Cl<sup>-</sup> were also similar at both heights at 0.89 µg m<sup>-3</sup> and 0.91 µg m<sup>-3</sup>, respectively. Variation in HCl concentrations at each height was more pronounced, with a mean value of 0.16 µg m<sup>-3</sup> at 0.6 m and 0.20 µg m<sup>-3</sup> at 2.4 m, and a median value of 0.12 µg m<sup>-3</sup> at 0.6 m and 0.15 µg m<sup>-3</sup> at 2.4 m. As for particulate NO<sub>3</sub><sup>-</sup> and gaseous HNO<sub>3</sub>, measured particulate Cl<sup>-</sup> concentrations were greater than those of gaseous HCl, by about a factor of 2 at each height.

15 In contrast, NH<sub>3</sub> concentrations were larger than those of particulate NH<sub>4</sub><sup>+</sup>; median concentrations of NH<sub>3</sub> were 1.15 µg m<sup>-3</sup> (2.4 m), while median concentrations of NH<sub>4</sub><sup>+</sup> were 0.64 µg m<sup>-3</sup> (2.4 m). The average concentrations of NH<sub>3</sub> were similar to those reported previously at the same site for the same time of year (Milford, 2004). Similarly, the average concentrations of HONO are higher than those of its particulate counterpart, NO<sub>2</sub><sup>-</sup>, with median concentrations for HONO of 0.04 µg m<sup>-3</sup> (2.4 m) and corresponding concentrations for NO<sub>2</sub><sup>-</sup> 0.02 µg m<sup>-3</sup> (2.4 m) respectively.

20 Maximum concentrations for NH<sub>3</sub> and HONO at 0.6 m were 21.4 µg m<sup>-3</sup> and 0.15 µg m<sup>-3</sup>. At 2.4 m, the maximum concentration for NH<sub>3</sub> and HONO were 13.8 µg m<sup>-3</sup> and 0.12 µg m<sup>-3</sup>. The maximum values at each height occurred at 11:00 on the 13<sup>th</sup> June for NH<sub>3</sub>, one hour after fertilisation of the South Field, and at 13:00 on the 13<sup>th</sup> June for HONO, four hours after fertilisation of the South Field.

25 The time series of measurements presented in Figures 3 and 4 show that both aerosol and trace gas concentrations are affected by prevailing meteorological conditions, with larger concentrations for each species during the drier, warmer period of 28<sup>th</sup> May to 6<sup>th</sup> June, followed by decreased concentrations from 6<sup>th</sup> to 10<sup>th</sup> June when precipitation increased and temperature decreased. Concentrations were lower – except for the peaks in NH<sub>3</sub> and HONO after fertilisation on the 13<sup>th</sup> June - during the  
30 period from 10<sup>th</sup> June to the end of the campaign, concurrent with the change in prevailing wind direction from the NE to the SW.

The concentrations of HNO<sub>3</sub> and SO<sub>2</sub> showed a strong diel cycle (Figure 4) from the 26<sup>th</sup> May to the 9<sup>th</sup> June, with maxima at both measurement heights occurring between 11:00 and 14:00, and minima occurring at night between 03:00 and 06:00. A

similar, but weaker, inverted pattern was exhibited by their particulate counterparts, with  $\text{NO}_3^-$  concentrations at both heights (Figure 3) having maxima between 02:00 and 04:00, and minima between 12:00 and 15:00.

Figure 5 shows the median diel concentrations of  $\text{NH}_3$ , HCl, HONO,  $\text{HNO}_3$  and  $\text{SO}_2$  at 2.4 m prior to fertilisation. The median concentrations of HONO remained above the detection limits of the instrument even during daytime, contrary to its expected photochemistry. While concentrations of HONO peaked during night-time and decreased during the day as incoming solar radiation increases, there remained a detectable concentration of HONO at both heights even for the measurement minima at 15:00. The median diel concentrations for HCl,  $\text{HNO}_3$  and  $\text{SO}_2$  show a shared pattern, with concentrations peaking during the day to reach a maximum between 11:00 to 14:00, followed by a decrease during the night, reaching minima between 02:00 and 04:00. The concentrations of  $\text{NH}_3$  showed little variation across the day. Figure 6 shows the median diel concentrations of  $\text{NH}_4^+$ ,  $\text{Cl}^-$ ,  $\text{NO}_3^-$  and  $\text{SO}_4^{2-}$  at 2.4 m prior to fertilisation. The median diel concentrations of  $\text{NH}_4^+$  reach a minimum at 16:00, with a maximum at 02:00. The concentrations of  $\text{NO}_3^-$  show a similar pattern of early morning median maxima (04:00) and afternoon minima (13:00). The median diel  $\text{SO}_4^{2-}$  concentrations had maxima at midnight and a minimum at 16:00. The  $\text{Cl}^-$  concentrations reached a maximum at 03:00 and a minimum at 13:00; however, the upper quartile range was high across all hours, with the maximum concentration of  $7.88 \mu\text{g m}^{-3}$  recorded at 03:00 (median at this time is  $0.5 \mu\text{g m}^{-3}$ ).

### 3.3 Fluxes, Deposition Velocities, and Canopy Resistance

#### 3.3.1 Fluxes of trace gases

Figure 7 shows the time series of the fluxes for the trace gases measured during the campaign. Data gaps are due to either absent data points (unpaired concentrations), or periods where data were filtered (refer to [Section 2.3.4](#)).

Bi-directional fluxes were present for both  $\text{NH}_3$  and HONO, with emission events for each gas occurring during the period of fertilisation of the South Field. For the other trace gases – HCl,  $\text{HNO}_3$  and  $\text{SO}_2$  – the flux was uni-directional, with deposition occurring throughout the campaign. The deposition for HCl,  $\text{HNO}_3$  and  $\text{SO}_2$  varied, with larger deposition fluxes occurring during the warmer, drier periods, particularly during the period 1<sup>st</sup> - 8<sup>th</sup> June, and smaller deposition fluxes close to zero during the colder, wetter period at the end of the campaign (15<sup>th</sup> - 24<sup>th</sup> June).

Summary statistics for the trace gas fluxes, deposition velocities, theoretical maximum deposition velocities, and canopy resistance values are presented in Table 42. The maximum  $\text{NH}_3$  flux was  $+1460 \text{ ng m}^{-2} \text{ s}^{-1}$ , recorded at 12:00 on the 13<sup>th</sup> June, three hours after fertilisation. The mean flux for  $\text{NH}_3$  was  $+15.24 \text{ ng m}^{-2} \text{ s}^{-1}$ , suggesting that emission was the predominant flux for  $\text{NH}_3$  during this campaign. For all other gases, the mean flux values were negative, suggesting that deposition was the net flux process overall. However, a maximum flux for HONO of  $+4.92 \text{ ng m}^{-2} \text{ s}^{-1}$ , recorded five hours after fertilisation, highlights the bi-directional flux pattern for HONO during the campaign. The maximum HONO flux measured here was

particularly large. Nitrous acid emissions have previously been reported post fertilisation of grassland using cattle slurry at the same field site ranging from +1.0 to +1.5 ng m<sup>-2</sup> s<sup>-1</sup> (Twigg et al. 2011). Table 2 also shows the median relative flux error, the typical flux detection limits ( $F_{LOD}$ ) and the fraction of 60-minute flux values that exceed the  $F_{LOD}$  of that period, based on actual concentration and turbulence. It should be noted that the uncertainty of the campaign averages is much smaller as random uncertainty reduces with the square root of the number of observation that enter the calculation of the ensemble average (e.g. Langford et al., 2015).

Median diel cycles for the deposition velocity and calculated theoretical maximum deposition velocity for the trace gases HCl, HONO, HNO<sub>3</sub> and SO<sub>2</sub> are shown in Figure 8. The calculation of median diel values for trace gas deposition velocities and canopy resistances excludes the period of flux divergence which occurred during fertilisation. The diurnal deposition velocities for HCl and HNO<sub>3</sub> were very close to the calculated maximum deposition velocities, which is expected as a result of their reactivity and high water solubility. The deposition velocity for SO<sub>2</sub> is near the theoretical maximum during night-time but is lower during daytime. The deposition velocity for HONO was consistently lower than its theoretical maximum throughout the entire day. While median values for the  $V_d$  for HNO<sub>3</sub> are close to the values for  $V_{max}$ , deposition velocities were recorded that exceeded their corresponding theoretical maximum. While most exceedances fall within the uncertainty range of the measurement, a maximum deposition velocity of 56.8 mm s<sup>-1</sup> was recorded at 14:00 on the 13<sup>th</sup> June, four hours after fertilisation.

### 3.3.2 Fluxes of water-soluble aerosol components

The measured surface fluxes of the aerosol species Cl<sup>-</sup>, NO<sub>3</sub><sup>-</sup>, SO<sub>4</sub><sup>2-</sup> and NH<sub>4</sub><sup>+</sup> are shown in Figure 9, as well as the summary statistics for the fluxes and deposition velocities in Table 53. A large data gap in NH<sub>4</sub><sup>+</sup> fluxes from 31<sup>st</sup> May to 10<sup>th</sup> June 2016 was due to NH<sub>4</sub><sup>+</sup> only being measured at one height on account of unreliable data for NH<sub>4</sub><sup>+</sup> at the lower height of 0.6 m.

Pre-fertilisation, all aerosol species exhibited deposition fluxes. The deposition fluxes were larger during the drier, warmer period from 31<sup>st</sup> May to 6<sup>th</sup> June, and close to zero during the wetter conditions at the end of the campaign. An important exception was the emission of NH<sub>4</sub><sup>+</sup> and NO<sub>3</sub><sup>-</sup> from 13:00 on the 13<sup>th</sup> June to 02:00 on the 14<sup>th</sup> June, starting 4 hours after fertilisation of the South Field.

Summary statistics for the fluxes and deposition velocities for the aerosol species measured are shown in Table 53. As for the trace gases, the median deposition velocities for the aerosol species excludes the period of flux divergence which occurred during fertilisation. The maximum flux for NH<sub>4</sub><sup>+</sup> of +18.16 ng m<sup>-2</sup> s<sup>-1</sup> was recorded at 16:00 on the 13<sup>th</sup> June, seven hours after fertilisation of the South Field. Similarly, the maximum flux for NO<sub>3</sub><sup>-</sup> (+31.84 ng m<sup>-2</sup> s<sup>-1</sup>) was also recorded soon after fertilisation, at 18:00 on the 13<sup>th</sup> June. Overall, however, the mean fluxes for all aerosol species were negative, confirming a predominant net deposition to the surface.

**Commented [RR15]:** Response to Reviewer #1 - The reviewer raises an important point that was considered during flux calculations, but which was not included in the manuscript. As outlined by Thomas et al. (2009), it is possible to calculate the minimum flux that the GRAEGOR can measure for each species, effectively providing a limit of detection for flux measurements. Fluxes presented have been filtered using these values, but discussion of their development, beyond mentioning that fluxes were filtered according to these values was not included, nor were they included in Tables 4 and 5. We will include a brief discussion of calculating this value in the Methods section of the revised manuscript, which, together with inclusion of minimum detectable flux values for each species in Tables 4 and 5, should resolve this issue.

**Commented [RR16]:** Response to Reviewer #2 - We have also taken care to exclude the period of flux divergence from the statistical analysis of canopy resistance and deposition velocity for the entirety of the campaign. This latter point was perhaps not clear in the paper and we will add text to stress this exclusion

**Commented [RR17]:** Response to Reviewer #2 - We have also taken care to exclude the period of flux divergence from the statistical analysis of canopy resistance and deposition velocity for the entirety of the campaign. This latter point was perhaps not clear in the paper and we will add text to stress this exclusion

### 3.4 HONO and NH<sub>3</sub> GRAEGOR measurement comparisons with LOPAP and QCL

#### 3.4.1 HONO Comparison Study between GRAEGOR and LOPAP

A comparison of HONO measurements from the GRAEGOR and two LOPAP instruments was conducted from the 26<sup>th</sup> May to the 6<sup>th</sup> June to investigate the potential artefacts in the WRD method used by the GRAEGOR. The LOPAPs were part of a study to investigate the mechanisms controlling HONO fluxes over managed grassland, including investigating the potential ground sources of HONO, details of which are presented in Di Marco *et al.* (in preparation). A series of simple linear regression analyses was conducted to determine the level of agreement between the concentrations of HONO measured by each sample box of the GRAEGOR and each of the LOPAPs. The two LOPAP instruments were operated at the two heights of 0.6 m and 2.0 m (hereafter referred to as LOPAP (0.6 m) and LOPAP (2.0m) respectively). In all comparisons, the GRAEGOR recorded a higher concentration of HONO than either of the LOPAPs. The linear regressions suggest that there is a consistent offset in all GRAEGOR concentrations, varying between 0.01  $\mu\text{g m}^{-3}$  and 0.02  $\mu\text{g m}^{-3}$ . In comparisons between the GRAEGOR Sample Box 1 at 0.6 m and both LOPAPs, the linear concentration relation for HONO varies from 0.92 to 0.97. The comparisons between the GRAEGOR Sample Box 2 (2.4 m) and the LOPAPs suggest that the linear concentration relation for HONO is 1.06 and 1.01 for LOPAP (2.0 m) and LOPAP (0.6m) respectively. In all comparisons, however, there exists a constant concentration offset, which results in a constant higher concentration recorded by both GRAEGOR sample boxes. The closest agreement is between GRAEGOR Sample Box 2 (set at height 2.4 m) and LOPAP (2.0 m), where the HONO concentration recorded by the GRAEGOR Sample Box 2 (2.4 m) is 1.06 that of LOPAP(2.0 m). This comparison also has the best statistical agreement, with an  $R^2$  value of 0.67, suggesting a reasonable agreement between the GRAEGOR Sample Box 2 and LOPAP (2.0 m) measurements.

#### 3.4.2 NH<sub>3</sub> Comparison Study between GRAEGOR and QCL

On the 7<sup>th</sup> June, a QCL with inlet at height 1.6 m was installed at the Easter Bush site and took measurements of NH<sub>3</sub> from 19<sup>th</sup> June to 7<sup>th</sup> August. Three days of concurrent NH<sub>3</sub> measurements taken by the GRAEGOR and the QCL were recorded in the period 21<sup>st</sup> – 24<sup>th</sup> June. The time series of the NH<sub>3</sub> measurements by each instrument are shown in Figure 10(a). An averaged NH<sub>3</sub> concentration at 1.0 m ( $\chi$  (1 m)) taken by the GRAEGOR was compared with the NH<sub>3</sub> concentrations taken by the QCL in a simple linear regression analysis, displayed in Figure 10(b). The linear regression shows that the GRAEGOR recorded a factor 1.22 higher concentrations of NH<sub>3</sub> than the QCL, with an associated  $R^2$  value of 0.76. However, the number of concurrent measurements is small, with only 41 shared hourly measurement values across three days and a period of 19 continuous hours missing between 02:00 and 23:00 of the 23<sup>rd</sup> June.

## 4 Discussion

### 4.1 Ion Balance

The ion balance for the hourly-measured cation ( $\text{NH}_4^+$ ) and anion ( $\text{NO}_3^-$  and  $\text{SO}_4^{2-}$ ) aerosol species pre-fertilisation is shown in Figure 11. Values are shown as molar equivalent concentration, derived from aerosol mass concentrations converted to molar concentrations and subsequently multiplied by their charge.  $\text{Cl}^-$  charge was not included, under the assumption that it would be entirely associated, in the form of sea salt, with  $\text{Na}^+$  which was not measured by the GRAEGOR. While the correlation between cation and anion species is very good ( $R^2 = 0.71$ ), the linear regression suggests a deficit of  $\text{NH}_4^+$ , suggesting that some of the  $\text{NO}_3^-$  and/or  $\text{SO}_4^{2-}$  was balanced by ions other than  $\text{NH}_4^+$ . A likely candidate is  $\text{Na}^+$ : some of the  $\text{SO}_4^{2-}$  is likely to have represented sea-salt  $\text{SO}_4^{2-}$  and some  $\text{NaNO}_3$  is formed by reaction of  $\text{NaCl}$  with  $\text{HNO}_3$ . Figure 11 is coloured by  $\text{Cl}^-$  concentration, and periods of anion excess tend to be associated with elevated  $\text{Cl}^-$  concentrations.

The formation of  $\text{NaNO}_3$  through the reaction of  $\text{HNO}_3$  or  $\text{NO}_x$  with sea salt has been previously observed in coastal sites (Andreae et al., 1999, 2000; Bardouki et al., 2003; Dasgupta et al., 2007)(Kutsuna & Ibusuki, 1994), and within the UK and Ireland, where the interaction with marine air with polluted air masses at coastal sites was shown to significantly shift the aerosol  $\text{NO}_3^-$  to the coarse mode (Yeatman et al., 2001; Twigg et al., 2015). Scavenging of atmospheric  $\text{H}_2\text{SO}_4$ , formed from  $\text{SO}_2$  (O'Dowd and de Leeuw., 2007), by sea salt may also be occurring, which would also shift some of the  $\text{SO}_4^{2-}$  from the fine to the coarse mode.

### 4.2 Deposition velocities and fluxes of water-soluble aerosol and trace gas species

#### 4.2.1 Fluxes of water-soluble aerosols and trace gases

Fluxes of  $\text{SO}_4^{2-}$  and  $\text{Cl}^-$  throughout the campaign were unidirectional deposition. However, during the fertilisation period of the South Field, bidirectional fluxes of  $\text{NH}_4^+$  and  $\text{NO}_3^-$  were observed. Prior to fertilisation these species were deposited to the site. An apparent emission flux of  $\text{NO}_3^-$  is consistent with the possibility of  $\text{NH}_4\text{NO}_3$  formation above grassland suggested by the divergence of  $\text{HNO}_3$   $V_4$  from  $V_{\text{max}}$  (Nemitz et al., 2009b) in the presence of high concentrations of  $\text{NH}_3$  near the surface. Concentrations of  $\text{NH}_3$  peak at  $21.4 \mu\text{g m}^{-3}$  on the 13<sup>th</sup> June, 11:00, which occurs three hours before peak  $\text{HNO}_3$   $V_4$  and 7 hours prior to the apparent peak in emissions of  $\text{NO}_3^-$  at 18:00.

Fluxes for the trace gases were bi-directional for  $\text{NH}_3$  and HONO, with deposition for all other species measured. Emissions of  $\text{NH}_3$  and HONO occurred throughout the campaign, with HONO emissions particularly present during the early morning. Both species reached peak emissions soon after fertilisation. Increases in atmospheric  $\text{NH}_3$  concentration and emissions of  $\text{NH}_3$  resulting from the application of solid urea fertiliser has been previously established (Akiyama et al., 2004; Sommer and Hutchings, 2001), with losses from volatilisation increased if the urea pellets are poorly mixed into the soil and if conditions are dry and warm. While conditions prior to the fertilisation event were cool, temperatures increased quickly throughout the

day, peaking at 19.2 °C at 13:00, four hours after fertilisation. Volatilisation was likely exacerbated by the dry conditions throughout the 13<sup>th</sup> June. The increase in concentration and upward flux of NH<sub>3</sub> provides the source for the formation of NH<sub>4</sub>NO<sub>3</sub> in the presence of HNO<sub>3</sub>. The mechanisms of the HONO emission fluxes are not discussed here but can be found in Di Marco *et al.* (in preparation).

#### 5 4.2.2 Aerosol deposition velocities

Deposition velocities for NO<sub>3</sub><sup>-</sup> reached a maximum value of 9.8 mm s<sup>-1</sup> during daytime, and a minimum of 0.2 mm s<sup>-1</sup> outside the period of apparent emission fluxes at night. A similar pattern was observed for sulfate, which reached a maximum value of 9.5 mm s<sup>-1</sup> during daytime and a minimum value, outside of apparent emission events, of 0.15 mm s<sup>-1</sup> during night. Median V<sub>d</sub> values for NO<sub>3</sub><sup>-</sup> and SO<sub>4</sub><sup>2-</sup> were 1.52 mm s<sup>-1</sup> and 1.45 mm s<sup>-1</sup>, respectively. For Cl<sup>-</sup>, the median V<sub>d</sub> was 3.14 mm s<sup>-1</sup>. The deposition velocities for SO<sub>4</sub><sup>2-</sup> were larger than those previously observed and derived for accumulation mode particles from theoretical considerations (Petroff *et al.*, 2008). For sulfate in the fine (<0.1 μm diameter) range, Allen *et al.* (1991) recorded a mean value of 1 mm s<sup>-1</sup> for deposition velocity over short grass, similar to observations made by Gallagher *et al.* (2002) who reported a mean value of 0.9 mm s<sup>-1</sup>.

15 The dry deposition of particles can be modelled using a process-orientated approach, which describes the deposition velocity as a function of particle size based on removal mechanisms acting within the vegetation canopy, such as Brownian diffusion, impaction, interception and sedimentation (Slinn and Slinn, 1980; Davidson *et al.*, 1982; Slinn, 1982). The models predict that for particles >0.1 μm in diameter deposition velocity increases with increasing particle size. Vong *et al.* (2004) recorded deposition velocities of greater than 2 mm s<sup>-1</sup> for PM<sub>10</sub> particles over grassland. If the sulfate and chloride were in particularly  
20 coarse particles, deposition velocities would potentially be skewed towards a higher deposition velocity.

Secondary ammonium compounds are typically found in the accumulation mode (0.1 to 1 μm), while seasalt is found in super-micron particles (Myhre *et al.*, 2006). Although measurements of particle size were not made during this campaign, measurements of aerosol species (including Cl<sup>-</sup> and SO<sub>4</sub><sup>2-</sup>) in the PM<sub>2.5</sub> and PM<sub>10</sub> size fractions were taken by a two-channel Monitor  
25 for Aerosols and Gases in Ambient Air (MARGA, Applikon B.V, The Netherlands) instrument located at Auchencorth Moss, 12 km south west of Easter Bush. [Aerosol concentration data was taken from an online database of MARGA measurements \(DEFRA, 2018\).](#) Agreement between MARGA and GRAEGOR aerosol concentrations were excellent (with correlations for SO<sub>4</sub><sup>2-</sup> with R<sup>2</sup> = 0.95, and for Cl<sup>-</sup> with R<sup>2</sup> = 0.91 between MARGA PM<sub>10</sub> and GRAEGOR TSP). As proxy for a particle size measurement, the proportion of PM<sub>2.5</sub> to PM<sub>10</sub> was used, with a lower proportion of PM<sub>2.5</sub> indicating a greater proportion of  
30 coarse aerosol, and a corresponding larger deposition velocity based on process-orientated modelling. To a first-order approximation, particle deposition velocities scale with u\* (Pryor *et al.*, 2008). Figure 12 shows plots of the normalised deposition velocities (V<sub>d</sub> / u\*) against the fraction of the PM<sub>10</sub> mass contained in PM<sub>2.5</sub> at Auchencorth Moss (f<sub>PM2.5</sub> = PM<sub>2.5</sub>/PM<sub>10</sub>) for nitrate (a), sulfate (b) and chloride (c).

**Commented [RR18]:** Response to Reviewer #1 - The processed and ratified MARGA data are publicly available online at [https://uk-air.defra.gov.uk/data/data\\_selector](https://uk-air.defra.gov.uk/data/data_selector) from which concentrations of any of the species measured by the MARGA can be selected. We will add the references and online resources to the paper.

Response to Reviewer #2 - The processed and ratified MARGA data are publicly available online at [https://uk-air.defra.gov.uk/data/data\\_selector](https://uk-air.defra.gov.uk/data/data_selector) from which concentrations of any of the species measured by the MARGA can be selected. We will add the references and online resources to the paper.

While the dynamic range of  $f_{PM_{2.5}}$  varied between compounds, third-order polynomial curves consistently describe the relation between the proportion of  $PM_{2.5}$  to overall PM and the normalised  $V_d$  for nitrate, sulfate and chloride, suggesting – in line with Slinn (1982) – that deposition velocity increases strongly with increasing particle size above  $0.1 \mu m$  particle diameter. However, the relationship – although statistically significant – shows significant variability, which may be due to measurement uncertainty, but might also reflect the additional effect of atmospheric stability on particle fluxes (e.g. Wesely et al., 1985; Petroff et al., 2008) or differences in the size distribution between the Auchencorth and Easter Bush measurement sites. It must be stressed that the proportion of  $PM_{2.5}$  to  $PM_{10}$  is a proxy measurement for particle size and can only differentiate the proportions of aerosol of diameter less than or greater than  $2.5 \mu m$ .

By contrast, the median deposition velocity of  $0.37 \text{ mm s}^{-1}$  for  $NH_4^+$  was much smaller and within the range of previous measurements of dry deposition velocities of accumulation mode particles to grassland. The average  $f_{PM_{2.5}}$  for  $NH_4^+$  recorded was 96%, compared to 78% for  $NO_3^-$  and 86% for  $SO_4^{2-}$ , suggesting that virtually all of the  $NH_4^+$  measured was contained in fine particles, within the measurement error. The average normalised deposition velocity ( $V_d/u_w$ ) of  $NH_4^+$  of 0.04 was in the range of the values for the other compounds evaluated at  $f_{PM_{2.5}} = 100\%$ .

Thus, the relatively high deposition velocities for  $Cl^-$ ,  $NO_3^-$  and  $SO_4^{2-}$  (compared with  $NH_4^+$ ) are a result of some of these compounds being contained in coarse aerosol. This is consistent with the ion balance (Fig. 11), which suggests that some of these compounds are balanced by seasalt  $Na^+$ , which is found mostly in the coarse fraction.

It should be noted that the increase in  $V_d$  with increasing contribution of coarse aerosol only accounts for the size-dependence of the processes of impaction and interception. As a non-turbulent process, gravitational sedimentation is not reflected in micrometeorological flux measurements and the sedimentation velocity would need to be added to the deposition velocity derived here.

#### 4.2.3 Trace gas deposition velocities

Median diel deposition velocities for  $HNO_3$  and  $HCl$  closely matched the theoretical maximum deposition velocities within the uncertainty of the measurement (Fig. 8), which closely conforms to their expected physico-chemical behaviour. Both  $HNO_3$  and  $HCl$  are reactive and highly water soluble, and consequently it is expected that their deposition velocities should equal the theoretical maximum, and that the canopy resistance for these species should be equal to zero (Dollard et al., 1987; Muller et al., 1993). The close agreement between  $V_d$  and  $V_{max}$  during most of the campaign suggests that chemistry is not affecting the fluxes and that the standard aerodynamic gradient method is therefore applicable. However, significant deviations of the calculated deposition velocity from the theoretical maximum for  $HNO_3$  exist:  $R_c$  values for  $HNO_3$  were particularly large 40 hours after fertilisation, from the 15<sup>th</sup> June to the 16<sup>th</sup> June, when the mean  $R_c$  value was  $14.8 \text{ s m}^{-1}$ . Conversely, there were

**Commented [RR19]:** Response to Reviewer #1 – “Finally, the good agreement between expected and measured deposition velocities for  $HNO_3$  and  $HCl$  may be taken as independent evidence (though not proof) of the high quality of the measured fluxes.”

periods when the  $V_d$  for  $\text{HNO}_3$  exceeded the  $V_{\max}$ , such as on the 13<sup>th</sup> June at 13:00 hours, when  $V_d$  for  $\text{HNO}_3$  was recorded as  $56.8 \text{ mm s}^{-1}$  compared with a calculated maximum of  $17.5 \text{ mm s}^{-1}$ .

5 Reductions in  $V_d$  for  $\text{HNO}_3$  (or in other words a non-zero  $R_c$ ) have been linked to ground-level sources or non-zero vapour pressures of  $\text{HNO}_3$  over nitrate-containing aerosol (particularly,  $\text{NH}_4\text{NO}_3$ ), which may evaporate from aerosol within the air space below the measurements or previously deposited to leaf surfaces (Brost et al., 1988; Kramm and Dlugi, 1994; Nemitz et al., 2000a, 2004). By contrast, values of  $V_d$  for  $\text{HNO}_3$  that exceed the theoretical maximum could suggest the presence of an additional sink for  $\text{HNO}_3$ , which would potentially arise as the result of  $\text{NH}_3$  reactions with  $\text{HNO}_3$  to form  $\text{NH}_4\text{NO}_3$  (Nemitz et al., 2000b; van Oss et al., 1998). The higher  $V_d$  values for  $\text{HNO}_3$  during the fertilisation period, followed by a higher  $R_c$  value 40 hours afterwards, could suggest the formation of  $\text{NH}_4\text{NO}_3$  immediately following fertilisation followed by its volatilisation soon after. Indeed, the exceedance of  $V_{\max}$  coincided with upward fluxes of  $\text{NH}_4^+$  and  $\text{NO}_3^-$  (Fig. 9) and this suggests that during the period after fertilisation, the increase in  $\text{NH}_3$  concentration lead to an exceedance of the equilibrium vapour pressures of  $\text{NH}_4\text{NO}_3$  near the ground, resulting in partitioning of  $\text{NH}_3$  and  $\text{HNO}_3$  into the aerosol phase. This would have constituted an additional airborne sink for  $\text{HNO}_3$  ( $V_d > V_{\max}$ ) as well as a source (apparent emission) for  $\text{NH}_4^+$  and  $\text{NO}_3^-$  as previously reported by Nemitz et al. (2009).

It should be noted that during this period the aerodynamic gradient method does not derive accurate fluxes because the condition of flux conservation is not met (Wolff et al., 2010), and this period has therefore not been included in the diel cycles and summary statistics presented above.

20 By contrast, fluxes of total ammonium ( $\text{tot-NH}_4^+ = \text{NH}_4^+ + \text{NH}_3$ ) and total nitrate ( $\text{tot-NO}_3^- = \text{NO}_3^- + \text{HNO}_3$ ) would be conserved, as the effect of gas-particle interactions are not considered, and their assessment provides additional information on the processes occurring during periods when fluxes are not conserved with height.

25 The time series for  $\text{tot-NO}_3^-$  and  $\text{tot-NH}_4^+$  fluxes are shown in Figure 13. Prior to the fertilisation event on the 13<sup>th</sup> June, the fluxes for  $\text{tot-NO}_3^-$  were universally depositional to the surface, while fluxes of  $\text{tot-NH}_4^+$  were bi-directional with significant variation. However, six hours after fertilisation, a significant emission event of  $\text{tot-NO}_3^-$  was observed lasting for six hours. Interestingly, this indicates that the apparent  $\text{NO}_3^-$  emission during this period (Fig. 9) exceeded the measured deposition of  $\text{HNO}_3$ , and that there must have been a net source of  $\text{NO}_3^-$  at the surface during this period. Upward fluxes have previously been reported in the literature where it was attributed to the volatilisation of  $\text{NH}_4\text{NO}_3$  from leaf surfaces (Nefitel et al., 1996) or alkyl nitrate chemistry (Farmer and Cohen, 2008). Primary emissions of  $\text{HNO}_3$  This could arise from the heterogeneous reaction of  $\text{NO}_2$  with water (Harrison, 1996):



**Commented [RR20]:** Response to Reviewer #2 - We have also taken care to exclude the period of flux divergence from the statistical analysis of canopy resistance and deposition velocity for the entirety of the campaign. This latter point was perhaps not clear in the paper and we will add text to stress this exclusion

Kleffman (2007) suggests that HNO<sub>3</sub> could be formed by the reduction of NO<sub>2</sub> on organic sources of humic acid, a process that would also lead to the production of HONO. The formation of HNO<sub>3</sub> inferred from observations coincided with emissions of HONO post-fertilisation. However, as discussed previously, this reaction is slow, and while possibly contributing to some of the observed HONO emission, may not be able to account for the majority of observed emissions.

5

A second potential pathway is the emission of HONO from the soil. As described by Scharko et al. (2015), the oxidation of ammonium by microbes in soils with high nitrification rates can lead to biogenic emissions of HONO. The addition of urea to the agricultural soil at Easter Bush would lead to an increase in soil NH<sub>4</sub><sup>+</sup> concentrations and subsequently, through oxidation by soil microbes, the observed emission of HONO. Further discussion of the sources of HONO emissions at Easter Bush will be described in a future paper by Di Marco *et al.* (in preparation).

10

### 4.3 Daytime Source of HONO

As shown in Figure 5, the median diel concentrations for HONO recorded by the GRAEGOR at 2.4 m do not drop below the detection limits of the instrument, determined to be 30 ng m<sup>-3</sup> from calibrations carried out during the campaign. This is contrary to what would be expected based solely on the photolysis rate of HONO, which would suggest that, after accumulation of HONO during night-time, rapid photolysis should reduce concentrations to below the detectable levels for measurement during early morning (Pagsberg et al., 1997). As measurement approaches have improved over the past 10 years, a growing number of measurements have revealed non-negligible HONO daytime concentrations at rural (Acker et al., 2006; Su et al., 2008; Sörgel et al., 2011), agricultural (Laufs et al., 2017) and urban (Lee et al., 2016) sites, including previous studies at the Easter Bush site (Twigg et al., 2011). Details on the discussion of a potential daytime source of HONO are further discussed in Di Marco *et al.* (in preparation).

15

20

### 4.4 Comparison of GRAGOR with other instrumentation

#### 4.4.1 Comparison of nitrous acid measurement between GRAEGOR and LOPAP

The comparison between the LOPAPs and the GRAEGOR revealed that both sample boxes of the GRAEGOR measured higher HONO concentrations than the LOPAP, principally due to the presence of a constant concentration offset of 0.01 to 0.02 µg m<sup>-3</sup> of HONO. Previous comparisons of measurements of HONO have been between the wet annular rotating denuder (WRD), as used in the GRAEGOR, and optical absorption techniques, primarily differential optical absorption spectroscopy (DOAS) instruments. In those comparisons, it has been found that HONO measurements by WRD, particularly during daytime and at low concentrations, tend to be significantly higher than DOAS measurements (Appel et al., 1990). By comparison, the LOPAP shows good agreement in HONO measurements with the DOAS (Kleffman et al., 2006), as the DOAS method is a molecule specific method and the LOPAP method measures any potential NO<sub>x</sub> artefact.

25

30

The higher concentrations recorded by the GRAEGOR can be explained by the presence of chemical interferences that occur on the inlet, at the air/liquid interface and within the sampling solution. As the WRD uses a liquid film to sample HONO, and as HONO can form heterogeneously on such surfaces, overestimation of HONO can occur. Furthermore, interferences by chemical reactions of NO<sub>2</sub> with hydrocarbons within the sampler can lead to a further interference (Gutzwiller et al., 2002), particularly in proximity to diesel emissions. It has also been shown that in high-alkalinity sampling solutions, mixtures of SO<sub>2</sub> and NO<sub>2</sub> can add a further interference to measurements (Spindler et al., 2003). Finally, photolytically induced artefacts can be introduced in the sampling lines that connect the GRAEGOR sampling box to the detector unit (Kleffman and Wiesen, 2008). The LOPAP, which is also a wet chemistry-based instrument, is designed to minimise the chemical interferences and artefacts that can be introduced in other wet chemistry instruments.

A comparison between daytime (06:00 to 18:00) GRAEGOR HONO concentrations and LOPAP HONO concentrations found only a slightly greater difference than the comparison between night time (19:00 to 05:00) concentrations recorded by the GRAEGOR and LOPAP. While previous comparisons between the DOAS and the WRD found that daytime concentrations measured by the WRD were higher than the DOAS compared to night-time measurements, these studies were generally conducted in urban areas where both HONO and NO<sub>x</sub> concentrations were high (Febo et al, 1996), in contrast to the low concentrations at Easter Bush. The implementation of thermal insulation material around the GRAEGOR sampling lines may have also reduced the influence of photolytic artefacts in exposed sampling lines during the day, which would have elevated daytime HONO measurements recorded by the GRAEGOR.

Spindler et al. (2003) developed the following quantification of the chemical artefact produced by the mixing of NO<sub>2</sub> and SO<sub>2</sub> in highly alkaline sampling solutions for HONO measurements in their investigation of SO<sub>2</sub> and NO<sub>2</sub> chemical interference, with all concentrations measured in ppb.

$$[\text{HONO}]_{\text{artefact}} = 0.0056[\text{NO}_2] + 0.0022 \text{ ppb}^{-1}[\text{NO}_2][\text{SO}_2] \quad (912)$$

The first term describes the heterogeneous formation of NO<sub>2</sub> with water alone, and the second describes the aqueous-phase reaction of NO<sub>2</sub> and SO<sub>2</sub>. Using measurements of SO<sub>2</sub> and NO<sub>2</sub> concentrations ~~taken at a long term monitoring site 300 m south east of the Easter Bush site,~~, the HONO artefact for the period of the GRAEGOR-LOPAP comparison was calculated and subtracted from the HONO concentrations recorded by the GRAEGOR. A linear regression between the concentrations recorded by GRAEGOR Sample Box 2 and LOPAP (2.0 m), which had the best agreement without artefact reduction, indicated better agreement after the correction for the artefact ( $\text{GRAEGOR}_{\text{artefact}}(2.4 \text{ m}) = 1.02 * \text{HONO}(\text{HONO}(\text{LOPAP}(2.0 \text{ m})))$ , intercept =  $5 \times 10^{-3} \mu\text{g m}^{-3}$ ,  $R^2 = 0.72$ ). Coefficient values were altered to produce the best possible agreement between GRAEGOR and LOPAP HONO values, arriving at a final artefact quantification of:

$$[\text{HONO}]_{\text{artefact}} = 0.0090[\text{NO}_2] + 0.0034 \text{ ppb}^{-1}[\text{NO}_2][\text{SO}_2] \quad (4013)$$

Use of these altered coefficients further reduced the offset in GRAEGOR HONO measurements, but also reduced the statistical agreement between GRAEGOR and LOPAP HONO measurements ( $\text{GRAEGOR}_{\text{artefact}(2.4 \text{ m})} = 0.98 \cdot \text{HONO}(\text{HONO}(\text{LOPAP}(2.0 \text{ m})))$ , intercept =  $2 \times 10^{-3} \mu\text{g m}^{-3}$ ,  $R^2 = 0.57$ ). Figure 14 shows the results of these analyses, with the linear regression between GRAEGOR Sample Box 2 (2.4 m) and LOPAP (2.0 m) without the artefact reduction applied to GRAEGOR Sample Box 2 (2.4 m) HONO concentrations, with Spindler's artefact reduction, and with the modified Spindler's artefact reduction. While the agreement between the LOPAP and GRAEGOR is improved by the introduction of an artefact reduction value, it does not fully close the gap even with altered coefficient values, with a constant concentration offset still present in measurements. The possibility that a further artefact is introduced from  $\text{NO}_2$  mixing with hydrocarbons would require further investigation, with concurrent measurements of hydrocarbons.

To determine if the HONO concentration offset in the GRAEGOR measurements impacted upon the measurements of HONO flux, a comparison between the HONO flux values derived from GRAEGOR and LOPAP measurements was conducted. Concurrent fluxes of HONO derived from LOPAP and GRAEGOR measurements exist for 72 hourly measurements, from the 26<sup>th</sup> May – 6<sup>th</sup> June. Figure 15 shows (a) the full time series of concurrent HONO flux values derived from GRAEGOR and LOPAP measurements and (b) a scatter plot of GRAEGOR against LOPAP HONO flux values. Overall, GRAEGOR HONO fluxes are biased towards deposition, with greater deposition values and lesser emission values compared to concurrent LOPAP values. This pattern would be consistent with the concept of an artefact formation dependent upon  $\text{SO}_2$  and  $\text{NO}_2$ .  $\text{SO}_2$  fluxes were unidirectionally depositional at Easter Bush during the campaign as measured by the GRAEGOR. Deposition of  $\text{SO}_2$  would lead to greater formation of artefact within the sample box set at a higher height, which is consistent with comparisons of HONO concentrations between each sample box of the GRAEGOR and each LOPAP instrument. In turn, this would lead to a bias in HONO flux values, resulting in a skew towards deposition. It should be noted that the sample size of concurrent measurements of HONO flux from GRAEGOR and LOPAP measurements is limited ( $n = 72$ ).

#### 4.4.2 Comparison of ammonia measurements with GRAEGOR and QCL

The comparison between the GRAEGOR and QCL found that, while there was reasonable agreement between the instruments, the GRAEGOR measured somewhat higher  $\text{NH}_3$  concentrations than the QCL, by a factor of 1.2. Due to lack of ancillary micrometeorological data during this campaign, the short overlap in measurements, and necessary filtering of unreliable data, there are too few concurrent measurements (15 hours) of flux between the QCL and the GRAEGOR for a reliable comparison. There are also only 41 hours of concurrent concentration measurements between the two instruments, which overlapped with a period of low  $\text{NH}_3$  concentrations.

A similar comparison between a WRD system (the Ammonia Measurement by Annular Denuder with Online Analysis, AMANDA) and the QCL system was conducted at the same site in 2004 and 2005 by Whitehead et al. (2008). This comparison

also found that the WRD system measured higher concentrations of  $\text{NH}_3$  compared to the QCL, but at a far greater factor of 1.67. This difference was particularly pronounced during periods of low  $\text{NH}_3$  concentrations, with better agreement recorded during a fertilisation and cutting event that occurred during that study. The older (pumped) QCL used during the earlier campaign did not derive its concentrations from first principles, in contrast to the QCL used during the comparison with the GRAEGOR reported here, which should be within 3% of the absolute value without further calibration, according to the manufacturer. An inter-comparison between eleven different measurement techniques for  $\text{NH}_3$  – including the AMANDA and two QCL instruments (the DUAL-QCLAS and the compact-QCLAS) – was conducted at the Easter Bush site in 2008 (von Bobrutski et al., 2011). While good statistical agreement was found in linear regression between the AMANDA and both QCL instruments for  $\text{NH}_3$  concentrations throughout the entirety of the campaign ( $R^2 = 0.92$  and  $R^2 = 0.97$  for the compact-QCL and DUAL-QCLAS, respectively), there was less agreement between the instruments during periods of low (<10 ppb)  $\text{NH}_3$  concentrations ( $R^2 = 0.81$  and  $R^2 = 0.52$  for the compact-QCL and DUAL-QCLAS respectively). During periods of low concentration, the QCL systems also underestimated  $\text{NH}_3$  concentrations compared to the AMANDA.

Any errors in the GRAEGOR's internal  $\text{NH}_3$  calibration system are unlikely to have an effect at low  $\text{NH}_3$  concentrations. As a test, the calibration values obtained from all the internal calibration checks which were carried out through the campaign (total calibrations = 5) were used to calculate the  $\text{NH}_3$  concentrations during the period of QCL measurements. No significant concentration difference was found between the concentrations obtained by different calibration values, due to no systematic difference in agreement between the different calibration periods.

While there remain significant differences in measured  $\text{NH}_3$  concentrations between the GRAEGOR and QCL, the improved agreement between those concentrations, particularly at low values, compared with the results from 2004 and 2005 suggests an improved methodology in use by the QCL system in place at Easter Bush. Further measurements, particularly of fluxes and during periods of high  $\text{NH}_3$  concentrations, would be required for a more detailed analysis.

## 5 Conclusion

In this paper, we have presented for the first time simultaneous measurements of the trace gases HCl, HONO,  $\text{HNO}_3$ ,  $\text{SO}_2$  and  $\text{NH}_3$ , and their associated water-soluble aerosols counterparts  $\text{Cl}^-$ ,  $\text{NO}_2^-$ ,  $\text{NO}_3^-$ ,  $\text{SO}_4^{2-}$ ,  $\text{NH}_4^+$ , before and after urea fertilisation of an agricultural grassland. The main findings for this study are:

1. Simultaneous measurements of the components of the  $\text{NH}_3$ - $\text{NO}_3$ - $\text{NH}_4\text{NO}_3$  triad suggested formation of ammonium nitrate post fertilisation. The use of the conservative exchange fluxes  $\text{tot-NH}_4^+$  and  $\text{tot-NO}_3^-$  indicates the presence of

a ground source of  $\text{HNO}_3$  post fertilisation, which would be rapidly scavenged by high post-fertilisation concentrations of  $\text{NH}_3$  to form  $\text{NH}_4\text{NO}_3$ . Through this mechanism, use of urea fertiliser becomes a source of regional, rather than local, pollution.

- 5        2. The deposition velocities measured for the aerosol compounds  $\text{Cl}^-$ ,  $\text{NO}_3^-$  and  $\text{SO}_4^{2-}$  were significantly larger than those measured for  $\text{NH}_4^+$ . After normalisation by turbulence, the measurements suggested a clear relationship between deposition velocity and particle size for  $\text{Cl}^-$ ,  $\text{NO}_3^-$  and  $\text{SO}_4^{2-}$ , as parameterised using the proxy of compound in  $\text{PM}_{2.5}/\text{PM}_{10}$ , although the relationship shows significant variability. Therefore, the high deposition velocities for aerosol compounds recorded at the site are a result of a fraction of the compounds being contained in super-micron aerosol, such as sea-salt sulphate and sodium nitrate.
- 10
3. Evidence for a HONO daytime source at the site throughout the campaign adds to the growing body of past measurements that has found evidence for HONO daytime formation in rural, urban and agricultural areas. There is also evidence for the emission of HONO post fertilisation at the site.
- 15

This also appears to be the first time a comparison between measurements of HONO concentrations determined by the LOPAP and the GRAEGOR instruments has been documented. While good linear agreement exists between HONO measurements taken by GRAEGOR and LOPAP at both measurement heights, a consistent offset in GRAEGOR HONO measurements suggest the presence of chemically induced artefacts within the GRAEGOR system. This is potentially linked to atmospheric  $\text{SO}_x$  and  $\text{NO}_x$  concentrations.

20

Furthermore, this paper presents a comparison between measurements of  $\text{NH}_3$  concentration determined by the GRAEGOR and a QCL system. While changes to the QCL operation system compared to previous studies conducted at the site have resulted in better agreement between the GRAEGOR and QCL, particularly for low  $\text{NH}_3$  concentrations, there still remain significant differences in  $\text{NH}_3$  concentrations with larger values reported by the denuder system.

25

Future measurements of aerosol deposition velocities should aim to investigate the effect of particle size upon deposition velocity, using a more robust measurement of particle size than used here. In addition, the ability of urea pellets to act as a potential surface on which heterogeneous formation of HONO and  $\text{HNO}_3$  occurs should be investigated, particularly as the formation of these compounds can give rise to the formation of the regional pollutant  $\text{NH}_4\text{NO}_3$ .

30

## Acknowledgments

This work was supported through studentship funded jointly by the Max Planck Institute for Chemistry and the University of Edinburgh School of Chemistry, and by the UK Natural Environment Research Council (NERC) through the project “Sources of Nitrous Acid in the Atmospheric Boundary Layer” (SNAABL, NE/M013405/1), with additional field-site support from NERC National Capability funding. The QCL was operated within the framework of the “UK-China Virtual Joint Centre for Improved Nitrogen Agronomy” funded through the Newton programme and administered by the UK Biotechnology and Biological Sciences Research Council (BBSRC). Data from the MARGA was obtained from [https://uk-air.defra.gov.uk/data/data\\_selector](https://uk-air.defra.gov.uk/data/data_selector) ~~uk-air.defra.gov.uk are and is~~ subject to Crown copyright, Defra, licenced under the Open Government Licence (OGL).

## 10 References

- Acker, K., Möller, D., Wieprecht, W., Meixner, F. X., Bohn, B., Gilge, S., Plass-Dülmer, C. and Berresheim, H.: Strong daytime production of OH from HNO<sub>2</sub> at a rural mountain site, *Geophys. Res. Lett.*, 33(2), 2–5, doi:10.1029/2005GL024643, 2006.
- Akiyama, H., McTaggart, I. P., Ball, B. C. and Scott, A.: N<sub>2</sub>O, NO, and NH<sub>3</sub> emissions from soil after the application of organic fertilizers, urea and water, *Water Air Soil Pollut.*, 156(1), 113–129, doi:10.1023/B:WATE.0000036800.20599.46, 2004.
- Allen, A. G., Harrison, R. M. and Erisman, J.-W.: Field measurements of the dissociation of ammonium nitrate and ammonium chloride aerosols, *Atmos. Environ.*, 23(7), 1591–1599, doi:https://doi.org/10.1016/0004-6981(89)90418-6, 1989.
- Allen, A. G., Harrison, R. M. and Nicholson, K. W.: Dry deposition of fine aerosol to a short grass surface, *Atmos. Environ. Part A, Gen. Top.*, 25(12), 2671–2676, doi:10.1016/0960-1686(91)90197-F, 1991.
- Andersen, H. V. and Hovmand, M. F.: Review of dry deposition measurements of ammonia and nitric acid to forest, *For. Ecol. Manage.*, 114(1), 5–18, doi:10.1016/S0378-1127(98)00378-8, 1999.
- Andreae, M. O., Elbert, W., Cai, Y., Andreae, T. W. and Gras, J.: Non-sea-salt sulfate, methanesulfonate, and nitrate aerosol concentrations and size distributions at Cape Grim, Tasmania, *J. Geophys. Res. Atmos.*, 104(D17), 21695–21706, doi:10.1029/1999JD900283, 1999.
- Andreae, M. O., Elbert, W., Gabriel, R., Johnson, D. W., Osborne, S. and Wood, R.: Soluble ion chemistry of the atmospheric aerosol and SO<sub>2</sub> concentrations over the eastern North Atlantic during ACE-2, *Tellus, Ser. B Chem. Phys. Meteorol.*, 52(4), 1066–1087, doi:10.1034/j.1600-0889.2000.00105.x, 2000.
- Appel, B. R., Winer, A. M., Tokiwa, Y. and Biermann, H. W.: Comparison of atmospheric nitrous acid measurements by annular denuder and differential optical absorption systems, *Atmos. Environ. Part A, Gen. Top.*, 24(3), 611–616, doi:10.1016/0960-1686(90)90016-G, 1990.

**Commented [RR21]:** Response to Reviewer #1 - The processed and ratified MARGA data are publicly available online at [https://uk-air.defra.gov.uk/data/data\\_selector](https://uk-air.defra.gov.uk/data/data_selector) from which concentrations of any of the species measured by the MARGA can be selected. We will add the references and online resources to the paper.

Response to Reviewer #2 - The processed and ratified MARGA data are publicly available online at [https://uk-air.defra.gov.uk/data/data\\_selector](https://uk-air.defra.gov.uk/data/data_selector) from which concentrations of any of the species measured by the MARGA can be selected. We will add the references and online resources to the paper.

- Bardouki, H., Liakakou, H., Economou, C., Sciare, J., Smolik, J., Ždímal, V., Eleftheriadis, K., Lazaridis, M., Dye, C. and Mihalopoulos, N.: Chemical composition of size-resolved atmospheric aerosols in the eastern Mediterranean during summer and winter, *Atmos. Environ.*, 37(2), 195–208, doi:10.1016/S1352-2310(02)00859-2, 2003.
- Behera, S. N., Sharma, M., Aneja, V. P. and Balasubramanian, R.: Ammonia in the atmosphere: A review on emission sources, atmospheric chemistry and deposition on terrestrial bodies, *Environ. Sci. Pollut. Res.*, 20(11), 8092–8131, doi:10.1007/s11356-013-2051-9, 2013.
- Bobbink, R., Hicks, K., Galloway, J., Spranger, T., Alkemade, R., Ashmore, M., Bustamante, M., Cinderby, S., Davidson, E., Dentener, F., Emmett, B., Erisman, J. W., Fenn, M., Gilliam, F., Nordin, A., Pardo, L. and De Vries, W.: Global assessment of nitrogen deposition effects on terrestrial plant diversity: A synthesis, *Ecol. Appl.*, 20(1), 30–59, doi:10.1890/08-1140.1, 2010.
- Brost, R. A., Delany, A. C. and Huebert, B. J.: Numerical modeling of concentrations and fluxes of HNO<sub>3</sub>, NH<sub>3</sub>, and NH<sub>4</sub>NO<sub>3</sub> near the surface, *J. Geophys. Res.*, 93(D6), 7137–7152, 1988.
- Camargo, J. A. and Alonso, Á.: Ecological and toxicological effects of inorganic nitrogen pollution in aquatic ecosystems: A global assessment, *Environ. Int.*, 32(6), 831–849, doi:10.1016/j.envint.2006.05.002, 2006.
- Cowan, N. J., Norman, P., Famulari, D., Levy, P. E., Reay, D. S. and Skiba, U. M.: Spatial variability and hotspots of soil N<sub>2</sub>O fluxes from intensively grazed grassland, *Biogeosciences*, 12(5), 1585–1596, doi:10.5194/bg-12-1585-2015, 2015.
- Dasgupta, P. K., Campbell, S. W., Al-Horr, R. S., Ullah, S. M. R., Li, J., Amalfitano, C. and Poor, N. D.: Conversion of sea salt aerosol to NaNO<sub>3</sub> and the production of HCl: Analysis of temporal behavior of aerosol chloride/nitrate and gaseous HCl/HNO<sub>3</sub> concentrations with AIM, *Atmos. Environ.*, 41(20), 4242–4257, doi:10.1016/j.atmosenv.2006.09.054, 2007.
- Davidson, C. I., Miller, J. M. and Pleskow, M. A.: The influence of surface structure on predicted particle dry deposition to natural grass canopies, *Water, Air, Soil Pollut.*, 18(1–3), 25–43, doi:10.1007/BF02419401, 1982.
- [DEFRA, UK Air – Air Information Resource, Data Selector: https://uk-air.defra.gov.uk/data/data\\_selector](https://uk-air.defra.gov.uk/data/data_selector), last access: 25<sup>th</sup> September 2018.
- Di Marco, C., Skiba, U., Weston, K., Hargreaves, K. and Fowler, D.: Field Scale N<sub>2</sub>O Flux Measurements from Grassland Using Eddy Covariance, *Water, Air, Soil Pollut. Focus*, 4(6), 143–149, doi:10.1007/s11267-004-3024-2, 2004.
- Di Marco et al. (2018). Characterisation of HONO fluxes over grassland. In preparation.
- Dollard, G. J., Atkins, D. H. F., Davies, T. J. and Healy, C.: Concentrations and dry deposition velocities of nitric acid, *Nature*, 326(6112), 481–483, 1987.
- Elliott, K. J., Vose, J. M., Knoepp, J. D., Johnson, D. W., Swank, W. T. and Jackson, W.: Simulated effects of sulfur deposition on nutrient cycling in class I wilderness areas., *J. Environ. Qual.*, 37, 1419–31, doi:10.2134/jeq2007.0358, 2006.
- Famulari, D., Fowler, D., Hargreaves, K. J., Milford, C., Nemitz, E., Sutton, M. A. and Weston, K.: Measuring eddy covariance fluxes of ammonia using tunable diode laser absorption spectroscopy., *Water, Air Soil Pollut. Focus*, 4, 151–158, doi:10.1007/s11267-004-3025-1, 2004.

- [Farmer, D. K. and Cohen, R. C.: Observations of  \$\Sigma\text{HNO}\_3\$ ,  \$\Sigma\text{AN}\$ ,  \$\Sigma\text{PN}\$  and  \$\text{NO}\_2\$  fluxes: evidence for rapid  \$\text{HO}\_3\$  chemistry within a pine forest canopy, \*Atmos. Chem. Phys.\*, 8\(14\), 3899–3917, 2008.](#)
- Febo, A., Perrino, C. and Allegrini, I.: Measurement of nitrous acid in Milan, Italy, by DOAS and diffusion denuders, *Atmos. Environ.*, 30(21), 3599–3609, doi:10.1016/1352-2310(96)00069-6, 1996.
- 5 Ferm, M.: Atmospheric ammonia and ammonium transport in Europe and critical loads: A review, *Nutr. Cycl. Agroecosystems*, 51(1), 5–17, doi:10.1023/A:1009780030477, 1998.
- Fiore, A. M., Naik, V. and Leibensperger, E. M.: Air Quality and Climate Connections, *J. Air Waste Manage. Assoc.*, 65(6), 645–685, doi:10.1080/10962247.2015.1040526, 2015.
- Flechard, C. R., Massad, R. S., Loubet, B., Personne, E., Simpson, D., Bash, J. O., Cooter, E. J., Nemitz, E. and Sutton, M.
- 10 A.: A dynamic chemical model of bi-directional ammonia exchange between semi-natural vegetation and the atmosphere, *Q.J.R. Meteorol. Soc.*, 125, 2611–2641, doi:10.1007/9789401772853, 1999.
- Flechard, C.R., 1998. Turbulent Exchange of Ammonia Above Vegetation. PhD Thesis. University of Nottingham, UK, 237 pp
- Foken, T.: *Micrometeorology*, 2nd ed., Springer, Berlin, 2008.
- 15 Foley, J. A., Ramankutty, N., Brauman, K. A., Cassidy, E. S., Gerber, J. S., Johnston, M., Mueller, N. D., O'Connell, C., Ray, D. K., West, P. C., Balzer, C., Bennett, E. M., Carpenter, S. R., Hill, J., Monfreda, C., Polasky, S., Rockström, J., Sheehan, J., Siebert, S., Tilman, D. and Zaks, D. P. M.: Solutions for a cultivated planet, *Nature*, 478, 337 [online] Available from: <http://dx.doi.org/10.1038/nature10452>, 2011.
- Fowler, D. and Unsworth, H. M.: Turbulent transfer of sulphur dioxide to a wheat crop, *Q. J. R. Meteorol. Soc.*, 105(446),
- 20 767–783, doi:10.1002/qj.49710544603, 1979.
- Fowler, D., Coyle, M., Skiba, U., Sutton, M. A., Cape, J. N., Reis, S., Sheppard, L. J., Jenkins, A., Grizzetti, B., Galloway, N., Vitousek, P., Leach, A., Bouwman, A. F., Butterbach-bahl, K., Dentener, F., Stevenson, D., Amann, M., Voss, M. and Fowler, D.: The global nitrogen cycle in the twenty-first century, *Philosophical Trans. R. Soc. B*, doi:<http://dx.doi.org/10.1098/rstb.2013.0164>, 2013.
- 25 Gallagher, M. W., Nemitz, E., Dorsey, J. R., Fowler, D., Sutton, M. a, Flynn, M. and Duyzer, J. H.: Measurements and parameterizations of small aerosol deposition velocities to grassland, arable crops, and forest: Influence of surface roughness length on deposition, *J. Geophys. Res.*, 107(D12), 549, doi:10.1029/2001JD000817, 2002.
- [Garland, J. A.: The dry deposition of sulphur dioxide to land and water surfaces, \*Proc R Soc London Ser A\*, 354\(1678\), 245–268, doi:10.1098/rspa.1977.0066, 1977.](#)
- 30 Galloway, J. N., Aber, J. D., Erisman, J. W., Seitzinger, S. P., Howarth, R. W., Cowling, E. B. and Cosby, B. J.: The Nitrogen Cascade, *Bioscience*, 53(4), 341, doi:10.1641/0006-3568(2003)053[0341:TNC]2.0.CO;2, 2003.
- Godfray, H. C. J., Beddington, J. R., Crute, I. R., Haddad, L., Lawrence, D., Muir, J. F., Pretty, J., Robinson, S., Thomas, S. M. and Toulmin, C.: Food Security: The Challenge of Feeding 9 Billion People, *Science* (80-. ), 327(5967), 812 LP-818 [online] Available from: <http://science.sciencemag.org/content/327/5967/812.abstract>, 2010.

- Gutzwiller, L., Arens, F., Baltensperger, U., Gäggeler, H. W. and Ammann, M.: Significance of semivolatile diesel exhaust organics for secondary HONO formation, *Environ. Sci. Technol.*, 36(4), 677–682, doi:10.1021/es015673b, 2002.
- Harrison, R. M., Peak, J. D. and Collins, G. M.: Tropospheric cycle of nitrous acid, *J. Geophys. Res. Atmos.*, 101(D9), 14429–14439, doi:10.1029/96JD00341, 1996.
- 5 Jones, S. K., Helfter, C., Anderson, M., Coyle, M., Campbell, C., Famulari, D., Di Marco, C., Van Dijk, N., Sim Tang, Y., Topp, C. F. E., Kiese, R., Kindler, R., Siemens, J., Schrupf, M., Kaiser, K., Nemitz, E., Levy, P. E., Rees, R. M., Sutton, M. A. and Skiba, U. M.: The nitrogen, carbon and greenhouse gas budget of a grazed, cut and fertilised temperate grassland, *Biogeosciences*, 14(8), 2069–2088, doi:10.5194/bg-14-2069-2017, 2017.
- Khlystov, A., Wyers, G. P. and Slanina, J.: The steam-jet aerosol collector, *Atmos. Environ.*, 29(17), 2229–2234, doi:10.1016/1352-2310(95)00180-7, 1995.
- 10 Kleffmann, J. and Wiesen, P.: Technical Note: Quantification of interferences of wet chemical HONO LOPAP measurements under simulated polar conditions, *Atmos. Chem. Phys.*, 8(22), 6813–6822, doi:10.5194/acp-8-6813-2008, 2008.
- Kleffmann, J., Lörzer, J. C., Wiesen, P., Kern, C., Trick, S., Volkamer, R., Rodenas, M. and Wirtz, K.: Intercomparison of the DOAS and LOPAP techniques for the detection of nitrous acid (HONO), *Atmos. Environ.*, 40(20), 3640–3652, doi:10.1016/j.atmosenv.2006.03.027, 2006.
- 15 Kleffmann, J.: Daytime sources of nitrous acid (HONO) in the atmospheric boundary layer, *ChemPhysChem*, 8(8), 1137–1144, doi:10.1002/cphc.200700016, 2007.
- Kramm, G. and Dlugi, R.: Modeling of the Vertical Fluxes of Nitric-Acid, Ammonia, and Ammonium-Nitrate, *J. Atmos. Chem.*, 18(4), 319–357, 1994.
- 20 [Langford, B., Acton, W., Ammann, C., Valach, A. and Nemitz, E.: Eddy-covariance data with low signal-to-noise ratio : time-lag determination , uncertainties and limit of detection. \*Atmos. Meas. Tech.\*, 4197–4213, doi:10.5194/amt-8-4197-2015, 2015.](#)
- Laufs, S., Cazaunau, M., Stella, P., Kurtenbach, R., Cellier, P., Mellouki, A., Loubet, B. and Kleffmann, J.: Diurnal fluxes of HONO above a crop rotation, *Atmos. Chem. Phys.*, 17(11), 6907–6923, doi:10.5194/acp-17-6907-2017, 2017.
- Lee, J. D., Whalley, L. K., Heard, D. E., Stone, D., Dunmore, R. E., Hamilton, J. F., Young, D. E., Allan, J. D., Laufs, S. and Kleffmann, J.: Detailed budget analysis of HONO in central London reveals a missing daytime source, *Atmos. Chem. Phys.*, 16(5), 2747–2764, doi:10.5194/acp-16-2747-2016, 2016.
- Kutsuna, S. and Ibusuki, T.: Fourier transform infrared measurement of the formation of nitrogen compounds on sodium chloride particles exposed to the ambient air in the Arctic, *J. Geophys. Res.*, 99(D12), 25,425-479, 1994.
- Medinets, S., Skiba, U., Rennenberg, H. and Butterbach-Bahl, K.: A review of soil NO transformation: Associated processes and possible physiological significance on organisms, *Soil Biol. Biochem.*, 80, 92–117, doi:10.1016/j.soilbio.2014.09.025, 2015.
- 30 Milford, C., 2004. Dynamics of Atmospheric Ammonia Exchange with intensively- managed Grassland. PhD Thesis. University of Edinburgh, Edinburgh, 219 pp.

- Milford, C., Theobald, M.R., Nemitz, E. and Sutton, M.A.: Dynamics of ammonia exchange in response to cutting and fertilising in an intensively-managed grass-land, *Water, Air, and Soil Pollution: Focus* 1, 167–176, 2001.
- Mozurkewich, M.: The dissociation constant of ammonium nitrate and its dependence on temperature, relative humidity and particle size, *Atmos. Environ. Part A, Gen. Top.*, 27(2), 261–270, doi:10.1016/0960-1686(93)90356-4, 1993.
- 5 Muller, H., Kramm, G., Meixner, F., Dollard, G., Fowler, D. and Possanzini, M.: Determination of HNO<sub>3</sub> dry deposition by modified Bowen ratio and aerodynamic profile techniques, *Tellus*, 45, 346–367, doi:10.1034/j.1600-0889.45.issue4.1.x, 1993.
- Myhre, G., Grini, A. and Metzger, S.: Modelling of nitrate and ammonium-containing aerosols in presence of sea salt, *Atmos. Chem. Phys.*, 6(12), 4809–4821, doi:10.5194/acp-6-4809-2006, 2006.
- Myles, L., Kochendorfer, J., Heuer, M. W. and Meyers, T. P.: Measurement of Trace Gas Fluxes over an Unfertilized Agricultural Field Using the Flux-gradient Technique, *J. Environ. Qual.*, 40(5), 1359, doi:10.2134/jeq2009.0386, 2011.
- 10 Nefel, A., Blatter, A., Hesterberg, R. and Staffelbach, T.: Measurements of concentration gradients of HNO<sub>2</sub> and HNO<sub>3</sub> over a semi-natural ecosystem, *Atmos. Environ.*, 30(17), 3017–3025, doi:10.1016/1352-2310(96)00011-8, 1996.
- Nemitz, E. and Sutton, M. A.: Gas-particle interactions above a Dutch heathland: III. Modelling the influence of the NH<sub>3</sub>-HNO<sub>3</sub>-NH<sub>4</sub>NO<sub>3</sub> equilibrium on size-segregated particle fluxes, *Atmos. Chem. Phys.*, 4(1988), 1025–1045 [online] Available from: <http://www.atmos-chem-phys.net/4/1025/2004/acp-4-1025-2004.html>, 2004.
- 15 Nemitz, E., Hargreaves, K. J., Nefel, A., Loubet, B., Cellier, P., Dorsey, J. R., Flynn, M., Hensen, A., Weidinger, T., Meszaros, R., Horvath, L., DäCURRENCY Signmmgen, U., Frühauf, C., Löpmeier, F. J., Gallagher, M. W. and Sutton, M. A.: Intercomparison and assessment of turbulent and physiological exchange parameters of grassland, *Biogeosciences*, 6(8), 1445–1466, doi:10.5194/bg-6-1445-2009, 2009a.
- 20 Nemitz, E., Dorsey, J. R., Flynn, M. J., Gallagher, M. W., Hensen, A., Erisman, J. W., Owen, S. M., Dämmgen, U. and Sutton, M. A.: Aerosol fluxes and particle growth above managed grassland, *Biogeosciences*, 6(8), 1627–1645, doi:10.5194/bg-6-1627-2009, 2009b.
- Nemitz, E., Sutton, M. A., Schjoerring, J. K., Husted, S. and Paul Wyers, G.: Resistance modelling of ammonia exchange over oilseed rape, *Agric. For. Meteorol.*, 105(4), 405–425, doi:10.1016/S0168-1923(00)00206-9, 2000b.
- 25 Nemitz, E., Sutton, M. A., Wyers, G. P., Otjes, R. P., Schjoerring, J. K., Gallagher, M. W., Parrington, J., Fowler, D. and Choulaton, T. W.: Surface/atmosphere exchange and chemical interaction of gases and aerosols over oilseed rape, *Agric. For. Meteorol.*, 105(4), 427–445, doi:10.1016/S0168-1923(00)00207-0, 2000a.
- Neuman, J. A., Huey, L. G., Ryerson, T. B. and Fahey, D. W.: Study of inlet materials for sampling atmospheric nitric acid, *Environ. Sci. Technol.*, 33(7), 1133–1136, doi:10.1021/es980767f, 1999.
- 30 Norman, M., Spirig, C., Wolff, V., Trebs, I., Flechard, C., Wisthaler, A., Schnitzhofer, R., Hansel, A. and Nefel, A.: Intercomparison of ammonia measurement techniques at an intensively managed grassland site (Oensingen, Switzerland), *Atmos. Chem. Phys.*, 9(8), 2635–2645, doi:10.5194/acp-9-2635-2009, 2009.
- O’Dowd, C. D. and de Leeuw, G.: Marine aerosol production: a review of the current knowledge, *Philos. Trans. R. Soc. A Math. Phys. Eng. Sci.*, 365(1856), 1753–1774, doi:10.1098/rsta.2007.2043, 2007.

- Oswald, R., Behrendt, T., Ermel, M., Wu, D., Su, H., Cheng, Y., Breuninger, C., Moravek, A., Mougín, E., Delon, C., Loubet, B., Pommerening-Röser, A., Sörgel, M., Pöschl, U., Hoffmann, T., Andreae, M. O., Meixner, F. X. and Trebs, I.: HONO emissions from soil bacteria as a major source of atmospheric reactive nitrogen., *Science*, 341(6151), 1233–5, doi:10.1126/science.1242266, 2013.
- 5 Pagsberg, P., Bjergbakke, E., Ratajczak, E. and Sillesen, A.: Kinetics of the gas phase reaction  $\text{OH} + \text{NO}(\text{+M}) \rightarrow \text{HONO}(\text{+M})$  and the determination of the UV absorption cross sections of HONO, *Chem. Phys. Lett.*, 272(5–6), 383–390, doi:10.1016/S0009-2614(97)00576-9, 1997.
- Petroff, A., Mailliat, A., Amielh, M. and Anselmet, F.: Aerosol dry deposition on vegetative canopies. Part I: Review of present knowledge, *Atmos. Environ.*, 42(16), 3625–3653, doi:10.1016/j.atmosenv.2007.09.043, 2008.
- 10 Phillips, G. J., Makkonen, U., Schuster, G., Sobanski, N., Hakola, H. and Crowley, J. N.: The detection of nocturnal  $\text{N}_2\text{O}_5$  as  $\text{HNO}_3$  by alkali- and aqueous-denuder techniques, *Atmos. Meas. Tech.*, 6(2), 231–237, doi:10.5194/amt-6-231-2013, 2013.
- Pilegaard, K.: Processes regulating nitric oxide emissions from soils, *Philos Trans R Soc L. B Biol Sci*, 368(1621), 20130126, doi:10.1098/rstb.2013.0126, 2013.
- Pio, C. A. and Harrison, R. M.: The equilibrium of ammonium chloride aerosol with gaseous hydrochloric acid and ammonia  
15 under tropospheric conditions, *Atmos. Environ.*, 21(5), 1243–1246, doi:10.1016/0004-6981(87)90253-8, 1987.
- Pryor, S. C., Gallagher, M., Sievering, H., Larsen, S. E., Barthelme, R. J., Birsan, F., Nemitz, E., Rinne, J., Kulmala, M., Grönholm, T., Taipale, R. and Vesala, T.: A review of measurement and modelling results of particle atmosphere-surface exchange, *Tellus, Ser. B Chem. Phys. Meteorol.*, 60 B(1), 42–75, doi:10.1111/j.1600-0889.2007.00298.x, 2008.
- Robertson, G. P., Bruulsema, T. W., Gehl, R. J., Kanter, D., Mauzerall, D. L., Rotz, C. A. and Williams, C. O.: Nitrogen-climate interactions in US agriculture, *Biogeochemistry*, 114(1–3), 41–70, doi:10.1007/s10533-012-9802-4, 2013.
- 20 [Rumsey, I. C. and Walker, J. T.: Application of an online ion-chromatography-based instrument for gradient flux measurements of speciated nitrogen and sulfur, \*Atmos. Meas. Tech.\*, 9\(6\), 2581–2592, doi:10.5194/amt-9-2581-2016, 2016.](#)
- Scharko, N. K., Schütte, U. M. E., Berke, A. E., Banina, L., Peel, H. R., Donaldson, M. A., Hemmerich, C., White, J. R. and Raff, J. D.: Combined Flux Chamber and Genomics Approach Links Nitrous Acid Emissions to Ammonia Oxidizing Bacteria  
25 and Archaea in Urban and Agricultural Soil, *Environ. Sci. Technol.*, 49(23), 13825–13834, doi:10.1021/acs.est.5b00838, 2015.
- Slanina, J., Ten Brink, H. M., Otjes, R. P., Even, A., Jongejan, P., Khlystov, A., Waijers-Ijpelaar, A., Hu, M. and Lu, Y.: The continuous analysis of nitrate and ammonium in aerosols by the steam jet aerosol collector (SJAC): extension and validation of the methodology, *Atmos. Environ.*, 35(13), 2319–2330, doi:10.1016/S1352-2310(00)00556-2, 2001.
- 30 Slinn, S. A. and Slinn, W. G. N.: Predictions for particle deposition on natural waters, *Atmos. Environ.*, 14(9), 1013–1016, doi:10.1016/0004-6981(80)90032-3, 1980.
- Slinn, W. G. N.: Predictions for particle deposition to vegetative canopies, *Atmos. Environ.*, 16(7), 1785–1794, doi:10.1016/0004-6981(82)90271-2, 1982.
- Sommer, S. G. and Hutchings, N. J.: Ammonia emission from field applied manure and its reduction - Invited paper, *Eur. J. Agron.*, 15(1), 1–15, doi:10.1016/S1161-0301(01)00112-5, 2001.

- Sörgel, M., Trebs, I., Serafimovich, A., Moravek, A., Held, A. and Zetzsch, C.: Simultaneous HONO measurements in and above a forest canopy: Influence of turbulent exchange on mixing ratio differences, *Atmos. Chem. Phys.*, 11(2), 841–855, doi:10.5194/acp-11-841-2011, 2011.
- Sörgel, M., Trebs, I., Wu, D. and Held, A.: A comparison of measured HONO uptake and release with calculated source strengths in a heterogeneous forest environment, *Atmos. Chem. Phys.*, 15(16), 9237–9251, doi:10.5194/acp-15-9237-2015, 2015.
- Soussana, J. F., Allard, V., Pilegaard, K., Ambus, P., Amman, C., Campbell, C., Ceschia, E., Clifton-Brown, J., Czobel, S., Domingues, R., Flechard, C., Fuhrer, J., Hensen, A., Horvath, L., Jones, M., Kasper, G., Martin, C., Nagy, Z., Neftel, A., Raschi, A., Baronti, S., Rees, R. M., Skiba, U., Stefani, P., Manca, G., Sutton, M., Tuba, Z. and Valentini, R.: Full accounting of the greenhouse gas (CO<sub>2</sub>, N<sub>2</sub>O, CH<sub>4</sub>) budget of nine European grassland sites, *Agric. Ecosyst. Environ.*, 121(1–2), 121–134, doi:10.1016/j.agee.2006.12.022, 2007.
- Spindler, G., Hesper, J., Brüggemann, E., Dubois, R., Müller, T. and Herrmann, H.: Wet annular denuder measurements of nitrous acid: Laboratory study of the artefact reaction of NO<sub>2</sub> with S(IV) in aqueous solution and comparison with field measurements, *Atmos. Environ.*, 37(19), 2643–2662, doi:10.1016/S1352-2310(03)00209-7, 2003.
- Su, H., Cheng, Y. F., Shao, M., Gao, D. F., Yu, Z. Y., Zeng, L. M., Slanina, J., Zhang, Y. H., and Wiedensohler, A., Nitrous acid (HONO) and its daytime sources at a rural site during the 2004 PRIDE-PRD experiment in China: *J. Geophys. Res.*, 113, D14312, doi:10.1029/2007jd009060, 2008.
- Su, H., Cheng, Y., Oswald, R., Behrendt, T., Trebs, I., Meixner, F. X., Andreae, M. O., Cheng, P., Zhang, Y. and Pöschl, U.: Soil nitrite as a source of atmospheric HONO and OH radicals, *Science* (80-.), 333(6049), 1616–1618, doi:10.1126/science.1207687, 2011.
- Suter, H., Sultana, H., Turner, D., Davies, R., Walker, C. and Chen, D.: Influence of urea fertiliser formulation, urease inhibitor and season on ammonia loss from ryegrass, *Nutr. Cycl. Agroecosystems*, 95(2), 175–185, doi:10.1007/s10705-013-9556-y, 2013.
- Sutton, M. A., Nemitz, E., Erisman, J. W., Beier, C., Bahl, K. B., Cellier, P., de Vries, W., Cotrufo, F., Skiba, U., Di Marco, C., Jones, S., Laville, P., Soussana, J. F., Loubet, B., Twigg, M., Famulari, D., Whitehead, J., Gallagher, M. W., Neftel, A., Flechard, C. R., Herrmann, B., Calanca, P. L., Schjoerring, J. K., Daemmgen, U., Horvath, L., Tang, Y. S., Emmett, B. A., Tietema, A., Peñuelas, J., Kesik, M., Brüggemann, N., Pilegaard, K., Vesala, T., Campbell, C. L., Olesen, J. E., Dragosits, U., Theobald, M. R., Levy, P., Mobbs, D. C., Milne, R., Viogy, N., Vuichard, N., Smith, J. U., Smith, P., Bergamaschi, P., Fowler, D. and Reis, S.: Challenges in quantifying biosphere-atmosphere exchange of nitrogen species, *Environ. Pollut.*, 150(1), 125–139, doi:10.1016/j.envpol.2007.04.014, 2007.
- Sutton, M. A., Nemitz, E., Milford, C., Campbell, C., Erisman, J. W., Hensen, A., Cellier, P., David, M., Loubet, B., Personne, E., Schjoerring, J. K., Mattsson, M., Dorsey, J. R., Gallagher, M. W., Horvath, L., Weidinger, T., Meszaros, R., Dämmgen,

- U., Neftel, A., Herrmann, B., Lehman, B. E., Flechard, C. and Burkhardt, J.: Dynamics of ammonia exchange with cut grassland: Synthesis of results and conclusions of the GRAMINAE Integrated Experiment, *Biogeosciences*, 6(12), 2907–2934, doi:10.5194/bg-6-2907-2009, 2009.
- Thomas, R. M., Trebs, I., Otjes, R., Jongejan, P. A. C. C., Ten Brink, H., Phillips, G., Kortner, M., Meixner, F. X. and Nemitz, E.: An automated analyzer to measure surface-atmosphere exchange fluxes of water soluble inorganic aerosol compounds and reactive trace gases, *Environ. Sci. Technol.*, 43(5), 1412–1418, doi:10.1021/es8019403, 2009.
- Trebs, I., Metzger, S., Meixner, F. X., Helas, G., Hoffer, A., Rudich, Y., Falkovich, A. H., Moura, M. A. L., Da Silva, R. S., Artaxo, P., Slanina, J. and Andreae, M. O.: The  $\text{NH}_4^+$ - $\text{NO}_3^-$ - $\text{Cl}^-$ - $\text{SO}_4^{2-}$ - $\text{H}_2\text{O}$  aerosol system and its gas phase precursors at a pasture site in the Amazon Basin: How relevant are mineral cations and soluble organic acids?, *J. Geophys. Res. Atmos.*, 110(7), 1–18, doi:10.1029/2004JD005478, 2005.
- Twigg, M. M., House, E., Thomas, R., Whitehead, J., Phillips, G. J., Famulari, D., Fowler, D., Gallagher, M. W., Cape, J. N., Sutton, M. A. and Nemitz, E.: Surface/atmosphere exchange and chemical interactions of reactive nitrogen compounds above a mowed grassland, *Agric. For. Meteorol.*, 151(12), 1488–1503, doi:10.1016/j.agrformet.2011.06.005, 2011.
- Twigg, M. M., Di Marco, C. F., Leeson, S., Van Dijk, N., Jones, M. R., Leith, I. D., Morrison, E., Coyle, M., Proost, R., Peeters, A. N. M., Lemon, E., Frelink, T., Braban, C. F., Nemitz, E. and Cape, J. N.: Water soluble aerosols and gases at a UK background site – Part 1: Controls of PM<sub>2.5</sub> and PM<sub>10</sub> aerosol composition, *Atmos. Chem. Phys.*, 15(14), 8131–8145, doi:10.5194/acp-15-8131-2015, 2015.
- Van der Eerden, L. J., Lekkerkerk, L. J., Smeulders, S. M. and Jansen, A. E.: Effects of atmospheric ammonia and ammonium sulphate on Douglas fir (*Pseudotsuga menziesii*), *Environ. Pollut.*, 76(1), 1–9 [online] Available from: <http://www.ncbi.nlm.nih.gov/pubmed/15092001>, 1992.
- Van Oss, R., Duyzer, J. and Wyers, P.: The influence of gas-to-particle conversion on measurements of ammonia exchange over forest, *Atmos. Environ.*, 32(3), 465–471, doi:10.1016/S1352-2310(97)00280-X, 1998.
- Vieno, M., Heal, M. R., Hallsworth, S., Famulari, D., Doherty, R. M., Dore, A. J., Tang, Y. S., Braban, C. F., Leaver, D., Sutton, M. A. and Reis, S.: The role of long-range transport and domestic emissions in determining atmospheric secondary inorganic particle concentrations across the UK, *Atmos. Chem. Phys.*, 14(16), 8435–8447, doi:10.5194/acp-14-8435-2014, 2014.
- Von Bobrutski, K., Braban, C. F., Famulari, D., Jones, S. K., Blackall, T., Smith, T. E. L., Blom, M., Coe, H., Gallagher, M., Ghalaieny, M., McGillen, M. R., Percival, C. J., Whitehead, J. D., Ellis, R., Murphy, J., Mohacsi, A., Pogany, A., Junninen, H., Rantanen, S., Sutton, M. A. and Nemitz, E.: Field inter-comparison of eleven atmospheric ammonia measurement techniques, *Atmos. Meas. Tech.*, 3(1), 91–112, doi:10.5194/amt-3-91-2010, 2010.
- Vong, R. J., Vickers, D. and Covert, D. S.: Eddy correlation measurements of aerosol deposition to grass, *Tellus, Ser. B Chem. Phys. Meteorol.*, 56(2), 105–117, doi:10.1111/j.1600-0889.2004.00098.x, 2004.
- Wang, J. and Bras, L. R.: A new method for estimation of sensible heat flux from air temperature, *Water Resour. Res.*, 34(9), 2281–2288, doi:10.1029/98WR01698, 1998.

Wesely, M. L., Cook, D. R. and Hart, R. L.: Sulfur Dry Deposition Over Grass, *J. Geophys. Res.*, 90(4), 2131–2143, 1985.

Whitehead, J. D., Twigg, M., Famulari, D., Nemitz, E., Sutton, M. a, Gallagher, M. W. and Fowler, D.: Evaluation of laser absorption spectroscopic techniques for eddy covariance flux measurements of ammonia., *Environ. Sci. Technol.*, 42(6), 2041–2046, doi:10.1021/es071596u, 2008.

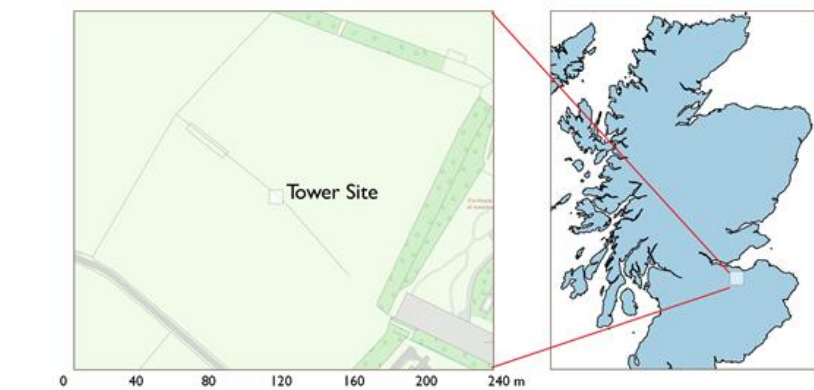
5 Wolff, V., Trebs, I., Ammann, C. and Meixner, F. X.: Aerodynamic gradient measurements of the  $\text{NH}_3\text{-HNO}_3\text{-NH}_4\text{NO}_3$  triad using a wet chemical instrument: an analysis of precision requirements and flux errors, *Atmos. Meas. Tech. Discuss.*, 2(5), 2423–2482, doi:10.5194/amtd-2-2423-2009, 2009.

Wolff, V., Trebs, I., Foken, T. and Meixner, F. X.: Exchange of reactive nitrogen compounds: Concentrations and fluxes of total ammonium and total nitrate above a spruce canopy, *Biogeosciences*, 7(5), 1729–1744, doi:10.5194/bg-7-1729-2010,  
10 2010.

Wyers, G. P., Otjes, R. P. and Slanina, J.: A continuous-flow denuder for the measurement of ambient concentrations and surface-exchange fluxes of ammonia, *Atmos. Environ. Part A, Gen. Top.*, 27(13), 2085–2090, doi:10.1016/0960-1686(93)90280-C, 1993.

Yeatman, S. G., Spokes, L. J. and Jickells, T. D.: Comparisons of coarse-mode aerosol nitrate and ammonium at two polluted  
15 coastal sites, *Atmos. Environ.*, 35(7), 1321–1335, doi:10.1016/S1352-2310(00)00452-0, 2001.

Zöll, U., Brümmer, C., Schrader, F., Ammann, C., Ibrom, A., Flechard, C. R., Nelson, D. D., Zahniser, M. and Kutsch, W. L.: Surface-atmosphere exchange of ammonia over peatland using QCL-based eddy-covariance measurements and inferential modeling, *Atmos. Chem. Phys.*, 16(17), 11283–11299, doi:10.5194/acp-16-11283-2016, 2016.



20 **Figure 1: Location of the Bush Tower Site (3°12'W, 55°52'N) in relation to surrounding agricultural land and within Scotland, UK.**

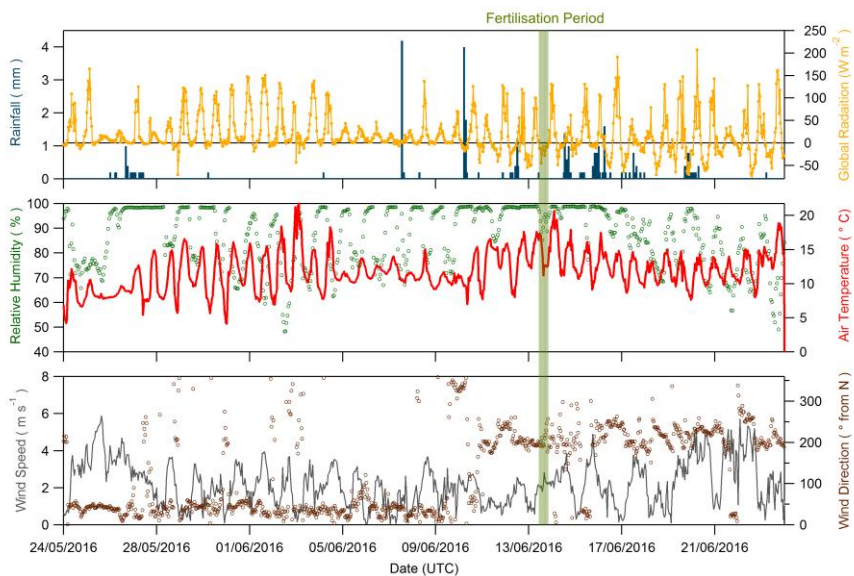


**Figure 2:** Global radiation (orange line), rainfall (blue bars), relative humidity (green dots), air temperature (red line), wind direction (brown circles) and wind speed (grey line) recorded during the Easter Bush Campaign, May to June 2016. The fertilisation period was 08:00 – 09:00 on 13<sup>th</sup> June and is highlighted in green.

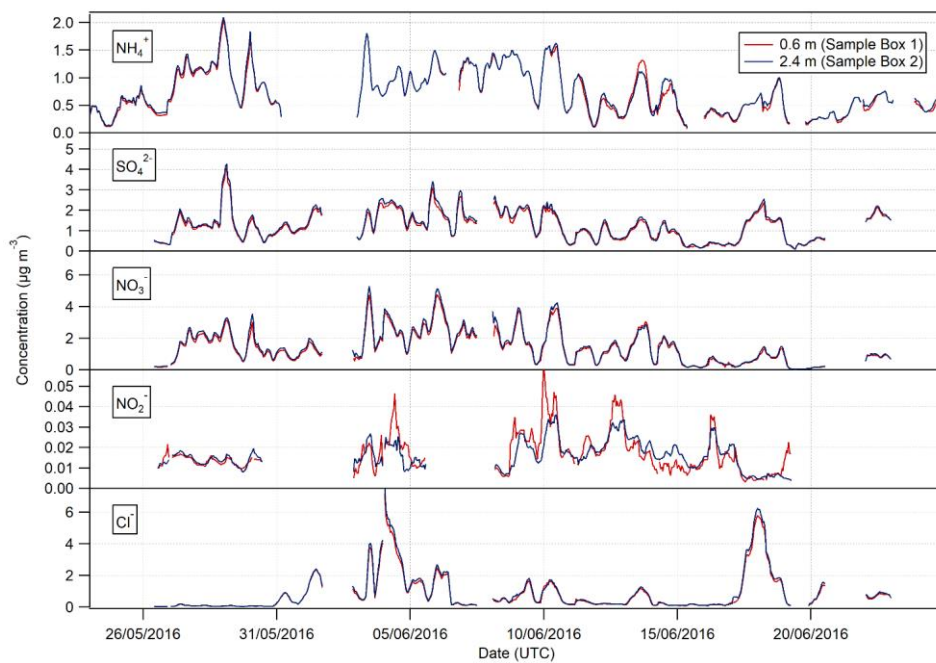


**Figure 3: Time series of hourly concentrations of the water-soluble aerosol species measured during the Easter Bush campaign. Results smoothed using a 5-hour moving point average.**

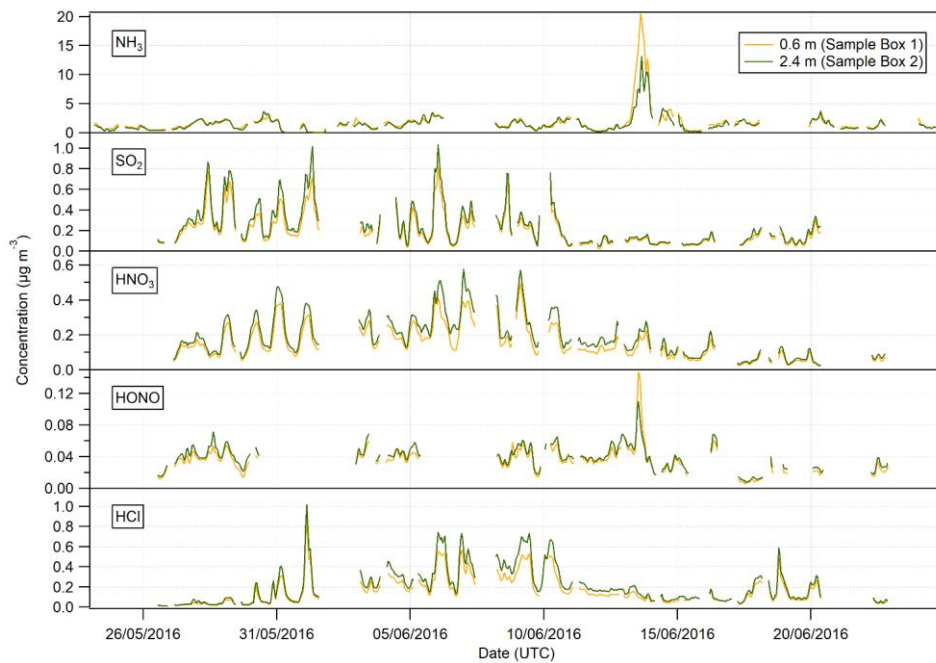


**Figure 4:** Time series of hourly concentrations of the gaseous species measured during the Easter Bush campaign. Results smoothed using a 5-hour moving point average.

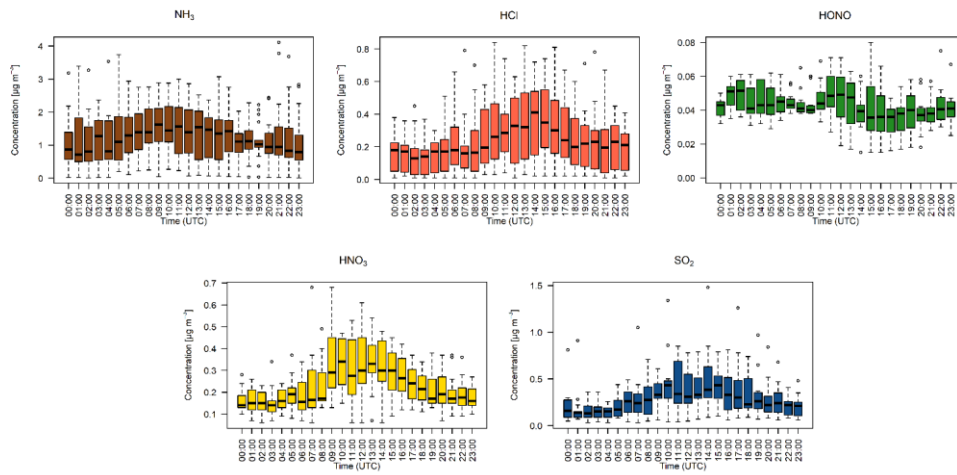


Figure 5: Hourly median diel trace gas concentrations measured by the GRAEGOR at 2.4 m. Boxes show the lower and upper quartiles and whiskers the 5% to 95% range, with outliers shown as circles.

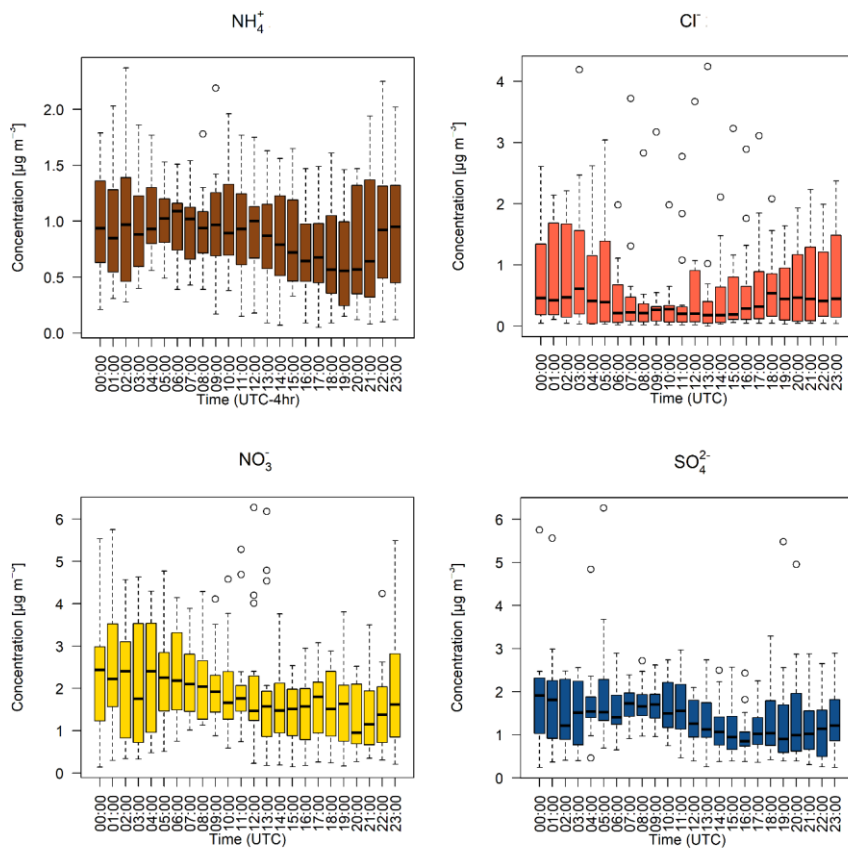
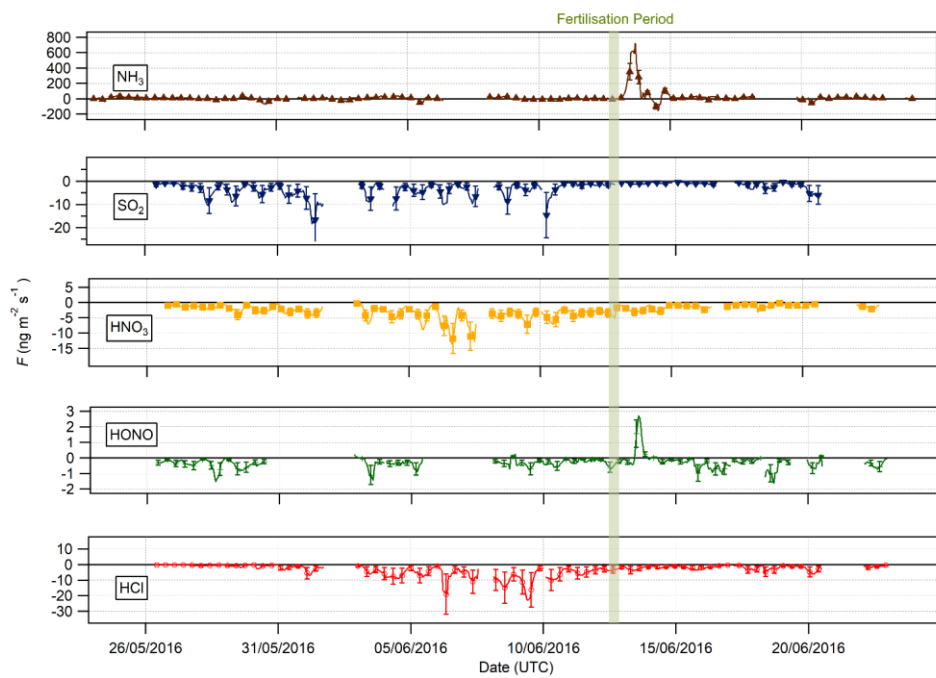


Figure 6: Hourly median diel water-soluble aerosol concentrations measured by the GRAEGOR at 2.4 m. Boxes show the lower and upper quartiles and whiskers the 5% to 95% range, with outliers shown as circles.



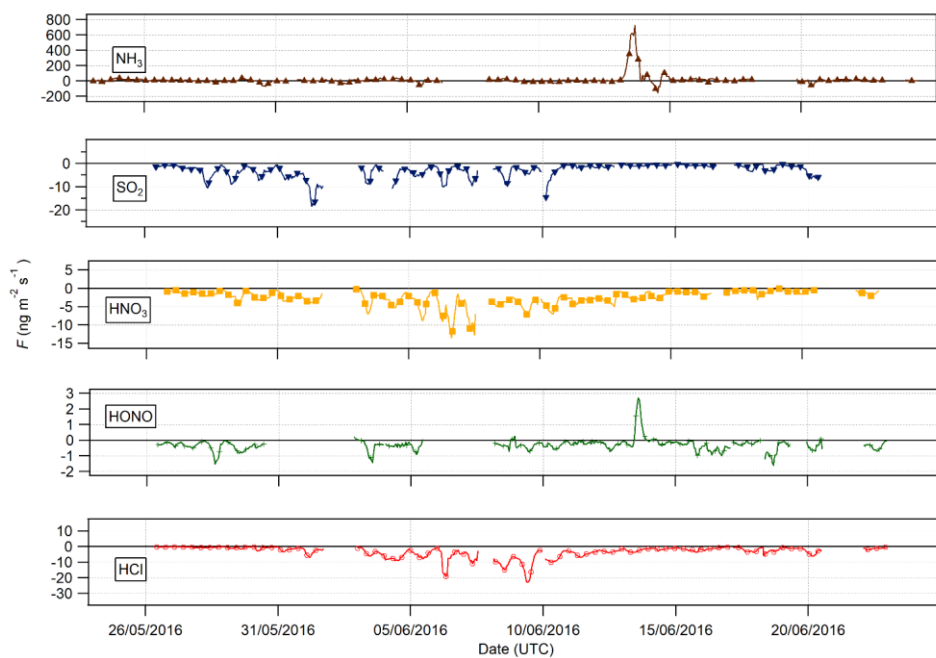
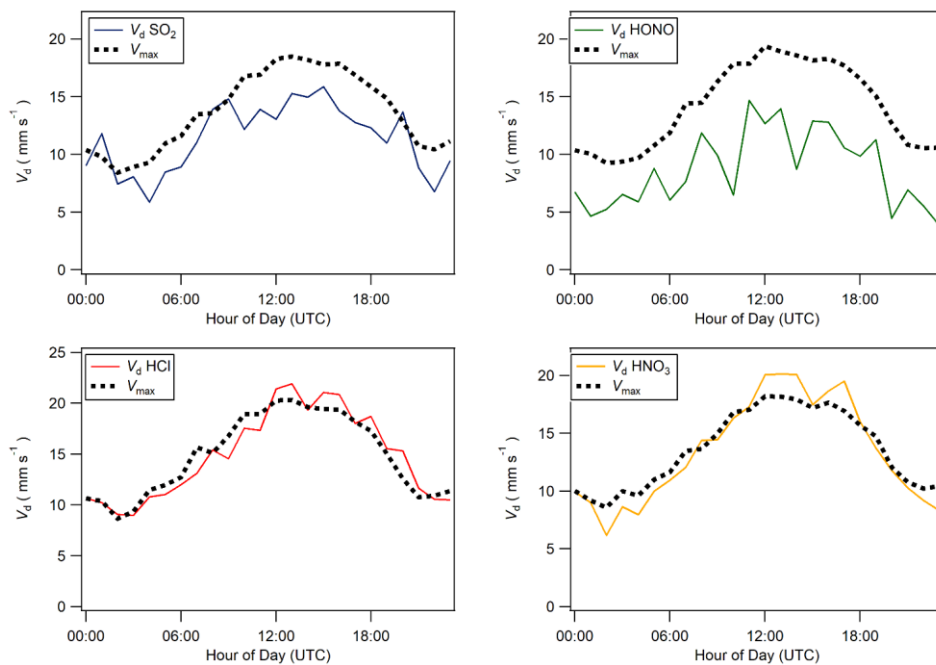
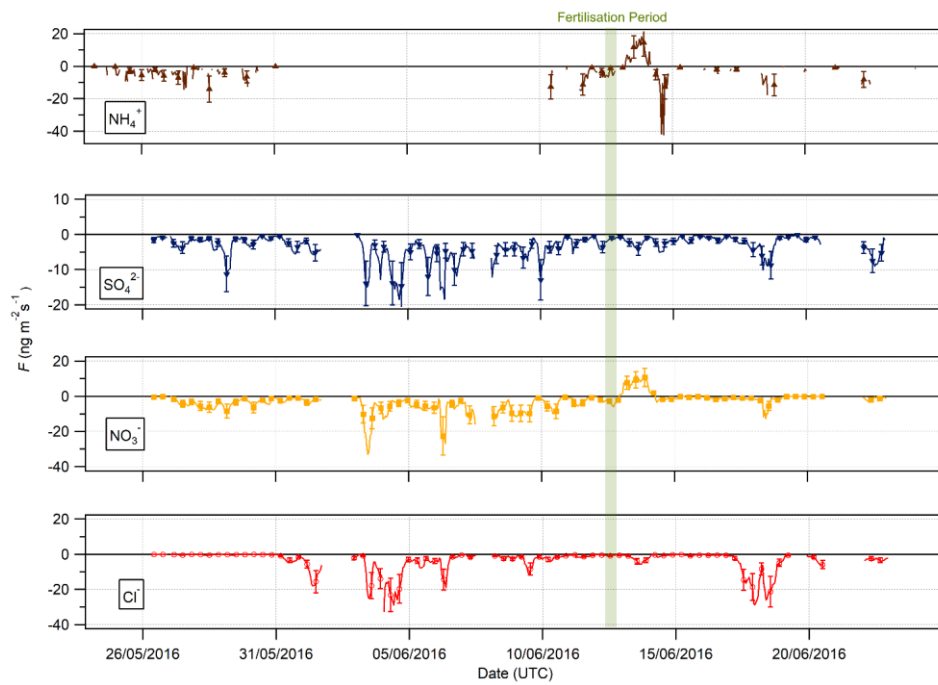


Figure 7: Time series of hourly trace gas fluxes measured during the Easter Bush campaign. Results smoothed using a 5-point moving point average. The fertilisation period was 08:00 – 09:00 on 13<sup>th</sup> June, and is highlighted in green. Flux uncertainties for each trace gas are included as error bars.

Commented [RR22]: Response to Reviewer #1 - We agree that it would be helpful to include error bars on the time series for fluxes and will add these to Figures 7 and 9 in the revised manuscript



**Figure 8: Median diel cycles for deposition velocity ( $V_d$ ) and maximum deposition velocity ( $V_{max}$ ) for (from top left clockwise)  $SO_2$ , HONO, HNO<sub>3</sub> and HCl.**



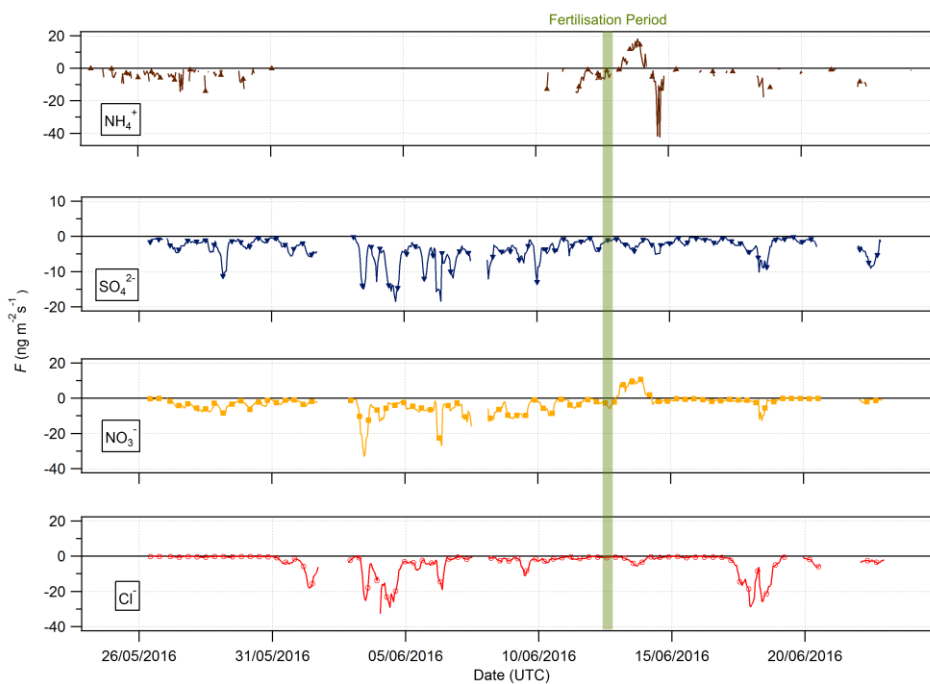


**Figure 9:** Time series of hourly fluxes of water-soluble aerosol species measured during the Easter Bush campaign. Results smoothed using a 5-point moving point average. The fertilisation period was 10.00 on 13th June, and is highlighted in green. **Flux uncertainties for each aerosol are included as error bars.**

**Commented [RR23]:** Response to Reviewer #1 - We agree that it would be helpful to include error bars on the time series for fluxes and will add these to Figures 7 and 9 in the revised manuscript

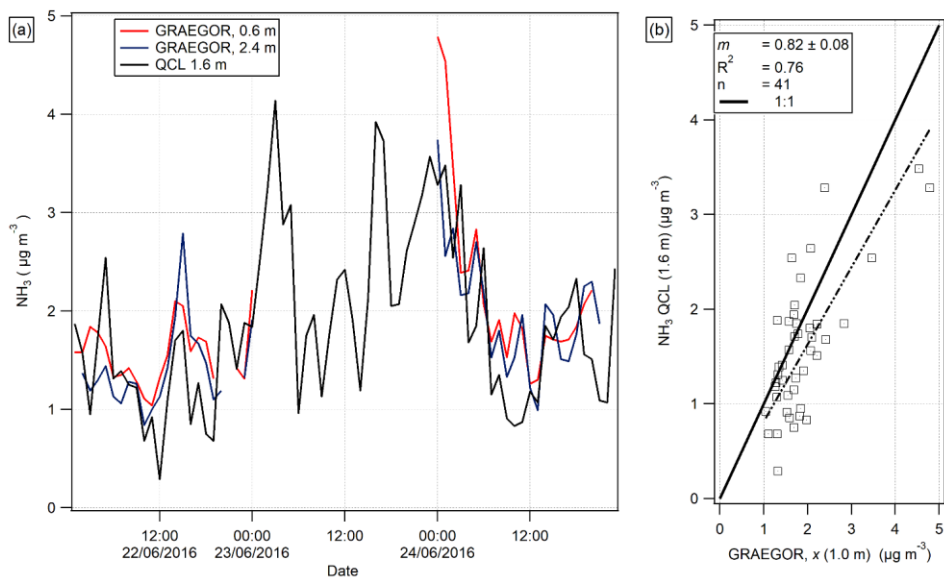


Figure 10 : (a). Time series of hourly averages of  $\text{NH}_3$  measurements recorded by GRAEGOR (0.6 m and 2.4 m) and QCL. (b). Linear regression analysis between QCL  $\text{NH}_3$  measurements and GRAEGOR (derived averaged concentration at 1.0 m)  $\text{NH}_3$  measurements.

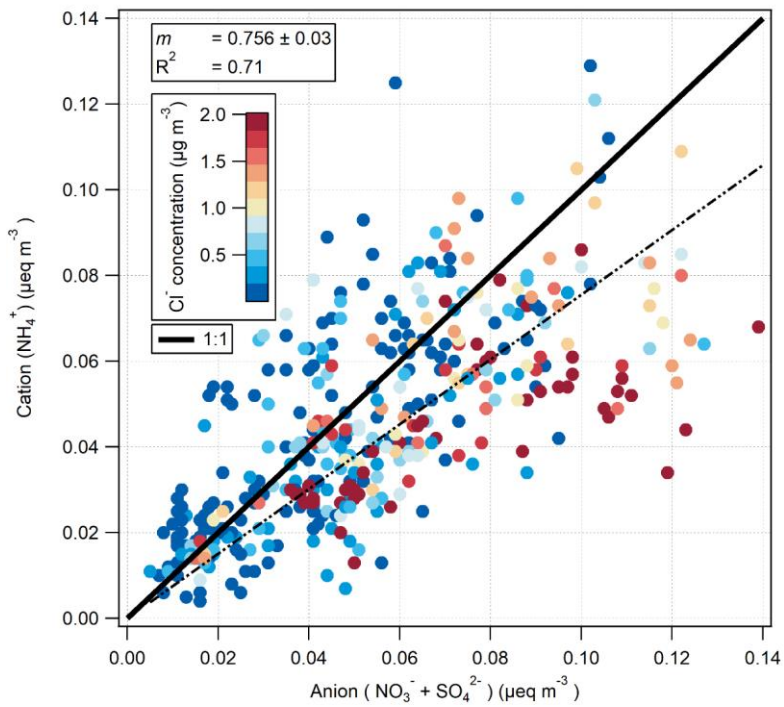


Figure 11: The ion balance of measured selected anions (NO<sub>3</sub><sup>-</sup> + SO<sub>4</sub><sup>2-</sup>) and measured cations (NH<sub>4</sub><sup>+</sup>) in μeq m<sup>-3</sup>. The colour scale is capped at 2 μeq m<sup>-3</sup> Cl<sup>-</sup> to highlight the association of anion excess with periods of sea salt influence.

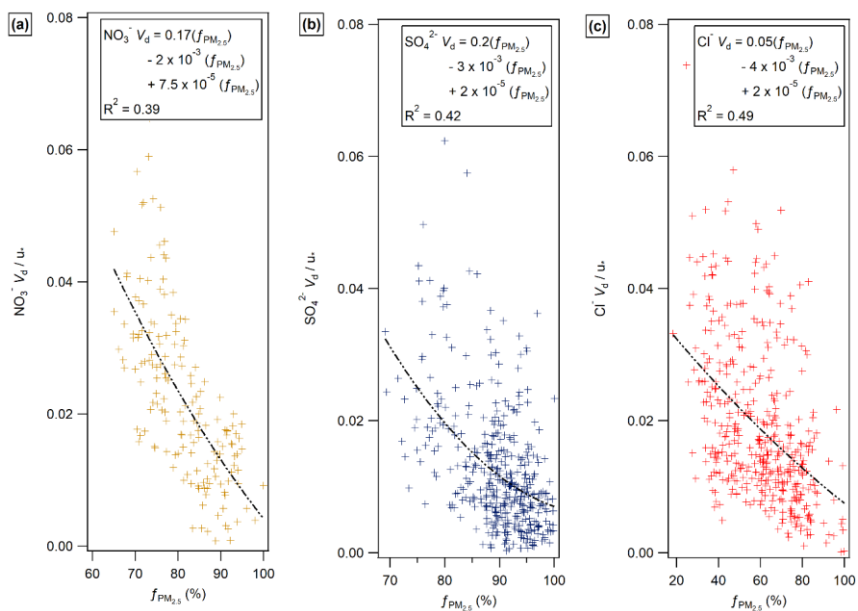


Figure 12: The normalised deposition velocity as a function of  $f_{PM_{2.5}}$  (expressed as a %) for (a) nitrate, (b) sulfate and (c) chloride, derived from the MARGA measurements at Auchencorth Moss.

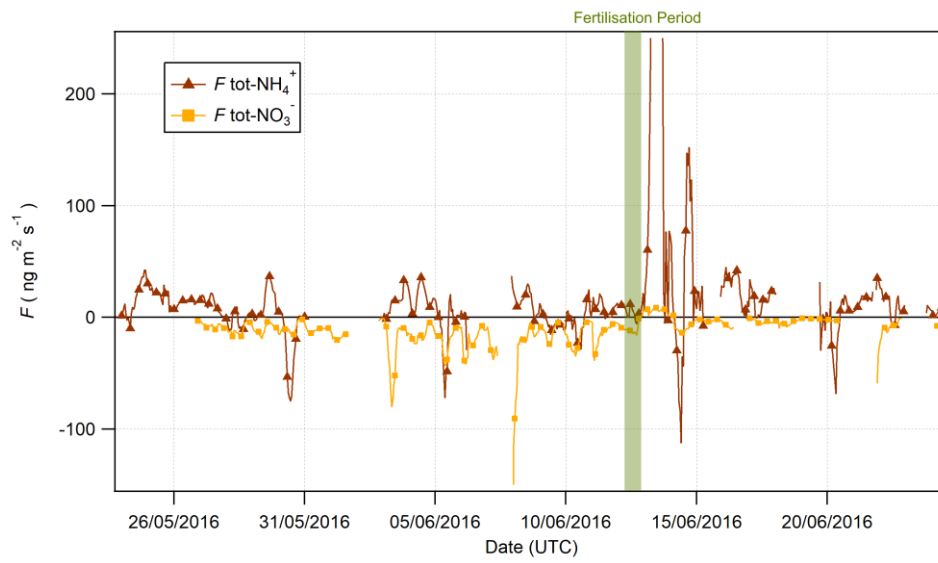


Figure 13: Fluxes of tot- $\text{NO}_3^-$  and tot- $\text{NH}_4^+$  pre-and post-fertilisation on the 13th June 2016 at 09:00 (marked in green).

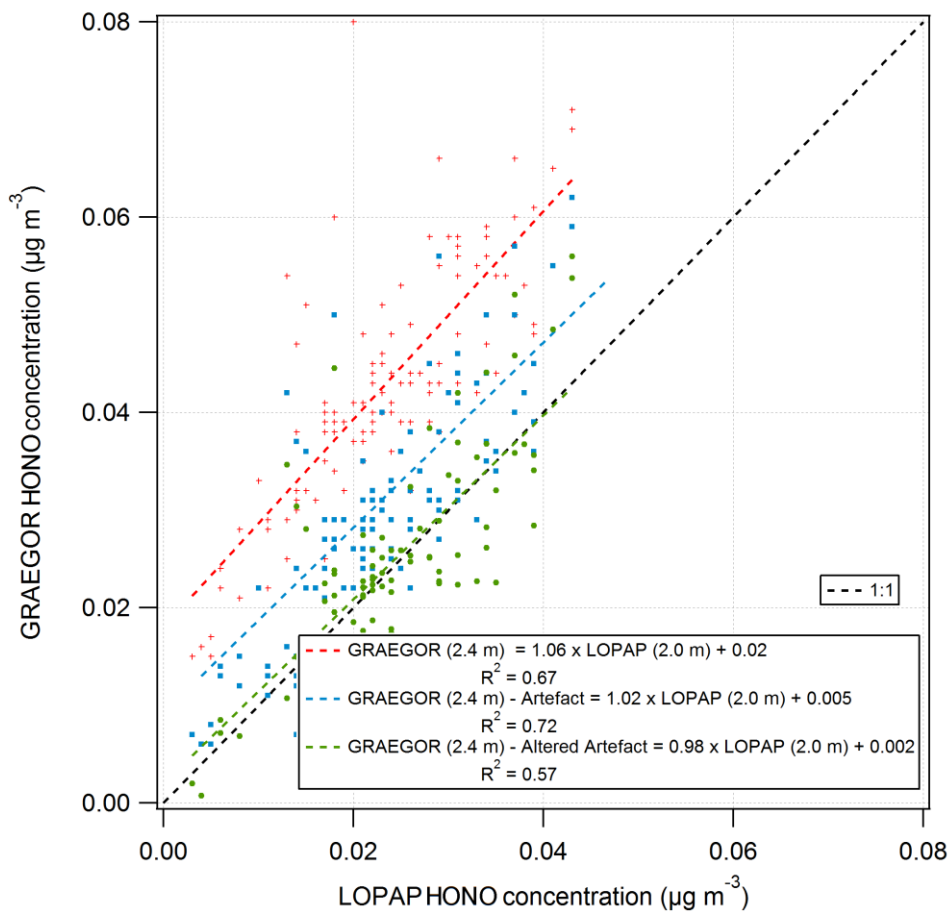


Figure 14: Simple linear regression analyses between GRAEGOR (2.4 m) and LOPAP (2.0 m) without artefact reduction (red), with Spindler's artefact reduction (blue), and with modified Spindler's artefact reduction (green) applied to GRAEGOR (2.4 m) HONO concentration.



Figure 15: (a) Time series of concurrent flux measurements of HONO derived from LOPAP (red) and GRAEGOR (green) measurements. (b) Scatter plot of GRAEGOR HONO flux values against LOPAP HONO flux values.

**Table 1: Limits of detection (LOD) for trace gases and water-soluble species measured, determined as three standard deviations (3σ) from averaged baseline signal.**

5

**Table 2, Table 3: Mean ( $\mu_A$ ), median ( $\mu_M$ ), min, max, and arithmetic standard deviation ( $\sigma_A$ ) for concentrations measured at 0.6 m and 2.4 m for trace gas and water-soluble aerosols measured during Easter-Bush campaign, calculated from hourly data. Number of measurements (N) for each compound at each height is also shown.**

- (0.6 m)	$\mu_A$ $\mu\text{g m}^{-3}$	$\mu_M$ $\mu\text{g m}^{-3}$	Min $\mu\text{g m}^{-3}$	Max $\mu\text{g m}^{-3}$	$\sigma_A$ $\mu\text{g m}^{-3}$	N
<b>NH<sub>4</sub><sup>+</sup></b>	0.77	0.67	<LOD	2.37	0.44	580
<b>Cl<sup>-</sup></b>	0.89	0.37	<LOD	7.31	1.25	484
<b>NO<sub>2</sub><sup>-</sup></b>	0.02	0.01	<LOD	0.07	0.01	334
<b>NO<sub>3</sub><sup>-</sup></b>	1.52	1.3	<LOD	5.91	1.13	507
<b>SO<sub>4</sub><sup>2-</sup></b>	1.28	1.21	<LOD	5.85	0.78	502
<b>NH<sub>3</sub></b>	1.71	1.32	<LOD	21.4	2.19	612
<b>HCl</b>	0.16	0.12	<LOD	1.21	0.15	507
<b>HONO</b>	0.03	0.04	<LOD	0.15	0.02	388
<b>HNO<sub>3</sub></b>	0.15	0.12	<LOD	0.53	0.09	513
<b>SO<sub>2</sub></b>	0.2	0.15	<LOD	1.22	0.17	479
-	-	-	-	-	-	-
(2.4 m)	$\mu_A$ $\mu\text{g m}^{-3}$	$\mu_M$ $\mu\text{g m}^{-3}$	Min $\mu\text{g m}^{-3}$	Max $\mu\text{g m}^{-3}$	$\sigma_A$ $\mu\text{g m}^{-3}$	N
<b>NH<sub>4</sub><sup>+</sup></b>	0.74	0.64	<LOD	2.33	0.43	580
<b>Cl<sup>-</sup></b>	0.91	0.36	<LOD	7.88	1.31	515
<b>NO<sub>2</sub><sup>-</sup></b>	0.02	0.02	<LOD	0.05	0.01	373
<b>NO<sub>3</sub><sup>-</sup></b>	1.53	1.32	<LOD	6.27	1.18	538
<b>SO<sub>4</sub><sup>2-</sup></b>	1.29	1.22	<LOD	6.26	0.83	540
<b>NH<sub>3</sub></b>	1.48	1.15	<LOD	13.79	1.5	602
<b>HCl</b>	0.2	0.15	<LOD	1.4	0.18	544
<b>HONO</b>	0.04	0.04	<LOD	0.12	0.02	410
<b>HNO<sub>3</sub></b>	0.19	0.16	<LOD	0.68	0.12	509
<b>SO<sub>2</sub></b>	0.24	0.18	<LOD	1.48	0.21	480

Formatted Table

10

**Table 1: Limits of detection (LOD, determined as three standard deviations from average baseline signal), mean ( $\mu_A$ ), median ( $\mu_M$ ), min, max, and arithmetic standard deviation ( $\sigma_A$ ) for concentrations measured at 2.4 m for trace gas and water-soluble aerosols**

**Commented [RR24]:** Response to Reviewer #1 and #2 – Due to concerns of length and the focus on concentration data, we have amalgamated three tables of concentration data into one. Limits of detection for each species are now contained in a single column, and the statistical data for only one height (2.4 m) is shown. Limits of detection for HNO<sub>3</sub> and SO<sub>2</sub> have also been corrected.

measured during Easter Bush campaign, calculated from hourly data. Number of measurements (N) for each compound is also shown.

	<b>LOD</b>	<b><math>\mu_A</math></b>	<b><math>\mu_M</math></b>	<b>Min</b>	<b>Max</b>	<b><math>\sigma_A</math></b>	<b>N</b>
(2.4 m)	$\text{ng m}^{-3}$	$\mu\text{g m}^{-3}$	$\mu\text{g m}^{-3}$	$\mu\text{g m}^{-3}$	$\mu\text{g m}^{-3}$	$\mu\text{g m}^{-3}$	
<b>NH<sub>4</sub><sup>+</sup></b>	190	0.74	0.64	<LOD	2.33	0.43	580
<b>Cl<sup>-</sup></b>	15	0.91	0.36	<LOD	7.88	1.31	515
<b>NO<sub>2</sub><sup>-</sup></b>	17	0.02	0.02	<LOD	0.05	0.01	373
<b>NO<sub>3</sub><sup>-</sup></b>	47	1.53	1.32	<LOD	6.27	1.18	538
<b>SO<sub>4</sub><sup>2-</sup></b>	109	1.29	1.22	<LOD	6.26	0.83	540
<b>NH<sub>3</sub></b>	172	1.48	1.15	<LOD	13.79	1.5	602
<b>HCl</b>	67	0.2	0.15	<LOD	1.4	0.18	544
<b>HONO</b>	30	0.04	0.04	<LOD	0.12	0.02	410
<b>HNO<sub>3</sub></b>	97	0.19	0.16	<LOD	0.68	0.12	509
<b>SO<sub>2</sub></b>	120	0.24	0.18	<LOD	1.48	0.21	480

5 Table 42: Mean ( $\mu_A$ ), median ( $\mu_M$ ), minimum and maximum values for flux, deposition velocity ( $V_d$ ), maximum deposition velocity ( $V_{max}$ ), and canopy resistances ( $R_c$ ) for trace gases measured during Easter Bush campaign, based on hourly values. Also shown are the median relative standard error ( $\sigma_r$ ), the flux limit of detection ( $F_{LOD}$ ) evaluated for typical conditions (median  $u^*$  and median concentration) as well as the fraction of the hourly flux value that exceed the flux detection limit evaluated for that hour ( $f_{LOD}$ ).

		<b>NH<sub>3</sub></b>	<b>HCl</b>	<b>HONO</b>	<b>HNO<sub>3</sub></b>	<b>SO<sub>2</sub></b>
<b>Flux (<math>\text{ng m}^{-2} \text{s}^{-1}</math>)</b>	$\mu_A$	15.24	-3.51	-0.3	-2.66	-3.04
	$\mu_M$	5.65	-1.98	-0.29	-1.99	-1.68
	Min	-324.5	-61.24	-2.46	-18.57	-35.57
	Max	1460	-0.03	4.92	0.82	-0.03
	No. of measurements	577	506	384	500	465
	$\sigma_r$ (%)		32	58	56	42
	$F_{LOD}$	1.28	0.75	0.18	0.89	0.97
	$f_{LOD}$ (%)	94	84	78	87	89
<b><math>V_d</math> (<math>\text{mm s}^{-1}</math>)</b>	$\mu_A$	-8.99	15.1	8.8	13.61	11.69
	$\mu_M$	-6.1	14.49	7.69	12.87	10.00
	Min	-215.3	0.01	-55.6	-4.72	0.34
	Max	92.90	52.83	59.81	56.78	55.38
<b><math>V_{max}</math> (<math>\text{mm s}^{-1}</math>)</b>	$\mu_A$	19.46	15.33	14.12	13.91	14.22
	$\mu_M$	18.8	15.26	13.99	13.75	14.02
	Min	1.7	0.04	0.04	0.04	0.45
	Max	57	40.41	36.99	36.93	36.99
<b><math>R_c</math> (<math>\text{s m}^{-1}</math>)</b>	$\mu_A$	-119.60	33.75	331.5	23.29	49.20

Formatted: Font: (Default) +Headings (Times New Roman)

Commented [RR25]: Response to Reviewer #1 - We will also add a summary of median flux error values to Tables 4 and 5...The reviewer raises an important point that was considered during flux calculations, but which was not included in the manuscript. As outlined by Thomas et al. (2009), it is possible to calculate the minimum flux that the GRAEGOR can measure for each species, effectively providing a limit of detection for flux measurements...We will include a brief discussion of calculating this value in the Methods section of the revised manuscript, which, together with inclusion of minimum detectable flux values for each species in Tables 4 and 5, should resolve this issue

Response to Reviewer #2 - The flux limits of detection for all trace gas and aerosol species measured will be added to Tables 4 and 5, respectively, of the manuscript.

Formatted Table

$\mu_M$  -92.050 1.82 13.07 5.71 27.61

**Commented [RR26]:** By convention, here cannot be a negative canopy resistance. A median and mean canopy resistance that is less than zero suggests that there was no canopy resistance throughout the campaign.

**Table 53:** Mean ( $\mu_A$ ), median ( $\mu_M$ ), minimum and maximum values for flux and deposition velocity ( $V_d$ ) for water soluble aerosols measured during Easter Bush campaign. Also shown are the median relative standard error ( $\sigma_F$ ), the flux limit of detection ( $F_{LOD}$ ) evaluated for typical conditions (median  $\mu$  and median concentration) as well as the fraction of the hourly flux value that exceed the flux detection limit evaluated for that hour ( $f_{LOD}$ ).

		$NH_4^+$	$Cl^-$	$NO_3^-$	$SO_4^{2-}$
<b>Flux (<math>ng\ m^{-2}\ s^{-1}</math>)</b>	$\mu_A$	-3.55	-4	-3.34	-3.56
	$\mu_M$	-2.97	-1.11	-1.76	-2.19
	Min	-42.23	-60.04	-89.32	-59.69
	Max	18.15	-1.06	31.84	-0.95
	No. of measurements	224	484	477	482
	$\sigma_F$ (%)	<u>58</u>	<u>41</u>	<u>48</u>	<u>45</u>
	$F_{LOD}$	<u>2.21</u>	<u>0.85</u>	<u>1.28</u>	<u>1.78</u>
	$f_{LOD}$ (%)	<u>91</u>	<u>81</u>	<u>84</u>	<u>87</u>
<b><math>V_d</math> (<math>mm\ s^{-1}</math>)</b>	$\mu_A$	0.93	3.65	1.97	1.89
	$\mu_M$	0.37	3.14	1.52	1.45
	Min	-0.04	-0.92	-9.43	-2.48
	Max	7.57	21.26	9.8	9.53

**Formatted Table**

**Formatted:** Font: Not Italic

**Commented [RR27]:** Response to Reviewer #1 - We will also add a summary of median flux error values to Tables 4 and 5...The reviewer raises an important point that was considered during flux calculations, but which was not included in the manuscript. As outlined by Thomas et al. (2009), it is possible to calculate the minimum flux that the GRAEGOR can measure for each species, effectively providing a limit of detection for flux measurements...We will include a brief discussion of calculating this value in the Methods section of the revised manuscript, which, together with inclusion of minimum detectable flux values for each species in Tables 4 and 5, should resolve this issue

Response to Reviewer #2 - The flux limits of detection for all trace gas and aerosol species measured will be added to Tables 4 and 5, respectively, of the manuscript.